Metabolic Engineering Aimed at the Production of Keto Acids
From Glycerol: An Industrial By-Product

by

Azhar Ahmed <u>Alhasawi</u>

Thesis submitted in partial fulfillment
of the requirements for the degree of
Doctor of Philosophy (PhD) in Biomolecular Sciences

The Faculty of Graduate Studies
Laurentian University
Sudbury, Ontario, Canada

ACCESSIBILITY CLAUSE AND PERMISSION TO USE

Abstract

Worldwide, energy consumption is at an all-time high and projected to increasingly grow in the upcoming years. Thus, it is critical to uncover alternative sources of energy that are independent of fossil fuels and environmentally neutral. The transformation of biomass into various energy-rich chemicals is an important strategy that is being pursued globally. Biodiesel can be an interesting substitute to fossil fuels. However, this process generates excessive amounts of glycerol, a byproduct that needs to be converted into valuable products if the biodiesel industry is to be sustainable.

The principle objective of this thesis is to study how glycerol can be used as a raw material by microbial systems to produce valuable products. The soil microbe, *Pseudomonas fluorescens* widely utilized in the numerous biotechnological applications due to its nutritional versatility is an obvious choice to tailor into a glycerol-transforming nanofactory. The abiotic modulators namely hydrogen peroxide (H_2O_2) and manganese (Mn) afforded uniquely facile means of triggering metabolic reprogramming aimed at the enhanced formation of pyruvate and α-ketoglutarate (KG). Under the influence of H_2O_2, *P. fluorescens* engineers an intricate metabolic network to synthesize ATP and pyruvate. As oxidative phosphorylation is severely impeded, the microbe invokes substrate level phosphorylation to generate energy. This is accomplished via the increased activities of various enzymes including pyruvate carboxylase (PC) and phosphoenolpyruvate carboxylase (PEPC) that were analyzed by blue-native polyacrylamide gel electrophoresis (BN-PAGE) and high performance liquid chromatography (HPLC). The high-energy phosphoenolpyruvate (PEP) is then converted into ATP and pyruvate, a process mediated by pyruvate phosphate dikinase (PPDK), phosphoenolpyruvate synthase

(PEPS) and pyruvate kinase (PK). Supplementation with a micro-nutrient such as Mn, a divalent metal involved in a variety of enzymes results in the reprogramming of the metabolic networks aimed at the accumulation of KG. The increased activities of isocitrate dehydrogenase (ICDH)-(NAD)P dependent and aminotransaminases aided the exocellular secretion of KG. The overexpression of pyruvate carboxylase (PC) that is evident in the Mn-treated cells provides oxaloacetate, an important precursor to the synthesis of citrate, a key ingredient in the synthesis of KG. Isocitrate lyase (ICL), fumarate reductase (FUMR), succinate semialdehyde dehydrogenase (SSADH), α-ketoglutarate decarboxylase (KDC) and γ-aminobutyric acid transaminases (GABAT) work in concert to produce KG. ^{13}C-NMR helped identify the metabolites participating in the metabolic networks. Immunoblot experiments confirmed the presence of overexpressed enzymes. These disparate metabolic pathways that promote the overproduction of the keto-acids in *P. fluorescens* have the potential of converting glycerol to value-added products commercially. As the process utilized is devoid of any genetic manipulation, it can be readily implemented in an industrial setting. In conclusion, both H_2O_2 and Mn can orchestrate metabolic changes in *P. fluorescens* inducing the production of pyruvate and KG from glycerol respectively. These chemical manipulations may also be applied to other microbial systems.

Acknowledgements

First and foremost, I would like to extend my gratitude to my supervisor and mentor, Dr. Vasu Appanna. This thesis without his guidance will not be possible. His knowledge and an incredible learning experience have inspired me to go over my obstacles and continue to move forward. His research and discussion have created the love of science. Truly, my future and success will be related to his teaching and I am grateful for his support and leadership. I also extend my gratitude to members of my supervisory committees, Dr. Abdel Omri and Dr. Crestina Beites. I thank them for their guidance and input and for spending time to look over all the details and providing helpful feedback. I also would thank Laurentian university of providing the opportunity to study and do the research in an excellent setting. I am also thankful to the Ministry of Higher Education for funding of my doctoral studies.

I'm also indebted to Dr. Pablo I. Nikel, Centre for Biosustainability: The Novo Nordisk Foundation, Technical University of Denmark, the external examiner and Dr. Ramesh Subramanian, Bharti School of Engineering, Laurentian University, internal examiner. Their advice was helpful in the completion of this thesis. I would like to thank my labmates past and present, Dr. Joseph Lemire, Dr. Christopher Auger, Dr. Sean Thomas (always supported me and eager to help), Dr. Adam Bignucolo, Dr. Varun Appanna and Nohaiah Aldarani for their friendship, mentorship, technical support and insights. Also, I would like to thank my father and mother in law who loved to see me in this position. Finally, I would also like to thank my family (brothers and sisters) for their continuous encouragements. Especially, Eman, Ali, Asia and Mohammed who were around me during my study and helped to take care of my kids.

Dedication

I dedicate this work to my Father Ahmed Alhasawi and Mother Anissah Al boqarin who surrounded me with their endless support, encouragement, love and prayers. They have been a great source of motivation and inspiration.

Table of Contents

List of Figures

List of Tables

List of publications

1. **Alhasawi A**, Appanna VD (2017). Enhanced extracellular chitinase production in *Pseudomonas fluorescens*: biotechnological implications. Aims Bioengineering 4, 366-376.

2. Tharmalingam S, **Alhasawi A,** Appanna VP, Lemire J, Appanna VD (2017). Reactive nitrogen species (RNS) resistant microbes: adaptation and medical implications. Biological Chemistry. doi.org/10.1515/hsz-2017-0152

3. Lemire J, **Alhasawi A,** Appanna VP, Tharmalingam S, Appanna VD (2017). Metabolic defense against oxidative stress: The road less travelled-so far. Journal Applied Microbiology. doi: 10.1111/jam.13509.

4. Aldarini N, **Alhasawi A,** Thomas SC, and Appanna VD (2017). The role of glutamine synthetase in energy production and glutamine metabolism during oxidative stress. Antonie van Leeuwenhoek. 110:629-639.

5. **Alhasawi A,** Appanna VD (2017) Manganese orchestrates a metabolic shift leading to the increased bioconversion of glycerol into α-ketoglutarate. Aims Bioengineering 4, 12-27.

6. Tharmalingam S, **Alhasawi A,** Appanna VP, Appanna, VD (2016) Decontamination of multiple-metal pollution by microbial systems: the metabolic twist. Handbook of metal-microbe interactions and bioremediation. Publisher Springer.

7. **Alhasawi A,** S.C. Thomas Appanna V (2016) Metabolic networks to generate ATP from glycerol during oxidative stress in *Pseudomonas fluorescens*. Enzyme and Microbial Technology. 85:51-56.

8. Thomas C, **Ahasawi A,** Auger C, A Omri A, Appanna VD (2015) Formate is a potent reductive force against oxidative stress. Antonie van Leeuwenhoek. 2015: 1-9.

9. Auger A, **Alhasawi A,** Contavadoo M, Appanna VD (2015) Dysfunctional mitochondrial bioenergetics and the pathogenesis of hepatic disorders. Frontiers Cell and Developmental Biology 3:40.

10. Auger A, Appanna ND, **Alhasawi A,** Appanna V (2015) Deciphering metabolic networks by blue native polyacrylamide gel electrophoresis: a functional proteomic exploration. EuPA Open Proteomics 7, 64-72.

11. **Alhasawi A,** Leblanc M, Appanna ND, Auger C, and Appanna, VD (2015) Aspartate metabolism and pyruvate homeostasis triggered by oxidative stress in *Pseudomonas fluorescens*: a functional metabolomic study. Metabolomics 11:1792-1801.

12. **Alhasawi A,** Appanna ND, Auger A, Appanna V (2015) Metabolic networks involved in the decontamination of a multiple metal environment by *Pseudomonas fluorescens*. Journal of Biotechnology 200, 38-43.

13. **Alhasawi A,** Castonguay A, Appanna ND, Auger C, Appanna VD (2015) Glycine metabolism and anti-oxidative defense mechanisms in *Pseudomonas fluorescens*. Microbiological Research 171: 26-31.

14. Appanna VP, **Alhasawi A,** C. Auger, Appanna VD (2015) Phospho-transfer networks and ATP homeostasis to counter oxidative stress in *Pseudomonas fluorescens*. Archive Biochemistry and Biophysics 606: 26e33.

15. Thomas SC, **Alhasawi A,** Appanna VP, Auger C, Appanna (2014) Brain metabolism and Alzheimer's disease: The prospect of a metabolite based therapy. Journal of Nutrition, Health and Aging 1-6.

16. **Alhasawi A,** Auger C, Appanna VP, Chahma MH, Appanna VD (2014) Zinc toxicity and ATP production in *Pseudomonas fluorescens*. Journal of Applied Microbiology 117, 65-73.

List of abbreviations

μM…………………………………………………………………...Micromolar

μL……………………………………..…………………………...Microlitre

μg…………………………………………………………………….Microgram

ACN……………………………………………………………Aconitase

ADP………………………………………………...Adenosine diphosphate

AK…………………………………………………………...Adenylate kinase

APS………………………………………………………….Ammonium persulfate

ATP………………………………………………………...Adenosine triphosphate

AU…………………………………………………………..……….Arbitrary units

BN…………………………………………………………………….Blue native

BN-PAGE…………………….Blue native polyacrylamide gel electrophoresis

BSA……………………………………………………………..Bovine serum albumin

BTU………………………………..…………………………..British thermal unit

C…………………...……………………………………………………….Celsius

CFE………………………………………..………………………Cell free extract

cm……………………………………………………………………….Centimeters

CoA……………………………………………………………………….Coenzyme A

CSB…………………...………………………………………...Cell storage buffer

DCIP…………………..……………………………………………Dichloroindophenol

ddH2O……………………..…………………………….Deionized and distilled water

LDH……………………………………………………...Lactate dehydrogenase

Mn………………………………………………………….Manganese

M…………………………………………………………..Molar

ME…………………………………..………………….Malic enzyme

MDH…………………………………………...Malate dehydrogenase

min……………………………………………………….Minutes

mL……………………………………………………Millilitre

mM…………………………………………………...Millimolar

mm……………………………...………………………..Millimeter

MS………………………………………………..Malate synthetase

N…………………………………...……………...Normal (normality)

nm……………………………………………………Nanometers

NaCl…………………………………………………Sodium chloride

NAD………….. ……....……..Nicotinamide adenine dinucleotide (oxidized)

NADH………. ……....………Nicotinamide adenine dinucleotide (reduced)

NADP…………...Nicotinamide adenine dinucleotide phosphate (oxidized)

NADPH…………..Nicotinamide adenine dinucleotide phosphate (reduced)

NAD-ICDH……………….…….NAD-dependent isocitrate dehydrogenase

NADP-ICDH…………………NADP-dependent isocitrate dehydrogenase

NDPK……………………………………….Nucleotide diphosphate kinase

O_2…………………………………………………..Molecular oxygen

Pi…………………………………………………….Inorganic phosphate

PPi……………………………………………………..Pyrophosphate

PC………………………………………………………….Pyruvate carboxylase

PDH………………………………………………….Pyruvate dehydrogenase

PEP…………………………………………………..Phosphoenolpyruvate

PEPC…………………………………………...Phosphoenolpyruvate carboxylase

PEPCK…………………………………….Phosphoenolpyruvate carboxykinase

PEPS……………………………………..Phosphoenolpyruvate synthase

PMS…………………………………………..Phenazine methosulfate

PPDK…………………………………………...Pyruvate, phosphate dikinase

ROS………………………………………………….Reactive oxygen species

SSA…………………………………………………..Succinate semialdehyde

SSADH…………………………………...Succinate semialdehyde dehydrogenase

1. Chapter I: Introduction

Globally, energy consumption is now at record levels and is estimated to steadily grow throughout the future (Figure 1.1). Rise in energy utilization has caused harmful environmental impacts due to greenhouse gas emissions and is contributing to the depletion of fossil fuel reserves (1). Considering the rapid depletion of petroleum and rising concerns regarding the environmental consequences of fossil fuel usage, an alternative beneficial approach is critical to decrease the reliance on fossil fuels. The possibility of using biofuels had already been noted. It was considered in the 1970s, but its development was restricted by challenges presented by the lack of adequate technology available at the time. Recent developments across numerous fields have once again generated attention in the production of biofuels. An innovative branch of biotechnology known as white biotechnology arose as a result of the concern over fossil fuel use. It focuses on using microbes to produce biodegradable products which have the benefits of necessitating less energy and forming less waste than the techniques that are currently in use (2).
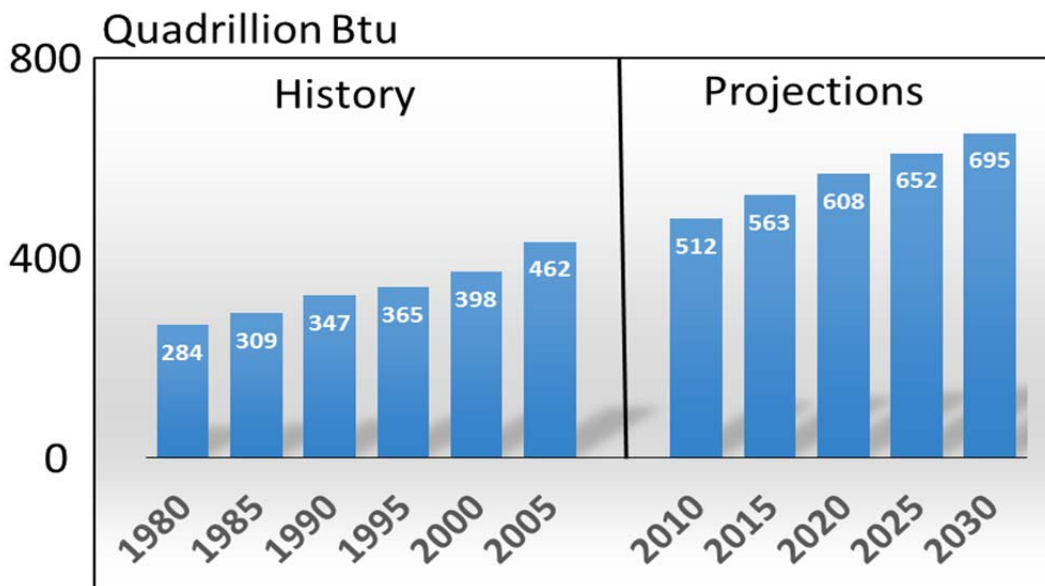
Figure 1.1: World marketed energy consumption 1980-2030 adapted from (1)

According to the aforementioned data from IEA 1980 to 2030, total world consumption of marketed energy is projected to increase by 57 % from 2004 to 2030 (1).

Due to the depletion of the fossil fuel reserves and environmental impacts of petroleum, alternative energy production process have received much attention, to balance market needs. Figure 1.2 illustrates numerous sources of energy used to meet the global demand in 2015. As depicted, fossil fuels were the main source of energy utilized by the world.
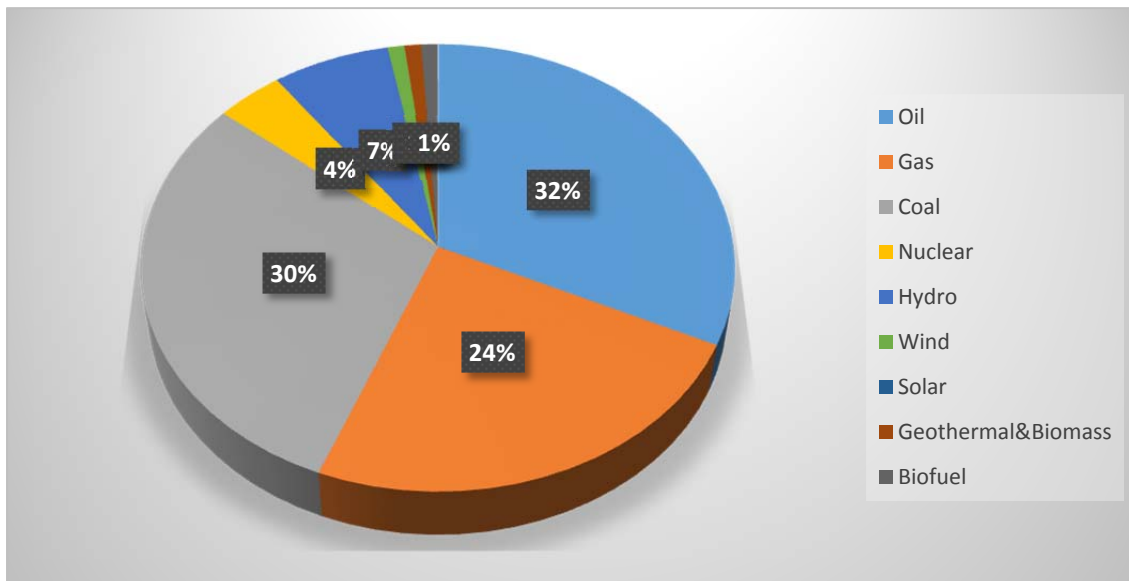
Figure 1.2: Numerous sources of energy to meet the global demand in 2015 adapted from (1).

1.1 Biomass Derived Energy

Biomass, made up of any biological materials is one of the most widely utilized materials and large scale energy production can be derived from such sources as woods, plants, organic wastes, and alcohol fuels (3). Biomass-derived energy can be obtained via three techniques: thermal, biochemical and chemical processes. Energy-derived from biomass is well-known to significantly diminish greenhouse gases and global warming. The use of fossil fuel leads to

excessive release of carbon dioxide into the atmosphere by emission of carbon that was fixed into fossils millions of years ago. In contrast, energy obtained from biomass does not release new carbon into the atmosphere. Thus, the dependence on expensive raw material as a carbon source to produce valuable added products can be mitigated by utilizing renewable biomass (4). Figure 1.3 demonstrates primary renewable feed stocks and the following biofuels produced by various kinds of feedstocks: plant oil and animal fat, sugar, starch and cellulose (5).
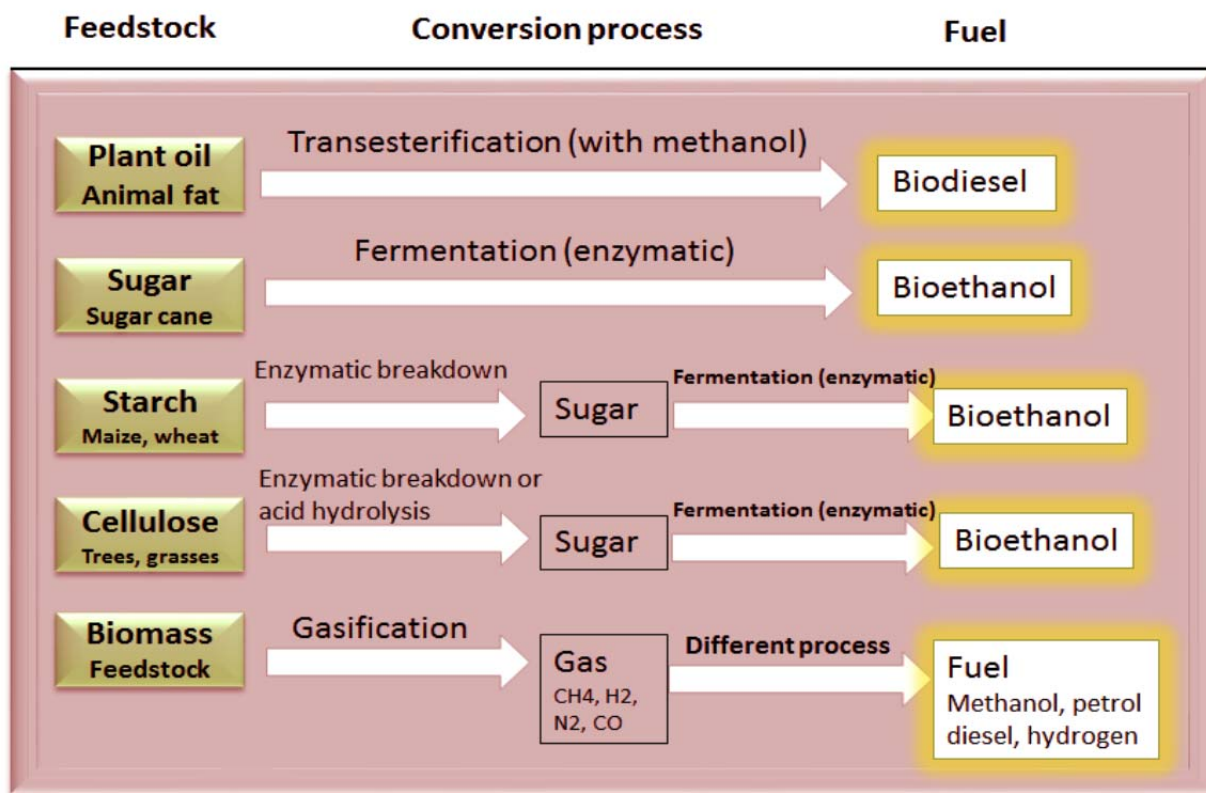
Figure 1.3: Utilization of diverse feedstocks in the production of biofuels for the transportation industry adapted from (5).

Bioethanol and biodiesel are two examples of biomass derived energy. Bioethanol is currently the alternate fuel to petroleum and used for road transport vehicles. It is produced via the chemical process of reacting ethylene with steam. Also, it can be produced by fermentation of sugars from diverse feed stocks. Although most cars on the road today in Canada and the U.S.

3

can run on blends of up to 10% ethanol without any modifications,   the use of 10% ethanol gasoline (E10) is restricted in some cities where risky levels of auto emissions are created (6). Numerous concerns regarding the large amount of arable land mandatory for the fuel crops become evident as the retail price of bioethanol approaches the cost of gas. This problem should be considered in the context of regenerating the bioethanol in order not to perturb the availability of biomass for human and animal consumption. Recently of note, the use of cellulose as raw material for bioethanol may alleviate some of these problems. Thus, cellulosic ethanol is becoming a promise for future renewable energy (7, 8).

Biodiesel is one of the foremost biodegradable fuels used as an alternative to fossil fuel because the former is obtained from 100% renewable resources and is non-toxic, making it safe for use. Biodiesel burns cleaner and provides lower emission of carbon monoxide and other air pollutants. Although biodiesel does not comprise petroleum, it can be mixed with petroleum to form biodiesel blend, which can be utilized in diverse vehicles. It also has an energy content equal to 90% of that of petroleum. Even though biodiesel has some inherent challenges, the nature of organic fuel contributes to increasing nitrogen species into the atmosphere. Consequently, the rise of nitrogen input would lead to more acid rains. Biodiesel production reduces reliance on imported crude fossil fuels from foreign countries and helps to improve the economy by growth of the agricultural sector (9, 10).

Chemically, biodiesel is defined as fatty acid methyl ester and synthesized from biological triglycerides such as plant oils or animal fats with alcohol in the presence of catalysts. For example, biodiesel can be produced from waste products including fats and greases by pre-treating them with sulfuric acid and methanol for esterification of higher free fatty acid content (Figure 1.4).

4
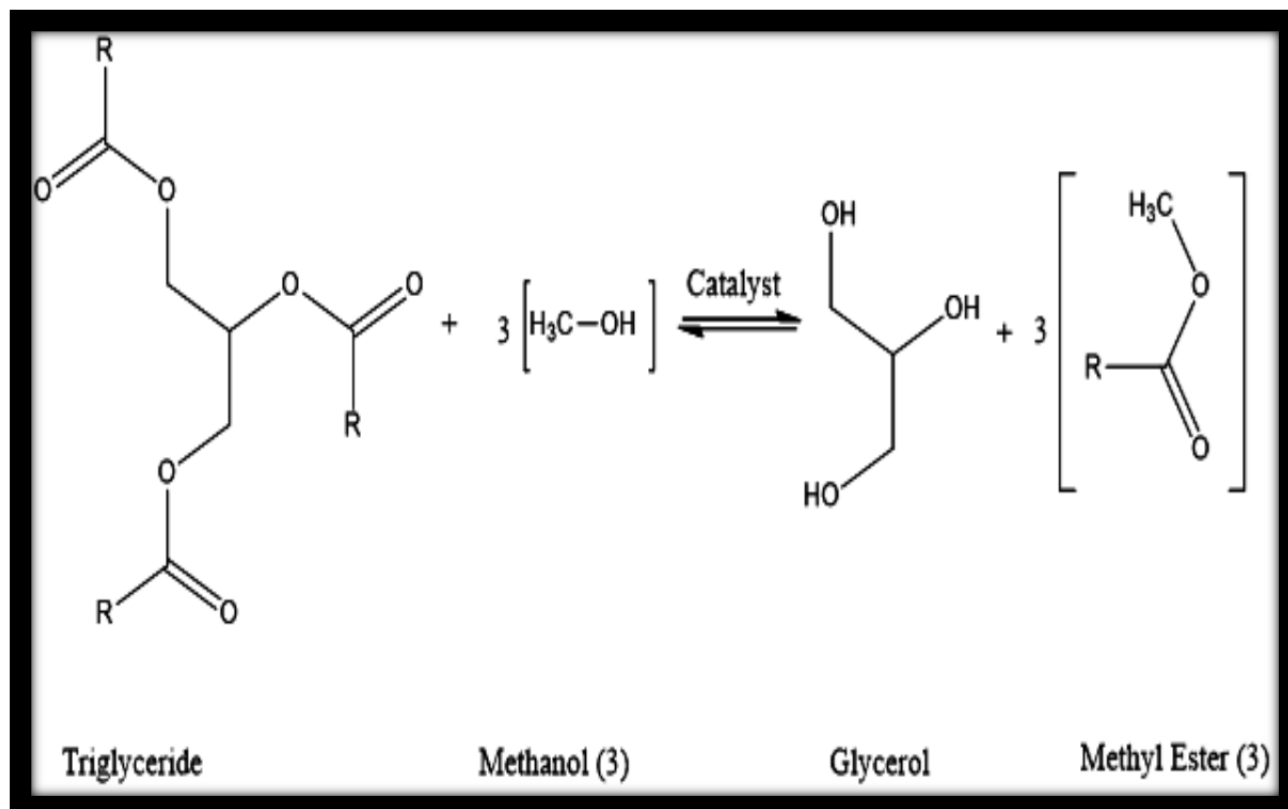
Figure 1.4: Transesterification reaction, crucial for the conversion of triglycerides (plant oil) into biodiesel adapted from (11).

The biodiesel industry is continually developing due to an increasing demand (11). However, the growth in biodiesel industry is contributing to crude glycerol accumulation. The United States produced 140 million gallons of biodiesel in 2016, resulting in 40 million kg of glycerol as a by-product (10, 12). Even though pure glycerol has numerous applications in food, cosmetics and drug industries, crude glycerol would have to undergo costly refining processes before it reaches the purity required to be utilized as such. Crude glycerol from transesterification reactions consists of about 50% glycerol; the rest is methanol, catalyst and

soap(13).
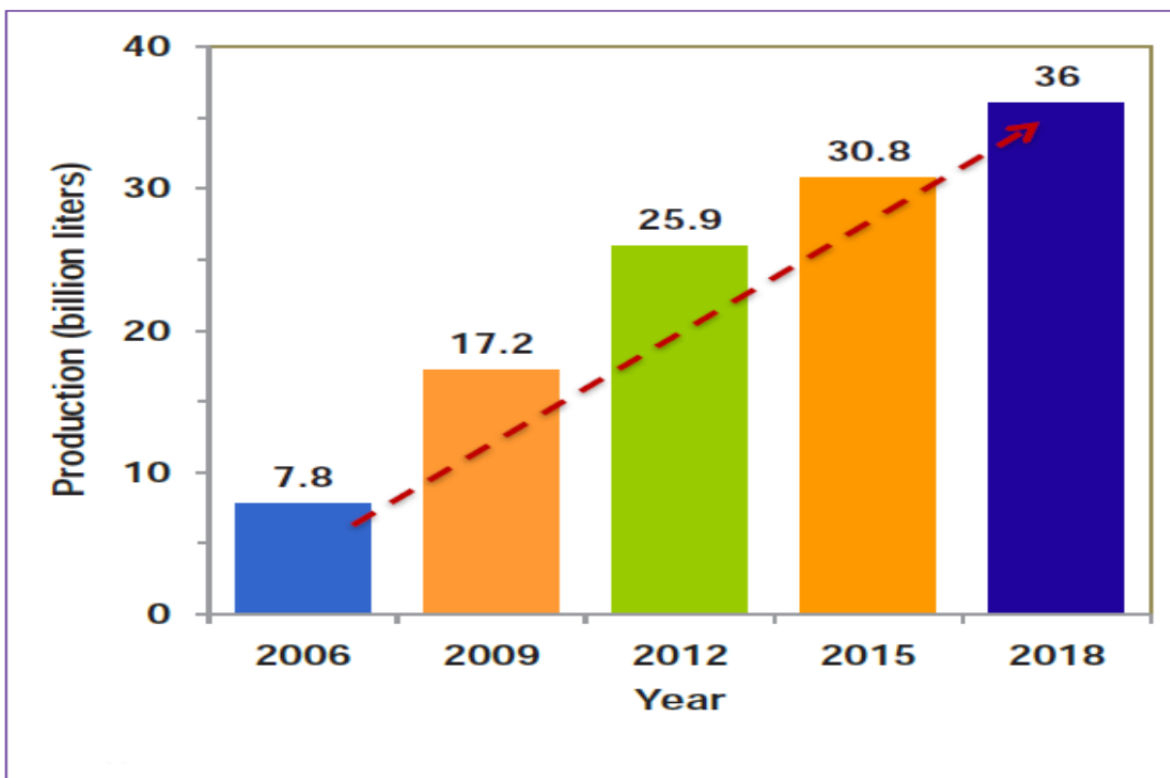
Figure 1.5: The global trend in the production of crude glycerol taken from (13).

1.2 Glycerol

Glycerol is a trihydric alcohol. It is a colorless, odorless, sweet-tasting and syrupy liquid (14). It has various applications in cosmetics, paints, foods, tobacco, pharmaceuticals and automobiles. It can be manufactured in different forms: raw, synthetic and purified. Raw glycerol formed by the biodiesel industry is approximately 60-80% pure compared to 100% in both the purified and synthetic glycerol. As aforementioned, glycerol requires extensive refining processes before it can be used to produce valuable products (15). The useful new applications

of glycerol in daily life and the chemical industry will advance the economic capability of the biodiesel industry.

1.3 Value-added products from glycerol

Worldwide, the conversion of crude glycerol resulting from biodiesel has grown from 200,000 tonnes in 2004 to 1.1224 million tonne in 2008 (16, 17). It is critical to establish a new era of research to convert crude glycerol in order to advance the economic sustainability of biodiesel facilities (2). Due to the surplus of crude glycerol and the higher price of corn, glycerol can be utilized as an animal feedstuff. Glycerol is a worthy energy source, which can be metabolized to glucose (10). However, more consideration should be paid to the crude glycerol for animal diets with regard to methanol and metals contamination. Indeed, the low cost of crude glycerol has attracted researchers to use it as a feedstock to generate value added products such as citric acid, lactic acid, propionic acid, polyhdroxyalkanoate (PHA), hydrogen and ethanol (9) (Figure 1.6).
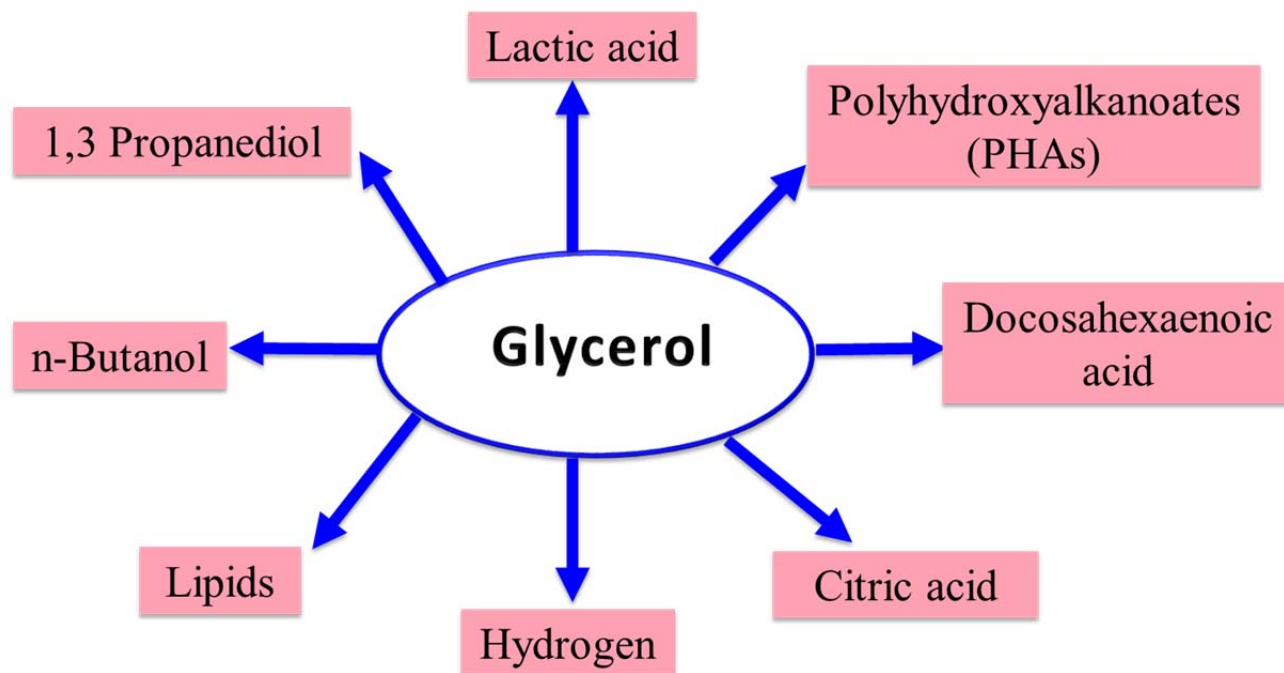
Figure 1.6: Numerous value-added products produced from glycerol (adapted from 9)

1.4 Conversion of glycerol to value-added products

Several techniques have been elucidated insofar as the conversion of glycerol to its constituent value-added products is concerned. Chemical catalysis is one of the foremost known methods of conversion. Studies have reported that glycerol can be oxidized and decomposed using a flow reactor. It has been demonstrated that utilizing polyfunctional molecules with simple oxidants are capable of producing oxygenated products including dihydroxyacetone, hydroxypyruvic acid, glyceric acid, oxalic acid and others. Metallic catalyst such as Pd, Pt and Au are utilized to perform the oxidation process. Furthermore, dehydration of glycerol under high temperature from 250C-350C is also another way to transform glycerol to valuable products. The selectivity of glycerol dehydration to acrolein has been optimized at appropriate temperatures. The latter reaction is catalyzed by acids such as sulfuric acid, phosphoric acids and

other catalysts such as zinc sulfate and zeolite. Also, catalytic acetylation of glycerol performed via acid oxides such as CeO_2/ZrO_2, CeO_2/Al_2O_3 was noted due to its stability, low costs, and regenerability and 100% conversion rate of glycerol. These reactions yield mono, di and tri esters of glycerol (acetin). Also, numerous researchers have utilized metals such as Zn, Cu, Mg, Pd, Ni in order to catalyze the reduction of glycerol. These methods can produce various products including ethylene-glycol, 1,2-propileneglycol, 1,3 propileneglycol, lactic acid, acetol, propanol, and or even acrolein. The selectivity of the products depends on varying the parameters involved including glycerol concentration, temperature, pressure to produce the desired products, etc. (18). All existing reactions highlight feasible techniques used to catalyze glycerol into valuable products. It is difficult to acquire good selectivity of the desired chemicals at high conversion rates of glycerol because of high hydroxylic functionality of the triol molecules of similar reactivity. Therefore, novel processes to convert glycerol into valuable products that are driven by microbial systems need to be devised.

One approach to effectively using crude glycerol from biodiesel sources is to program microorganisms to grow on crude glycerol as carbon source and produce large arrays of value-added products with varied functionalities. Therefore, understanding how microorganisms are capable of metabolizing crude glycerol is very essential since it is sustainable, economical, and environmentally-neutral. It is possible to produce valuable chemicals by using different types of microorganisms (bacteria, fungi and algae) driving different metabolic pathways, depending on the required products. However, various by-products which are usually produced during the fermentation process affect the yield of desired products. Hence, this can be solved using genetic engineering via inactivating the genes that are responsible for inhibitor formation or overproduction of genes that lead to the targeted products. While 1, 3 propanediol can be

produced by numerous types of organisms, *Klebsiella pneumoniae* and *Clostridium butyricum* were noted to be the most widely utilized microorganisms that have efficiently converted glycerol to 1, 3 propanediol. *Clostridium butyricum* is known to produce 76.2 g/L of this product by using fed-batch ferementation with 1L which was scaled up to 200L and the productivity was 2.g/g/L/H (19). Also, *E.coli* was genetically engineered to metabolize glycerol and produce 1, 2 propanediol and this was performed via the overexpression of genes involved in dihydoxyacetone phosphate metabolism including methylglyoxal synthase (mgsA), glycerol dehydrogenase (gldA), and aldehyde oxidoreductase (yqhD) (20).

These manipulations contribute to high production of this industrial value added-product. *Clostridium pasteurianum* is known to produce n-butanol under anaerobic conditions and the product butanol has been optimized using simultaneous dual substrate cultivation stratagems. Also, the deletion of 2, 3-butanediol biosynthesis pathways by deactivating the genes that are responsible for the production of butanediol and overexpressing enzymes that lead to synthesis of butanol were achieved in *Klebsiella pneumoniae,* which promises to be a good approach to the production of butanol (21). Indeed, citrate is also another useful chemical that is produced by microorganisms using crude glycerol as sole source of carbon. *Yarrowia lipolytica*, is an acetate negative mutant that has been established to produce high amount of citric acid under nitrogen limitation conditions (22). Polyhydroxyalkanoate (PHA) which is poly-ester biopolymer used as alternative to fossil fuels has effectively been produced by different types of microorganisms including *Paracoccus denitrificans*, *Cupriavidus necator* JMP and *Zobellella denitrificans*. The latter is used in the large-scale production of PHA with crude glycerol due to its lower sensitivity to NaCl compared to the former. Furthermore, it was expected that a 10 million gallon per year biodiesel plant would have the prospective of generating 20.9 ton PHB.

The production of ethanol also is easy from glycerol and it has been noted that *Pachysolen tannophilus* is an efficient microbe to produce ethanol. *E.coli* is also used to produce ethanol from glycerol and ethanol production was maximized when the strain was constructed by inactivating fumarate reductase and phosphate acetyltransferase resulting in the production of 1 mole of ethanol per mole consumed of glycerol (23).

1.5 Abiotic stress and metabolite production

Although microbial conversion of glycerol to valuable products has emerged as a much sought-after goal, it has some drawbacks including low yield due to inhibitory compounds. These compounds inhibit cell growth of the microorganisms. Adaptation of the microorganism under diverse stress conditions has been shown to increase the product yields. *Clostridium butyricum* DSP1 has been adapted to an environment of high osmotic pressure to grow in high concentration of pure glycerol (90 g/L) and crude glycerol (70g/L) to produce 1, 3 propanediol (24). Indeed, *Novosphingobium* sp. could produce PHA in the presence of phosphate and nitrogen starvation and it utilizes crude glycerol to elaborate this biopolymer. This biopolymer has the potential to be utilized in biomedical applications due to the formation of endotoxin-free polyhydroxyalkanoates (PHAs) from this gram-negative bacteria (25). Also, poly hydroxybutyrate (PHB) was harvested in *B. megaterium* growing in crude glycerol under oxygen and pH controlled environments (26). Further studies have revealed the formation of lactic acid in dairy products and molasses, a process mediated by the bacterium *Lactobacillus plantarum* (27, 28). Changing the environments including varying the pH and the nature of the substrates were shown to optimize the production of highest amount of lactic acid (27, 28).

Another common example is *Arabidopsis thaliana*, which produces huge amounts of phosphatase as an adaptation to phosphate starvation (29). This could be explained due to the phosphate mobilization in the metabolism of reactive oxygen species in stressed or senescent parts of the plant. Indeed, adaptation to metal-contaminated environments lead to favorable microbial associations that are very prominent in bioremediation processes. Certainly plenty of microbial organisms isolated from extreme environments are utilized in numerous industrial processes. The aim of these adaptations is to help assist the generation and secretion of desired products (30, 31). Studies were shown how *Pseudomonas fluorescens* adapted to multiple metal stressors engineers its metabolic network to increase oxalate production as a common metal chelator (32). This has broad stroke implications in bioremediation strategies (32). Hence, enrichment of certain attributes by natural means is also a common strategy utilized to coach microbes to accomplish specific chosen tasks.
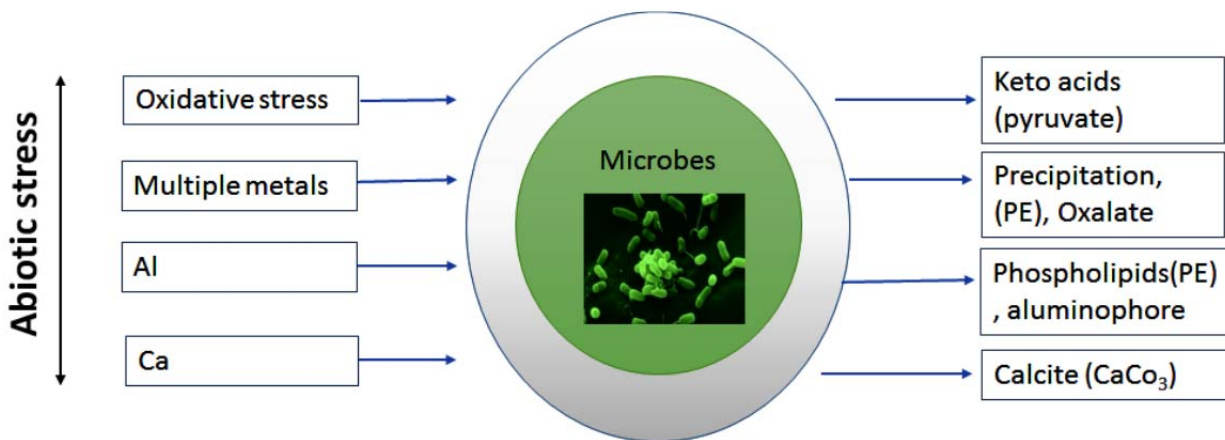
Figure 1.7: Abiotic stress induces microbes to accomplish specific chosen task.

1.6 *Pseudomonas fluorescens*, a potent biotechnological microbe

Pseudomonas fluorescens is a gram-negative, rod-shaped, and non-pathogenic bacterium that is known to thrive mainly in the soil, plants, and water surfaces. Its name stems from its ability to give fluorescent pigments under iron-limiting conditions. It has simple nutritional necessities and can readily grow in mineral media accompanied with numerous carbon sources owing to its versatile metabolism. It has been shown to survive in extreme environments. The adaptation of this microbe creates a unique prominence in biotechnological routes aimed at producing a targeted product. Studies have revealed how *P. fluorescens* increases biofilm production under turbulent conditions. This proves that this microbe alters its metabolism when the nutrients and oxygen were transported via the flow and turbulence (33). Also, *Pseudomonas fluorescens* increases biomass and yielded ajmalicine in *Catharanthus roseus* under drought stress (34). *P. fluorescens* is one of the most promising microbes for use in bioremediation. It has been demonstrated that under multiple metal stress, *P. fluorescens* can modulate its metabolic network to increase the formation of oxalate, as a chelator. Indeed, under oxidative stress, this microbe adapted by accumulating pyruvate, a known keto-acid to detoxify ROS. This was achieved by shutting down enzymes responsible for NADH production, a pro-oxidant and increasing the synthesis of NADPH, an anti-oxidant. This microbe has the ability to adapt to stress by engineering different metabolic networks. Overall, this feature may have enormous industrial applications. Proper mineral nutrition is known to elicit biochemical reconfigurations that may be tapped for commercial value (32).

2. Chapter 2: Thesis objectives

Considering our reliance on petroleum and the growing concern about the environmental penalties due to our heavy dependence on fossil fuels, a substitute and an economically favourable approach is seriously required to diminish our dependence on fossil fuels. Biomass use is an encouraging alternative owing to its abundant accessibility in nature and numerous uses in chemical, fuel and bioplastic engineering. Biodiesel is gaining importance as an alternative fuel of immense economic value. However, the processing of this biofuel contributes to the accumulation of surplus glycerol. The latter has emerged as an important raw material to produce value-added products as it is less expensive and it has the ability to get readily transformed. Metabolic modulation has become the technology of choice in the bioconversion of glycerol as it is economical, environmentally-friendly and creates relatively less by-products. Microorganisms are widely utilized for the fermentation of glycerol. To effectively utilize glycerol as a source of carbon, it is necessary to understand the biological systems capable of producing enzymes, a key participant in the conversion of glycerol into value-added products. Here I plan to nutritionally tailor the soil microbe *P. fluorescens* to generate products of commercial value. Abiotic modulators will be utilized to achieve this goal.

Since oxidative stress is known to perturb the TCA cycle and electron transport chain, the production of energy is severely affected. There is a dearth of understanding related to the stratagem involved in fulfilling the need for ATP under stressed situations. Also, effectors of substrate level phosphorylation and phospho-transfer system in promoting the biosynthesis of ATP have not been fully evaluated. Furthermore, studies in our laboratory have demonstrated the role of metabolic networks and keto acid in combating ROS. Keto acids can accumulate during oxidative stress in numerous organisms. These moieties react with ROS to generate CO_2 and corresponding carboxylic acids. Hence, the biochemical pathways *P. fluorescens* invokes to synthesize ATP and to over-produce pyruvate, a critical metabolite under H_2O_2 stress will be investigated in the presence of glycerol as the sole carbon source.

Micro-nutrients like manganese (Mn) can also stimulate significant metabolic alteration contributing to value-added products. This divalent metal is vital for the ideal activity of numerous enzymes including pyruvate carboxylase (PC), pyruvate kinase (PK), and phosphoenol pyruvate carboxylase (PEPC) that are essential to the metabolism of glycerol. Manganese-dependent enzymes are also a key in combatting oxidative stress and in the metabolic networks elaborating the transformation of carbohydrates. Hence, the ability of this element to remodel metabolic networks aimed at the production of such keto-acids as α-ketoglutarate will be assessed. A functional metabolomic and proteomic approach will be taken to uncover how this microbe can generate value-added products in an environment supplemented with H_2O_2 and Mn respectively. These molecular insights into the conversion of glycerol to value-added products will lay the foundation for the industrial applications of these processes. These abiotic metabolic factors may be readily implemented commercially.

3. Chapter 3: The metabolic reprogramming evoked by ROS to generate valuable products

It is a general misconception that central metabolic networks are static, where as they are quite flexible. Normally, the metabolism of glucose produces 2 ATP and 2 molecules of pyruvate, which are then metabolized through the TCA cycle. The latter produces the reducing agent NADH, which can be utilized to produce ATP for cellular processes. However, ATP production is not the only goal of these metabolic networks. They also help generate metabolites that are crucial for sustaining life. For instance, succinate, a product of TCA cycle is involved in the production of heme while 3-phosphoglycerate resulting from glycolysis can result in the amino acid cysteine and serine (35, 36). Hence, specific pathways can be selectively promoted to obtain desired products from glycerol.

H_2O_2 is known to severely block oxidative phosphorylation and affects enzymes of the TCA cycle. This abiotic stress forces *P. fluorescens* to reprogram its metabolic networks in order to counter the toxicity of the oxidant. This metabolic adaptation resulted in enhanced production of pyruvate, PEP and ATP.

Metabolic networks to generate pyruvate, PEP and ATP from glycerol in *Pseudomonas fluorescens*

(Original research)

Azhar Alhasawi, Sean C. Thomas and Vasu D. Appanna*

(Published in Enzyme and Microbial Technology)

Abstract

Glycerol is a major by-product of the biodiesel industry. In this study we report on the metabolic networks involved in its transformation into pyruvate, phosphoenolpyruvate (PEP) and ATP. When the nutritionally–versatile *Pseudomonas fluorescens* was exposed to hydrogen peroxide (H_2O_2) in a mineral medium with glycerol as the sole carbon source, the microbe reconfigured its metabolism to generate adenosine triphosphate (ATP) primarily via substrate – level phosphorylation (SLP). This alternative ATP-producing stratagem resulted in the synthesis of copious amounts of PEP and pyruvate. The production of these metabolites was mediated via the enhanced activities of such enzymes as pyruvate carboxylase (PC) and phosphoenolpyruvate carboxylase (PEPC). The high energy PEP was subsequently converted into ATP with the aid of pyruvate phosphate dikinase (PPDK), phosphoenolpyruvate synthase (PEPS) and pyruvate kinase (PK) with the concomitant formation of pyruvate. The participation of the phospho-transfer enzymes like adenylate kinase (AK) and acetate kinase (ACK) ensured the efficiency of this O_2-independent energy-generating machinery. The increased activity of glycerol dehydrogenase (GDH) in the stressed bacteria provided the necessary precursors to fuel this process. This H_2O_2-induced anaerobic life-style fortuitously evokes metabolic networks to an effective pathway that can be harnessed into the synthesis of ATP, PEP and pyruvate. The bioconversion of glycerol to pyruvate will offer interesting economic benefit.

pyruvate carboxylase (PC), phosphoenolpyruvate carboxylase (PEPC), phosphoenolpyruvate synthase (PEPS), pyruvate orthophosphate dikinase (PPDK), reactive oxygen species (ROS), reduced nicotinamide adenine dinucleotide phosphate (NADPH), tricarboxylic acid (TCA).

Introduction

Metabolism is pivotal for the maintenance of life. It enables organisms to grow, produce energy, communicate, and repair damage. Adaptation is crucial if an organism is to survive adverse environmental conditions like salt, oxidative, metal and temperature stress. Metabolic reconfiguration is a key adaptive strategy living systems invoke to counter the fluxes in their environments (36-38). When confronted with osmotic stress, some organisms are known to enhance the formation of Fe-S clusters and acidic amino acids (39). While gallium toxicity stimulates the production of NADPH, oxalate synthesis is promoted to nullify the burden of aluminum (Al) over-load (40, 41). Manganese has been shown to elicit enhanced production of an exopolysaccharide, a moiety involved in metal sequestration (42).

As aerobic organisms are constantly exposed to oxidative stress, they have evolved intricate systems to adapt to this situation. Superoxide dismutase is used to neutralize the highly reactive superoxide (O_2^-) while catalase helps neutralize H_2O_2 (43, 44). Other important enzymes that orchestrate the production of the anti-oxidant NADPH are malic enzyme (ME), glucose-6-phosphate dehydrogenase, nicotinamide adenine dinucleotide kinase (NADK), and NADP-dependent isocitrate dehydrogenase (45-48). The role of ketoacids in countering the oxidative burden via their reaction with reactive oxygen species (ROS) is also known (41). These metabolites decompose ROS with the concomitant formation of the corresponding carboxylic acid and CO_2. For instance, pyruvate reacts with H_2O_2 with the concomitant formation of acetate by non-enzymatic decarboxylation (41). Oxidative stress is also known to severely impair

20

oxidative phosphorylation (OP), a process that produces ATP in an O_2-dependent manner. Disparate enzymes that participate in this network, need Fe-S and heme clusters that are rendered ineffective by ROS (49). Although, the detoxification mechanisms responsible for the elimination of ROS have been well-studied, there is a dearth of information on how ROS-tolerant microbes satisfy their ATP requirements. Substrate level phosphorylation (SLP) is the other ATP-producing machine that is commonly utilized by biological systems in oxygen-limited environments. High energy compounds that are obtained following various biochemical transformations help phosphorylate adenosine monophosphate (AMP) and/or adenosine diphosphate (ADP) into ATP (50). PEP and succinyl CoA are two metabolites that can be readily converted into ATP (51-52). While pyruvate kinase mediates the transformation of PEP into ATP in the presence of ADP (53), succinyl CoA synthetase is responsible for the conversion of succinyl CoA into nucleoside triphosphates (52).

As part of our efforts to decipher the metabolic adaptations and uncover the biotechnological potential of the nutritionally-versatile soil microbe *Pseudomonas fluorescens,* (54), we have subjected this organism to H_2O_2 stress in a mineral medium with glycerol as the sole carbon source. The biodiesel industry is eagerly seeking bioprocesses that will convert this waste into valuable products, a feature that will contribute to its profitability. In this study, we demonstrate the ability of the microbe to produce elevated levels of PEP and pyruvate while fulfilling its energy need via substrate-level phosphorylation. This H_2O_2-induced metabolic shift aimed at ATP production, limiting the synthesis of NADH, a pro-oxidant and augmenting the formation of the anti-oxidant NADPH also provides a route to value-added products from glycerol.

Material and methods

Microbial growth conditions and isolation of cellular fractions

The bacterial strain *Pseudomonas fluorescens* 13525 was purchased from American Type Culture Collection (ATCC) and cultured in a mineral medium containing (per liter of deionized water) Na_2HPO_4 (6.0 g); KH_2PO_4 (3.0 g); $MgSO_4$ (0.2 g) and NH_4Cl (0.8 g). Trace elements (1 ml) were added as previously described (55). The pH was adjusted to 6.8 with 2 N NaOH. The media were dispensed in 200 ml aliquots in 500 ml Erlenmeyer flasks and autoclaved before inoculation. Glycerol (10%; v/v; 1.37 M) was added as sole source of carbon (Sigma Aldrich, Oakville, Canada). Hydrogen peroxide (H_2O_2) (500 µM) was utilized for oxidative stress as this concentration is known to elicit the optimal anti-oxidative response in this organism (41, 46). The media were then inoculated with 1 ml of stationary-phase cells (450 µg protein equivalent) of the control culture .The cultures were incubated at 26°C in a gyratory water bath shaker. To keep the level of ROS constant a second dose of H_2O_2 was introduced 30 hours after incubation. The level of H_2O_2 in medium was monitored as described in (56). Cells from glycerol (control) and H_2O_2– containing cultures were isolated at similar growth phases for analysis (40 h for control cells and 60 h for H_2O_2–stressed cells). *P. fluorescens* cells were harvested by centrifugation at 10,000 x g for 15 min at 4°C. The supernatant was removed and the pellet was washed with 0.85% NaCl. These cells were then re-suspended in a cell storage buffer (pH 7.3) consisting of 50 mM Tris-HCl; 5 mM $MgCl_2$ and 1mM phenylmethylsulfonylfluoride (PMSF). These were ruptured via sonication with a Brunswick sonicator for 15 seconds at 4 intervals. The power level was set at 4 and the samples were kept on ice. The unbroken cells were removed at 10,000 x g. Centrifugation at 180,000 x g for 3 hours at 4^oC yielded a soluble fraction, and a membrane pellet (57). The Bradford assay was performed in triplicate to determine the protein concentration of both fractions (58).

Metabolite analysis

Metabolite levels were analyzed using high performance liquid chromatography (HPLC). Cells were grown in control and H_2O_2-stressed conditions. At similar growth phases the cells were isolated and disrupted via sonication as described previously (36). Soluble fractions were boiled immediately for 10 min to precipitate proteins before analysis. Samples of spent fluid and cell free extract (CFE) were injected into an Alliance HPLC equipped with a C18 reverse-phase column (Synergi Hydro-RP; 4μm; 250 x 4.6mm, Phenomenex) operating at a flow rate of 0.7 ml/min at ambient temperature as described in (36). Briefly, the mobile phase consisting of 20 mM KH_2PO_4, (pH 2.9) was utilized to separate organic acids. Select metabolites were detected with the aid of known standards, and peaks were quantified with the aid of the Empower software (Waters Corporation) (36). To monitor the metabolism of glycerol, 2 mg/mL protein equivalent of soluble CFE was incubated for 30 min in reaction buffer containing 2 mM glycerol, 1 mM AMP, Pi. The reactants and products were followed by HPLC. To evaluate the biotechnological potential, the whole cells (2 mg protein equivalent) obtained at the same phase of growth were incubated in the glycerol media without NH_4Cl for 6h. The consumption of glycerol and the formation of pyruvate were monitored.

Enzyme activities in metabolic networks aimed at generating ATP, pyruvate and PEP

Blue native (BN) polyacrylamide gel electrophoresis (PAGE) was performed as described in (52, 59). Briefly, 60 micrograms of proteins were loaded into each well and electrophoresed under native conditions. The blue cathode buffer (50 mM Tricine, 15 mM Bis-Tris, 0.02% (w/v) Coomassie G-250 (pH 7) at 4°C) was used to help visualizing the running front and was substituted by a colourless cathode buffer (50 mM Tricine, 15 mM Bis-Tris, pH 7

at 4°C).Upon completion, the gel was equilibrated in reaction buffer for 15-30 min and visualization of enzyme activity was determined by associating the formation of NAD(P)H to 0.2 mg/mL of phenazine methosulfate (PMS) and 0.4 mg/mL of iodonitrotetrazolium (INT), or by coupling the formation of $NAD(P)^+$ to 16.7 μg/mL, 2,6-dichloroindophenol (DCPIP) and 0.4 mg/mL INT. Complex I was detected by the addition of 5 mM KCN, 5 mM NADH and 0.4 mg/mL INT while 20 mM succinate, 1 mM FAD, 5 mM KCN, 0.2 mg/mL of PMS and 0.4 mg/mL of INT was utilized as the visualizing medium for Complex II. Complex IV was assayed by the addition of 10 mg/mL of diaminobenzidine, 10 mg/mL cytochrome C, and 562.5 mg/mL of sucrose. Isocitrate dehydrogenase (ICDH-$NADP^+$ or NAD^+) activity was tracked with reaction mixture containing 5 mM isocitrate, 0.5 mM $NADP^+$ or NAD^+, 0.2 mg/mL PMS and 0.4 mg/mL INT. For malic enzyme, the gel was incubated in equilibrium buffer consisting of 5 mM malate, 0.5 mM $NADP^+$, 0.2 mg/ml PMS and 0.4 mg/ml INT. The activity of glucose 6 phosphate (G6PDH) gel was revealed in buffer system consisting of 5 mM glucose 6-phosphate, 0.5 mM $NADP^+$, 0.2 mg/ml PMS and 0.4 mg/ml INT. Glycerol dehydrogenase (GDH) was also incubated in reaction buffer consist of 5 mM glycerol, 0.5 mM NAD^+, 0.2 mg/mL PMS and 0.4 mg/mL INT. Glycerol-3 phosphate dehydrogenase (G3PDH) was assayed by the addition of glycerol 3 phosphate, NAD^+, 0.2 mg/ml PMS and 0.4 mg/ml INT. The activities of PEPC, PK, PEPS and PPDK were imaged as described previously (54). The activity of acetate kinase (ACK) and adenylate kinase (AK) were examined with the aid of an enzyme-coupled procedure including hexokinase and glucose-6-phosphate dehydrogenase (53, 60).

A destaining solution (40% methanol, 10% glacial acetic acid) was utilized to stop the reaction once the activity bands had reached the desired intensity. Reactions performed without the addition of a substrate or cofactor or inhibitor in the reaction mixture ensured the specificity of

the enzymes. Furthermore, select activity bands were excised and incubated in appropriate reaction buffer and monitored by HPLC to confirm the nature of the enzyme. Densitometry was performed using Image J for Windows. Spectrophotometric data for ICDH-NAD$^+$ was obtained by incubating 1 mg of membrane CFE from control and H$_2$O$_2$-treated cells with 2 mM isocitrate and 0.5 mM NAD$^+$ for 3 min. NADH production was monitored at 340 nm. For malate dehydrogenase (MDH), malate was used as substrate while NAD-dependent glycerol dehydrogenase was monitored with the aid of 2 mM glycerol. The membrane CFE was given 2 mM pyruvate, 0.5 mM ATP or Pi, 0.5 mM HCO$_3^-$, 10 units of MDH and 0.5 mM NADH to study pyruvate carboxylase (PC) activity. Negative controls were performed without the substrates or cofactors (46). Glycerol was monitored colorimetrically as described (61).

Statistical analysis

Data were expressed as means ± standard deviations (SD). All experiments were accomplished at least twice and in triplicate.

Results and Discussion

Cellular growth, metabolite distribution and NADPH-generating enzymes

Pseudomonas fluorescens was able to proliferate in a mineral medium with 10% glycerol. Although in the presence of H$_2$O$_2$ the growth rate was slower, at stationary phase of growth the cellular yield was similar to that observed in the control cultures (Figure 3.1A). There was a marked variation in the metabolite levels in these cultures. While the spent fluid from the H$_2$O$_2$ culture had higher levels of pyruvate and acetate, the cell-free extract were characterized by prominent peaks attributable to PEP, AMP and ATP (Figure 3.1B, C). Only 7.0% of the initial

H$_2$O$_2$ was detected after 60 h of growth. To adapt to the oxidative stress triggered by H$_2$O$_2$, the microbe appeared to have enhanced metabolic pathways aimed at NADPH production. There was a sharp increase in activities of such enzymes as G6PDH, ME and ICDH-NADP$^+$. Three isoenzymes of G6PDH were evident in the in-gel activity assay. There was a 3-fold increase in the activity of ME (Figure. 3.2A). However, a slight increase in the activity of MDH was observed (Table 3.1A).
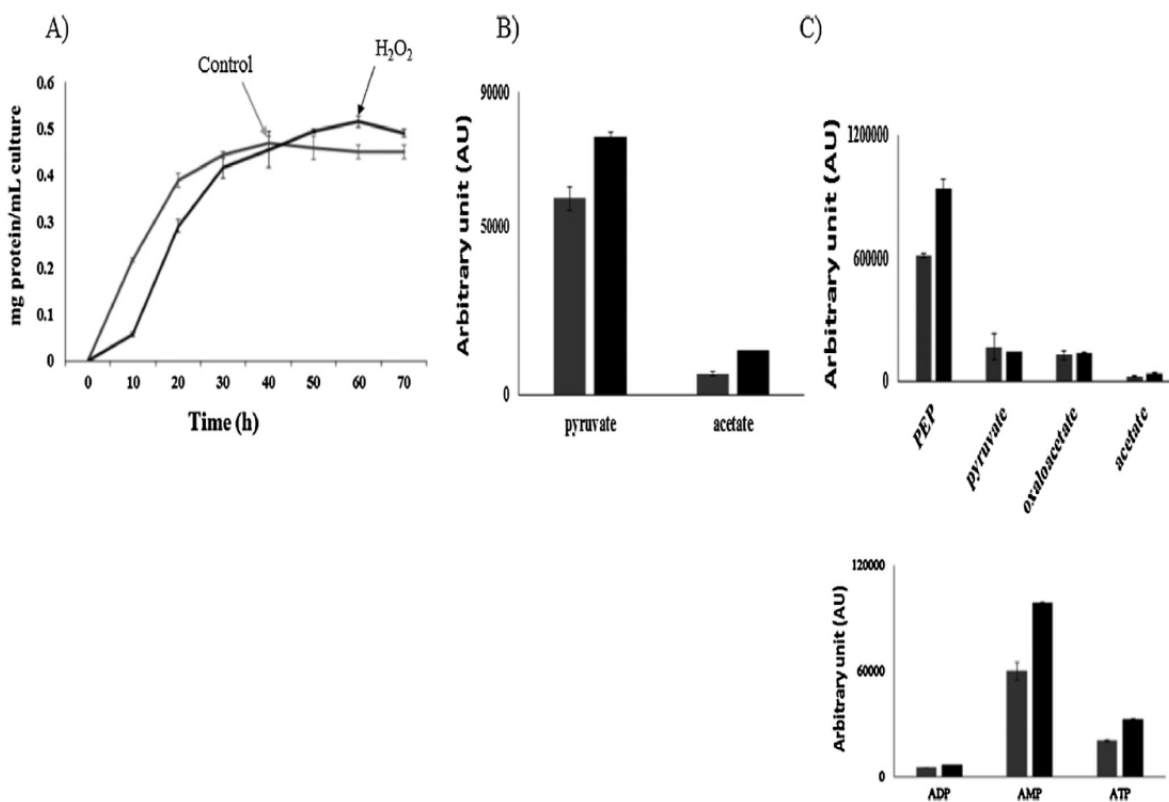
Figure 3.1: Cellular growth in glycerol medium of *Pseudomonas fluorescens* and metabolite analysis.

Growth profile of *Pseudomonas fluorescens* grown in 10 % of glycerol media as the only source of carbon. The black curve indicates stressed *Pseudomonas fluorescens* whereas the grey curve indicates the growth of a control culture. B) HPLC analyses of select metabolites in spent fluid. C) HPLC analysis of soluble CFE from control and H$_2$O$_2$-challenged cells and nucleotides in the CFE obtained from control and stressed cells. (Cells were obtained at stationary growth phase) (n=3).

Table 3.1 Enzyme activities monitored by spectrophotometric assay

Enzymes	Ctl	Stress
NAD+-dependent isocitrate dehydrogenase [a]	0.42±0.03	0.32±0.01
Malate dehydrogenase [a]	0.50±0.04	0.69±0.01
NAD+-dependent glycerol dehydrogenase [a]	0.072±0.04	0.37±0.06
Pyruvate carboxylase [b]	0.71±0.02	0.92±0.08

[a] μmol NADH produced min^{-1} mg protein^{-1} as monitored at 340 nm (n = 3 ±standard deviation).

[b] μmol NADH consumed min^{-1} mg protein^{-1} as monitored at 340 nm (n = 3 ±standard deviation).

TCA cycle enzymes, electron transport chain, and metabolite synthesis

The presence of H_2O_2 in the medium led to a drastic reduction in the tricarboxylic acid (TCA) cycle enzymes and the electron carrier proteins responsible for oxidative phosphorylation. Complex I, II, IV and ICDH-NAD$^+$ were barely evident in the BN-PAGE analyses (Figure 3.2B, Table 3.1). The degradation of glycerol in the stressed cells was mediated via GDH-NAD$^+$ as this enzyme had increased activity (Figure. 3.2C, Table 3.1). The control cells were characterized with increased activity of the glycolytic enzyme G3PDH (Figure 3.2C). To evaluate how the organism was producing ATP, the soluble CFE was incubated with glycerol, AMP and Pi. Approximately a 2-fold increase in ATP level was detected in the CFE extract from the stressed cells (Figure 3. 2D).
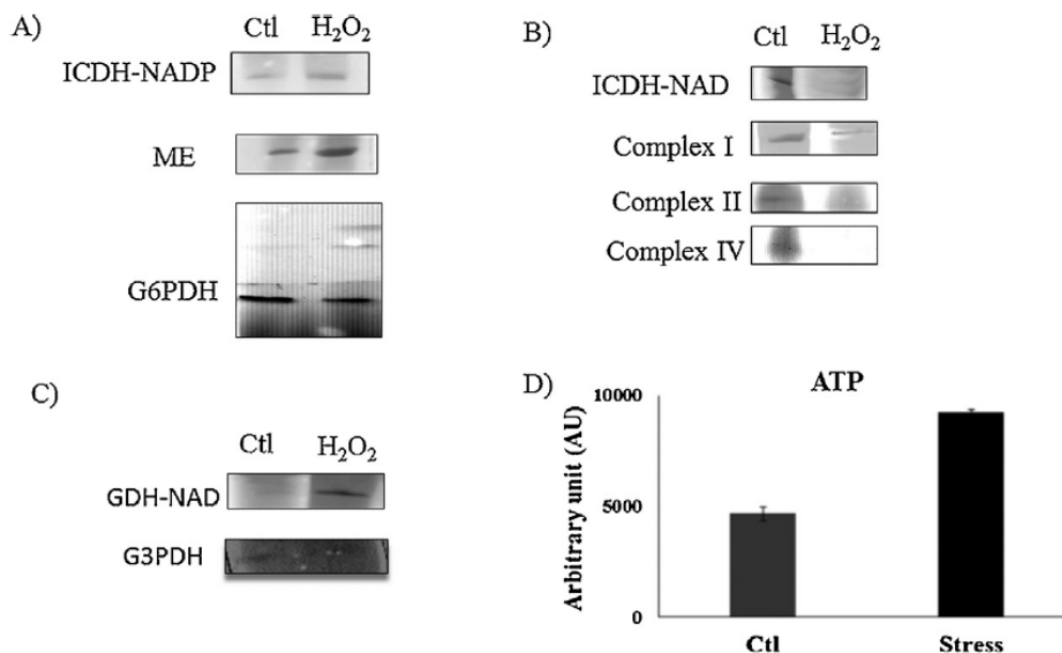
Figure 3.2: NADPH-producing enzymes, oxidative metabolism and glycerol metabolism.

In-gel activity: NADP-dependent isocitrate dehydrogenase (ICDH-NADP$^+$) and Malic enzyme (ME) and glucose 6-phosphate dehydrogenase (G6PDH). B) Select TCA cycle and oxidative phosphorylation enzymes (ICDH-NAD$^+$ and Complex I, II, IV). C) In-gel enzymatic activities of glycerol dehydrogenase (GDH), glycerol 3 phosphate dehydrogenase (G3PDH) from control and H$_2$O$_2$-stress cells. D) HPLC analysis of CFE treated with 2 mM glycerol, 0.5 mM Pi and 1mM AMP for 30 min. Gels are representative of 3 independent experiments. Ctl = Control; H$_2$O$_2$-treated. Gels are representative of 3 independent experiments. The black graph indicates stressed *Pseudomonas fluorescens* whereas the grey graph indicates the metabolites of a control culture.

Oxaloacetate that was generated by the increased activity of PC in the stressed cells was converted to PEP by PEPC, a process that does not necessitate high energy phosphate. In the control cultures the ATP-utilizing PEPCK was preferentially utilized in the synthesis of PEP (Figure. 3.3A). The PC activity band yielded more oxaloacetate upon incubation with pyruvate, HCO$_3^-$ and either ATP or Pi. Phosphoenol pyruvate was the metabolite of choice utilized by H$_2$O$_2$-stressed *P. fluorescens* to produce ATP as the TCA cycle and OP were severely impeded. Both PPDK and PEPS that require PPi and Pi respectively to generate ATP from AMP and PEP

were upregulated in the stressed cultures (Figure 3.3B, Table 3.1). Two isoenzymes of PEPS were evident in the soluble CFE isolated from H_2O_2-challenged bacteria. When the CFE was incubated with oxaloacetate, AMP and PPi, approximately 2-fold more ATP was produced compared to the control (Figure 3.3C).

Since acetate is a metabolite generated as a consequence of the interaction of pyruvate with ROS, it was important to decipher how this carboxylic acid was aiding in the ATP-generating network. Acetate kinase (ACK), an enzyme that mediates the conversion of acetate into acetate phosphate with the concomitant formation of ADP for ATP was increased in activity in the stressed cells (Figure 3.3D). The ADP from the reaction was a ready source of AMP, a process catalyzed by adenylate kinase. This enzyme aids in the transformation of ADP into AMP and ATP. Its activity was elevated in the stressed cells (Figure 3.3D). As the CFE extract from the stressed cells produced copious amounts of PEP, it was important to evaluate the ability of the intact cells to produce value-added metabolites from glycerol. After 6 h of incubation, the intact cells from the stressed cells produced approximately 3-fold more pyruvate in the spent fluid compared to the control (Figure 3.4A). Relatively more glycerol was consumed in the stressed cells compared to the control. After 6h of incubation, the stressed whole cells consumed 70% of the initial glycerol while the control cells utilized only 60% as monitored colorimetrically.
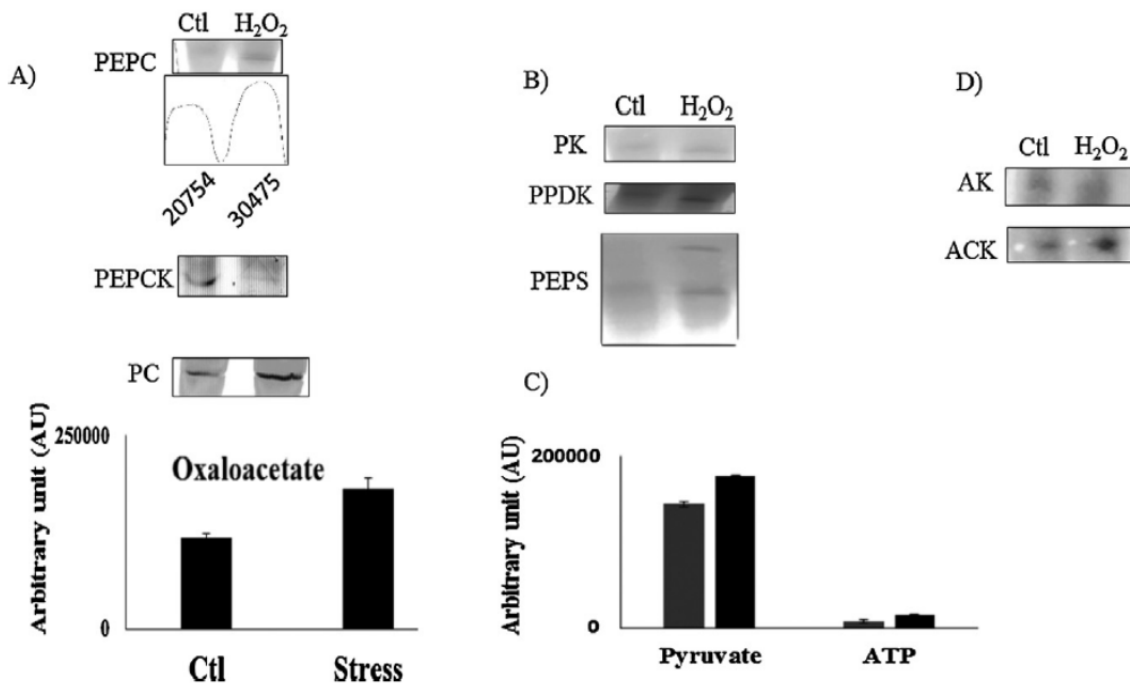
Figure 3.3: Phosphoenol pyruvate and ATP-producing system under oxidative stress.

A) In-gel activity of phosphoenolpyruvate carboxylase (PEPC), phosphoenolpyruvate carboxylase kinase (PEPCK), Pyruvate carboxylase (PC) and HPLC analysis of cut band reaction of pyruvate carboxylase (PC) and oxaloacetate production for 30 min. B) In-gel activity of pyruvate kinase (PK), pyruvate orthophosphate dikinase (PPDK) and phosphoenolpyruvate synthase (PEPS). C) HPLC analysis of CFE treated 2 mM oxaloacetate, 0.5 mM PPi and 1mM AMP for 30 min. D) In-gel activity of acetate kinase (ACK) and adenylate kinase (AK). Gels are representative of 3 independent experiments. Ctl = Control; H_2O_2-treated. Densitometry was performed using Image J for windows.

Discussion

Metabolic networks to produce ATP, PEP and pyruvate from glycerol

The foregoing data reveal that *P. fluorescens* evokes the participation of an elaborate metabolic network aimed at fulfilling its requirement in ATP in a condition that severely impedes the TCA cycle and oxidative phosphorylation. As expected the enzymes participating in these processes are down-regulated while those in the synthesis of the anti-oxidant, NADPH are

upregulated in activities (46, 47). The production of PEP is key to this strategy as this high energy moiety is eventually fixed into the universal energy currency, ATP The upregulation of PEPC and PC provide an effective route to PEP as these enzymes use Pi instead of ATP in this process. The participation of PPDK and PEPS in the subsequent reactions affords a very economic means of producing ATP. These enzymes require as cofactor PPi, Pi and AMP only (53, 60), unlike PK, the commonly utilized phosphorylating enzyme during glycolysis, ADP is not involved in this reaction. In this instance, the ADP generated from the interaction of ACK with acetate and ATP, is converted to ATP and AMP by AK, an enzyme with increased activity in the stressed cells. This interplay amongst these enzymes ensures that this metabolic network is fine-tuned for ATP production in the microbial system with an ineffective oxidative phosphorylation.

The necessity to produce ATP by this alternative metabolic module provides a unique route to PEP and pyruvate. Indeed, the cell-free extract was able to generate high amounts of PEP while the intact cells were more apt at secreting pyruvate in spent fluid following the utilization of glycerol (Figure. 3.4A). Glycerol is an important by-product of the biodiesel industry (62, 63). Hence, the ability of this microbial system to generate these two value-added metabolites can be optimized into a commercial process aimed at the increasing the profitability of the biodiesel production (Figure 3.4B). In conclusion, these results show that *P. fluorescens* is a potent biofactory that can be exploited to generate value-added products from glycerol. Its capacity to reconfigure its metabolic networks to counter the challenge posed by H_2O_2, reveals very effective biotechnological routes to produce ATP, pyruvate and PEP.
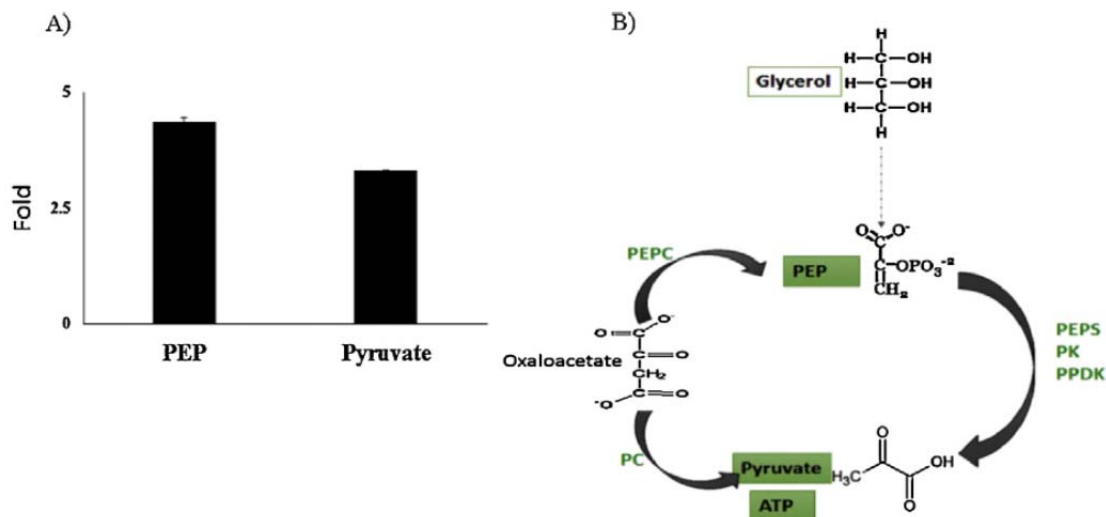
Figure 3.4: Value-added product formation in stressed *P. fluorescens*.

A) (Pyruvate production in whole cells after 6 h and PEP production in soluble CFE after 30 min compared to control). Note: (70% and 60% of glycerol were consumed in the stressed and control cells respectively, SD±2.0%, n=3). B) Scheme depicting the production of pyruvate, PEP and ATP from glycerol in *P. fluorescens.*

Conflict of Interest

All authors declare that they have no conflict of interest.

4. Chapter 4: Metabolic engineering triggered by manganese results in the production of α-ketoglutarate

Manganese (Mn) is one of the most crucial micronutrients necessary for all organisms, including humans, animals, plants and microbes. It plays a vital role in numerous biological processes required for normal growth, development and cellular homeostasis (64). In addition, this divalent metal is essential for normal immune function, adenosine triphosphate (ATP) regulation, bone growth and digestion. It is an important component for several enzymatic reactions comprising the synthesis of amino acids, proteins, lipids and carbohydrates (65). Mn is the component of metalloenzymes including manganese superoxide dismutase (Mn-SOD), arginase and pyruvate decarboxylase. The latter is responsible to add CO_2 to pyruvate with the associated formation of oxaloacetate- uses ATP as the co-factor.

In this chapter, the data point to the ability of *P. fluorescens* to produce ketoglutarate (KG) from glycerol in the presence of Mn. The metabolic reprograming provoked by the interaction of the microbe with Mn exposes a stimulating approach of how microbial systems can be trained to accomplish a preferred commercial job. The overexpression in the activities of such Mn-dependent enzymes as PC, PPDK and PEPC offers an active route to oxaloacetate and ATP. Oxaloacetate is an important precursor of KG, a value-added product that was made easily accessible due the enhanced activities of transaminases and ICDH. The metabolic alteration provoked by Mn represents a facile opportunity to program microbes aimed at producing metabolites of commercial value.

Manganese orchestrates a metabolic shift leading to the increased bioconversion of glycerol into

α-ketoglutarate.

(Original research)

Azhar A. Alhasawi and Vasu D. Appanna*

(Published in Aims Bioengineering)

Alhasawi A, Appanna VD (2017) Manganese orchestrates a metabolic shift leading to the

increased bioconversion of glycerol into α-ketoglutarate. Aims bioengineering. 2017,

4(1): 12-27.

Abstract

Glycerol is a major by-product of the biodiesel industry and its transformation into value-added products is an ongoing technological challenge. Here we report on the ability of the nutritionally-versatile *Pseudomonas fluorescens* to synthesize copious amount of α-ketoglutarate (KG) in a glycerol medium supplemented with manganese (Mn). The enhanced production of this keto-acid was mediated by the increased activities of isocitrate dehydrogenase (ICDH)-(NAD)P dependent and aminotransaminases. At stationary phase of growth when the optimal quantity of KG was recorded, these enzymes exhibited maximal activities. Two isoforms of pyruvate carboxylase (PC) that were identified in the Mn-treated cells provided an effective route for the synthesis of oxaloacetate, a metabolite critical in the production of KG. Furthermore, the increased activities of phosphoenol pyruvate carboxylase (PEPC) and pyruvate orthophosphate dikinase (PPDK) ensured the efficacy of this KG-generating metabolic system by supplying pyruvate and ATP from the oxaloacetate synthesized by PC. Mn-exposed whole cells converted 90% of industrial glycerol into KG. This Mn-evoked metabolic network can be optimized into the economic transformation of glycerol into KG.

Keywords: Bioconversion; glycerol; α-ketoglutarate; manganese; pyruvate carboxylase; metabolic networks

List of abbreviations: Manganese (Mn), α-ketoglutarate (KG), cell free extract (CFE), isocitrate dehydrogenase (ICDH), pyruvate carboxylase (PC), phosphoenolpyruvate carboxylase (PEPC), pyruvate orthophosphate dikinase (PPDK), pyruvate kinase (PK), tricarboxylic acid (TCA), aspartate aminotransferase (AST), glycine transaminase (GT), glutamate dehydrogenase (GDH), aconitase (ACN) and spent fluid (SF).

Introduction

The search for renewable energy triggered by environmental concerns and the finite nature of oil reserves have propelled scientists to seek alternative technologies aimed at transforming biomass into fuels (66,67). Bio-based processes are the most widely utilized technology in the generation of such combustible energy sources as ethanol, butanol and propanol (68). Microbial systems have been tailored to produce these fuels from plant-derived biomass like starch or cellulose (69, 70). In this instance, following the liberation of glucose, a reaction mediated by the enzyme amylase or cellulase, the monosaccharide is subsequently converted to the desired end product. The enhanced formation of the intermediary metabolites like pyruvate, acetate and acetyl CoA is critical to the economic success of these microbial nano-factories (71, 72). The liberation of energy-rich gases H_2 and CH_4 from biomass is another avenue being pursued to satisfy the global need for clean energy as is the production of biodiesel (73, 74).

In the biodiesel industry, plant or animal-derived triglycerides are the starting material that are converted to fatty acids. These fatty acids can then be either esterified or decarboxylated to hydrocarbons and utilized as fuels. One of the major draw-back of the biodiesel industry is the generation of glycerol as a by-product (75). Indeed approximately 10% (w/w) of this trihydroxylated moiety is released and it is projected that this problem will exacerbate as the global demand for biodiesel increases. Hence, it is critical that this waste product be converted into value-added commodities if the biodiesel industry is to be economically viable. Currently, chemicals such as propane 1,3-diol, succinic acid and citric acid are among some of the microbially-mediated products that are synthesized (18, 62, 76).

In this study we have utilized the metabolically-versatile soil microbe *Pseudomonas fluorescens* to transform glycerol into KG. Metabolic engineering is an important strategy that can aid in fine-tuning the precise molecular pathways responsible for the transformation of this trihydroxy alcohol into products of economic significance. Although genetic manipulation may be utilized to modulate metabolic activities in order to induce the formation of a desired metabolite, micro-nutrients like manganese can also promote significant metabolic shift leading to value-added products (77-78). This divalent metal is required for the optimal activity of a variety of enzymes including pyruvate carboxylase (PC), phosphoglyceromutase (PG), pyruvate kinase (PK), and phosphoenol pyruvate carboxylase (PEPC) that are central to the metabolism of glycerol (79, 80). Manganese-dependent enzymes are also pivotal in combatting oxidative stress and in the metabolic networks involved in the transformation of carbohydrates (81, 82). In fact, the ability of this element to promote exopolysaccharide production in micro-organisms has been attributed to its close ionic similarity to magnesium, an avid cation for monosaccharides and their phosphorylated derivatives (42). Some microbes have been shown to produce KG, a metabolite of significant industrial applications from different carbon sources (83). However, this is the first demonstration of ability of Mn to elicit a metabolic reconfiguration resulting in the enhanced formation of this dicarboxylic acid from industrial glycerol. Here we report on the influence of this divalent metal on glycerol metabolism in *P. fluorescens* and on various enzymes responsible for enhanced synthesis of KG. The metabolic pathways mediating the fixation of the trihydroxy alcohol into oxaloacetate and its eventual conversion into KG are delineated. Furthermore, the effectiveness of the Mn-evoked transformation of industrial glycerol into this keto-acid by intact microbial cells is also discussed.

Materials and methods

Bacterial culturing techniques and biomass measurement

The bacterial strain *Pseudomonas fluorescens* 13525 from American Type Culture Collection (ATCC) was grown in a mineral medium containing (per liter of deionized water) Na_2HPO_4 (6.0 g); KH_2PO_4 (3.0 g); NH_4Cl (0.8 g); and $MgSO_4$ (0.2 g). Trace elements (1 mL) were added as previously described (55, 84-86). The pH was adjusted to 6.8 with the addition of 2 N NaOH.   Glycerol (10% v/v: 1.37 M) from Sigma Aldrich (Oakville, Canada) was added to the medium as the sole source of carbon. Prior to inoculation, the media were dispensed in 200 mL aliquots in 500 mL Erlenmeyer flasks. Various concentrations of $MnCl_2$ ranging from 25 μM to 1 mM were utilized to optimize the conditions for maximal production of KG. The media were inoculated with 1 mL of stationary phase cells (450 μg protein equivalent) of the control culture and were then incubated at 26∘C in a gyratory water bath shaker, model 76 (New Brunswick Scientific) at 140 rpm. Cells were harvested at different time intervals by centrifugation at 10000 x g for 20 min. The bacterial pellets were treated with 1 mL of 1 N NaOH and the biomass was measured with the aid of the Bradford assay (58). The spent fluid (SF) was analyzed by a variety of techniques. All comparative studies were done with cells at the same growth phases i.e. 40 h for the controls and 48 h for the Mn-treated cells.

Regulation experiments and Cellular fractionation

To confirm if the metabolic changes were indeed induced by the addition of Mn, control cells were added to Mn-treated media while cells isolated from the Mn cultures were incubated in control media. To afford an accurate comparison, these cells were gathered at the same growth phase. Following their incubation at 26°C for 6 h in a gyratory water bath, the cells were harvested as aforementioned. The cellular fractions were isolated by centrifugation and assayed

for select enzymatic activities. The spent fluid was removed for further analysis and the pellet was washed with 0.85 % NaCl (10 mL). Cells were then resuspended in a cell storage buffer (pH 7.3) containing (50 mM Tris–HCl; 5 mM MgCl$_2$ and 1 mM phenylmethylsulfonylfluoride (PMSF) and disrupted by sonication using a Brunswick Sonicator on power level 4 for 15 sec 4 times and with 5 min pauses. To obtain the cell free extracts [(CFE) soluble and membranous fractions], cells were centrifuged for 3 h at 180,000 x g at 4 $^{\circ}$C. Unbroken cells were initially removed by centrifugation at 10000 x g for 20 min. The Bradford assay was performed in triplicate to determine the protein concentration of both fractions using bovine serum albumin (BSA) as the standard (58).

Metabolite analysis

Metabolite levels were monitored by high performance liquid chromatography (HPLC). Soluble cell free extract (CFE) was taken immediately in order to minimize any degradation and then boiled for 10 min to precipitate proteins before analysis. Quenching with 60% methanol afforded similar results (56). Samples of spent fluid and CFE were injected into an Alliance HPLC equipped with a C18 reverse-phase column (Synergi Hydro-RP; 4 μm; 250 x 4.6 mm, Phenomenex) operating at a flow rate of 0.7 mL/min at ambient temperature and Waters dual absorbance detector were utilized as described in (56). Activity bands obtained by electrophoresis were excised from the gel and placed in a reaction mixture containing 2 mM substrates. After 30 min of incubation, 100 μL of the sample was removed and diluted with Milli-Q water for HPLC analysis. Mobile phase containing 20 mM KH2PO4 (pH 2.9) was used at a flow rate of 0.7 mL/min at ambient temperature to separate the substrates and products, which were measured at 210 nm to detect carbonyl groups and 280 nm to identify nucleic acids. To ensure the metabolite identity biological samples were spiked with known standards, and

peaks were quantified using the Empower software (Waters Corporation). In order to assess the biotechnological potential, the whole cells (4 mg protein equivalent) collected at the same phase of growth were incubated in 10 % glycerol (commercial and industrial, ROTHSAY biodiesel company, Ontario, Canada) media devoid of NH_4Cl for various times (0 h, 3 h, 6 h and 24 h) and the production of KG was monitored both by HPLC and the 2, 4 dinitrophenyl hydrazine (DNPH) assay (87). The consumption of glycerol was monitored colorimetrically as described (61).

Spectrophotometric analysis of various enzymes and α-ketoglutarate determination assay

Spectrophotometric data for ICDH-NAD/NADP activity were achieved by incubating 0.1 mg protein equivalent of membrane or soluble CFE from control and Mn-treated cells in reaction buffer containing (25 mM Tris-HCl, 5 mM $MgCl_2$, pH 7.4) with 2 mM isocitrate. NAD or NADP (0.5 mM) was utilized as the cofactor and the reaction mixtures were monitored for 3 min for NAD(P)H production at 340 nm. Negative controls were accomplished without the substrates or cofactors. The activity of aconitase (ACN, EC 4.2.1.3) was determined in the soluble fractions of the CFE. Tricarballylic acid (10 mM), a citrate analogue was added to the whole cells prior to cellular disruption to ensure the stability of this enzyme (49). The assay consisted of activity buffer (25 mM Tris-HCl, 5 mM $MgCl_2$, pH 7.4), 10 mM substrate (citrate) and 200 μg/mL soluble protein. The reaction was monitored at 240 nm for the formation of cis-aconitate as previously described. Aconitate served as the standard and specific activities were calculated. Blanks were prepared in a similar fashion however, substrate or protein was omitted from the mixture (49).

The carbonyl group of ketoacids were readily measured by DNPH assay (87). Spent fluid obtained from control and Mn-cultures at different time intervals were monitored. Absorbance was measured at 490 nm and concentrations were calculated using α-ketoglutarate as the standard. Following a 10-fold dilution, glycerol concentration in the spent fluid was also assessed (61). Commercial glycerol (Sigma Aldrich (Oakville, Canada)) was the standard.

Monitoring enzymatic profiles by BN-PAGE

Blue native polyacrylamide gel electropohoresis (BN-PAGE) was accomplished as described (54, 59, 60). Briefly, membrane and soluble fractions were isolated and prepared in a non-denaturing buffer (50 mM Bis-Tris, 500 mM ε-aminocaproic acid, pH 7.0, 4°C) at a concentration of 4 μg/μL. For membrane solubilisation, 10% maltoside was included in the buffer. A 4-16% gradient gel was prepared with the Bio-Rad MiniProteanTM 2 system using 1 mm spacers to afford optimal protein separation. Sixty micrograms of proteins were loaded into each well prior to electrophoresis under native conditions at 80 V to ensure proper stacking, then at 300 V for proper migration through the gel. The blue cathode buffer (50 mM Tricine, 15 mM Bis-Tris, 0.02% (w/v) Coomassie G-250 (pH 7) at 4°C) was used to aid visualize the running front and was exchanged to a colorless cathode buffer (50 mM Tricine, 15 mM Bis-Tris, pH 7 at 4°C) when the running front was halfway through the gel. Upon completion, the gel was equilibrated in the reaction buffer for 15-30 min. The in-gel visualization of enzyme activity was determined by associating the formation of NAD(P)H to 0.2 mg/mL of phenazine methosulfate (PMS) and 0.4 mg/mL of iodonitrotetrazolium (INT), or by coupling the formation of NAD(P) to 16.7 μg/mL, 2,6-dichloroindophenol (DCPIP) and 0.4 mg/mL INT. Isocitrate dehydrogenase (NAD or NADP) was analyzed in-gel with a reaction mixture consisting of 5 mM isocitrate, 0.5 mM NAD(P), 0.2 mg/mL of PMS and 0.4 mg/mL of INT. Aspartate transaminase (AST) was

incubated in equilibrium buffer, 5 mM KG, 5 mM aspartate, 5 units of glutamate dehydrogenase (GDH), 0.5 mM NAD, 0.2 mg/mL PMS and 0.4 mg/mL INT (56). Glycine transaminase (GLT) was monitored as described with the aid of lactate dehydrogenase in order to visualize glyoxylate production (36). Glutamate dehydrogenase (GDH) was tracked using a reaction buffer with 5 mM glutamate, 0.5 mM NAD, 0.2 mg/mL PMS and 0.4 mg/mL INT.   For pyruvate carboxylase (PC) analysis, the membrane CFE was electrophoresed and was incubated with 5 mM pyruvate, 0.5 mM ATP, 0.5 mM HCO_3^-, 10 units of malate dehydrogenase (MDH), 0.5 mM NADH, 16.7 µg/mL DCPIP and 0.4 mg/mL INT. The product oxaloacetate was traced with assistance of MDH. Bromopyuvate was used as the inhibitor of PC (88). α-Ketoglutarate dehydrogenase (KGDH) was monitored by using 5 mM KG, 0.5 mM CoA, 0.5 mM NAD, 0.2 mg/mL PMS and 0.4 mg/mL INT (41). Pyruvate dehydrogenase (PDH) activity was tracked with the reaction buffer consisting of 5 mM pyruvate, 0.1 mM CoA, 0.5 mM NAD, 0.2 mg/mL PMS and 0.4 mg/mL INT (41). PEPC, PPDK and PK activities were visualized as described previously (53, 54). In this instance, the formation of oxaloacetate and pyruvate were detected with MDH and LDH respectively. Complex IV was examined by the addition of 10 mg/mL of diaminobenzidine, 10 mg/mL cytochrome C, and 562.5 mg/mL of sucrose (54). To ensure equal protein loading, the gels were stained by Coomassie blue G-250.   Enzymes like GDH and complex IV that had relatively similar activities in both cultures were also utilized in order to confirm that equal quantities of proteins were being electrophoresed. The activity of select enzymes including ICDH-NADP(2 mM isocitrate and 0.5 NADP for 30 min), PC (2 mM pyruvate, 0.5 ATP and 2 mM HCO_3^- for 30 min), PPDK (2 mM PEP and 1 mM AMP and 0.5 mM PPi) PC/AST were incubated in reaction buffer containing 2 mM glutamate, 2 mM pyruvate and 2 mM HCO_3^-) and the isozymes for PC were further confirmed by incubating the activity

42

bands with the appropriate substrates and monitoring the products by HPLC. Inhibitors like 5 mM rotenone for complex I and 5 mM bromopyruvate for PDH and PC were utilized to confirm the specificity of the desired enzymes.

Reactions were stopped using a destaining solution (40% methanol, 10% glacial acetic acid) once the activity bands had reached the necessary intensity. Reactions performed without the addition of a substrate or cofactor or inhibitor in the reaction mixture ensured specificity. Densitometry was performed using Image J for Windows.

Pyruvate metabolism by select enzymes monitored by NMR and HPLC

To establish if indeed these enzymes were a source of oxaloacetate, pyruvate and ATP, the activity bands attributable to these enzymes were added sequentially to the substrates and the products were assessed. 13C-NMR analyses were accomplished using a Varian Gemini 2000 spectrometer operating at 50.31 MHz for 13C. Samples were analyzed with a 5 mm dual probe (35u pulse, 1-s relaxation delay, 8 kilobytes of data, and 3000 scans). Chemical shifts were confirmed by comparing to standard compounds under analogous conditions (52).   The formation of oxaloacetate was first investigated by incubating the excised band of PC from the membrane CFE of Mn cultures for 1 h in phosphate reaction buffer containing (2 mM pyruvate labelled 13C-3, 0.5 mM ATP, 10 mM HCO_3^-). The reaction was stopped by removing the excised gel and heating at 60 0C. Following the identification of the labelled oxaloacetate peak, it was incubated with the excised band corresponding to the activity of PEPC and PPDK (Note: These bands were localized at the same spot in the gel and AMP (0.5 mM) was added to this incubation mixture). Once, the reaction was complete, the products were analysed by NMR and HPLC. The metabolites were identified by comparing to known standards. As PC and AST

43

activities located in the membrane CFE co-migrated on the gel, the activity band was excised and incubated with 2 mM pyruvate, 0.5 mM ATP, 10 mM HCO_3^- and 2 mM glutamate for 1 h. The formation of KG oxaloacetate and aspartate was monitored by HPLC.

Statistical analysis

Data were expressed as means ± standard deviations (SD). Statistical correlations of the data were checked for significance using the Student t test (*p ≤ 0.05, ** p ≤ 0.01). All experiments were performed at least twice and in triplicate.

Results

Influence of manganese on cellular growth and metabolite profile

P. fluorescens was able to grow in a mineral medium with 10% glycerol. However, in the cultures supplemented with Mn, there was a distinct difference in the nature and levels of metabolites in these cultures. The spent fluid from the Mn-cultures was characterized with prominent peaks indicative of KG and succinate (Figure. 4.1A). The inclusion of 50 μM Mn in the growth medium elicited the production of maximal amount of KG. At least a 4-fold increase in KG was observed compared to the controls. A marked diminution was observed at lower and higher concentrations of Mn (Figure. 4.1B). As 50 μM Mn evoked the optimal response, this concentration was utilized to decipher the metabolic networks responsible for the enhanced production of the keto-acid. Although the rate of growth was slightly slower in the Mn-media, at the stationary phase of growth the cellular yield was similar to that observed in the control cultures (Figure. 4.1C). The concentration of KG in the spent fluid as monitored by DNPH assay in the Mn-cultures increased with the time of incubation and was found to be maximal at stationary phase of growth (Figure. 4.1D). There was no significant difference in the

consumption of glycerol in these cultures. At stationary phase of growth almost 90% of this carbon source was utilized in the control and Mn-supplemented media. The pH at stationary phase of growth was 6.0 most likely due to secretion of KG. To elucidate the metabolic networks responsible for this seminal observation, the select metabolite profile of the soluble CFE was analyzed. Although peaks attributable to KG, pyruvate, isocitrate, oxaloacetate, succinate and ATP were evident, there was a marked variation in the levels of isocitrate, oxaloacetate and succinate in the Mn-grown cells compared to the cells obtained from the control cultures (Figure. 4.2A). This observation prompted the analysis of complex IV, an enzyme critical in energy production via oxidative phosphorylation. There was no significant variation in the activity of this enzyme in both cultures; the activity of complex I also did not appear to be influenced by the presence of Mn in the medium (Figure. 4.2B). PDH, an enzyme that supplies acetyl CoA and is inhibited by bromopyruvate was relatively similar in both cultures (Figure. 4.2C).
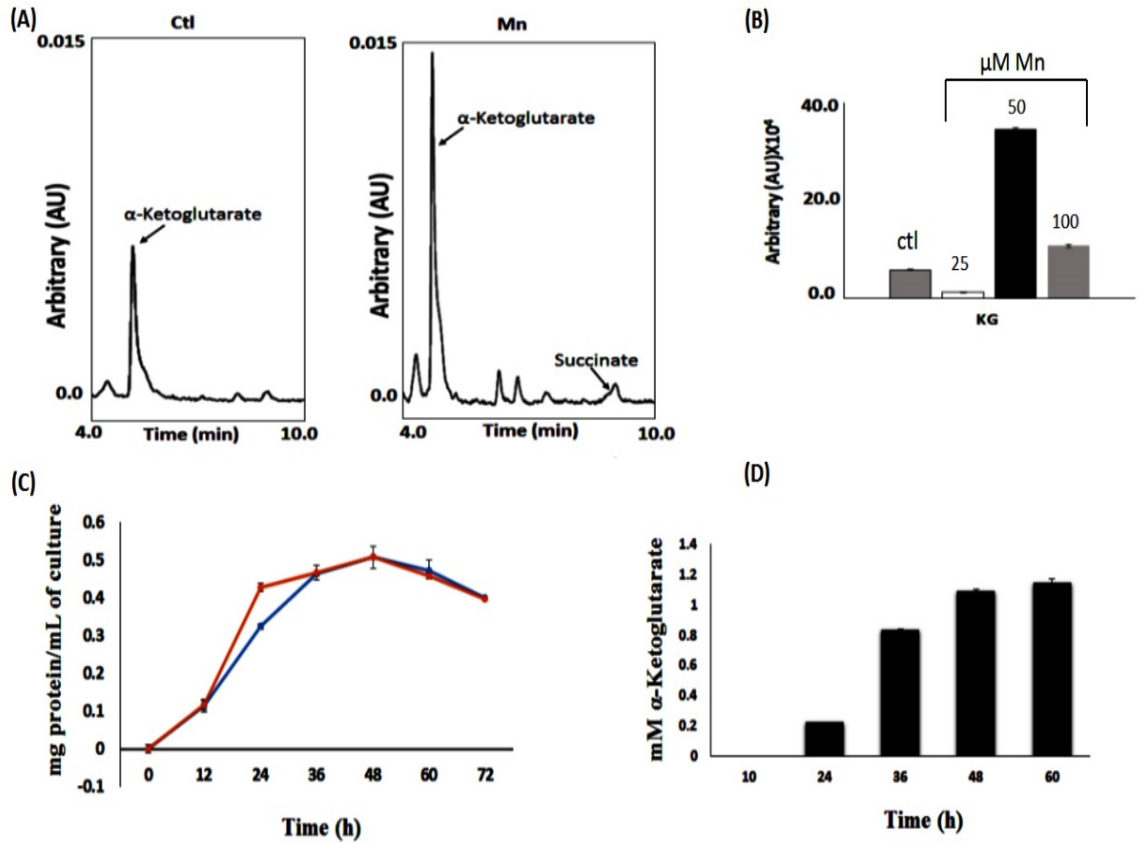
Figure 4.1: Influence of Mn on KG production

A) HPLC analyses of spent fluid in control and Mn cultures. B) KG production at different Mn concentrations. C) Growth profile of *P. fluorescens* grown in 10% glycerol with 50 µM Mn. The black curve indicates Mn cultures; the grey curve control culture. D) KG concentrations in spent fluid at various time intervals in Mn-cultures (50 µM). (n = 3).
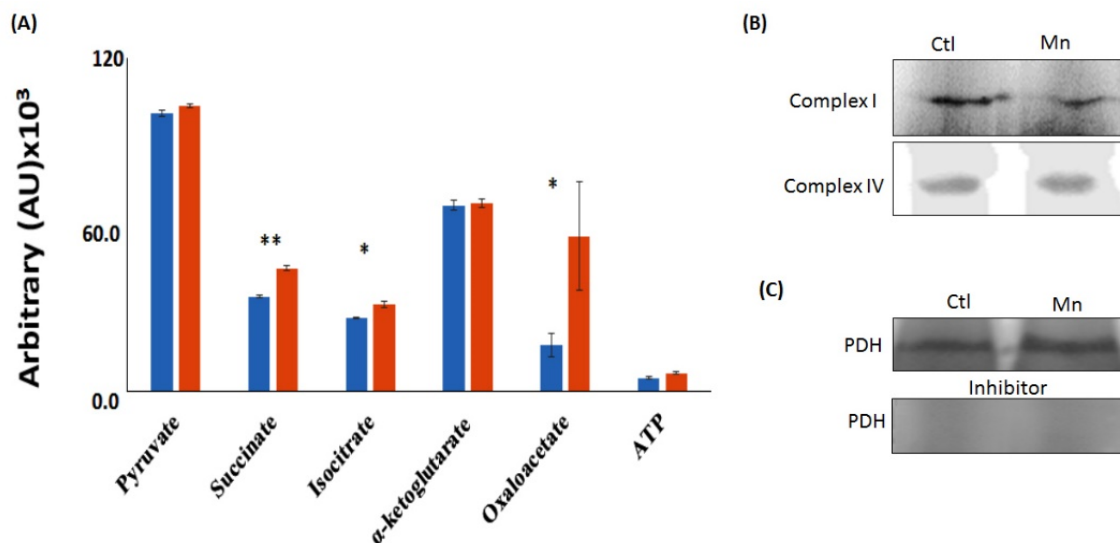
Figure 4.2: Functional metabolomics and select energy-producing enzymes

A) HPLC of targeted metabolites from control and Mn-treated cells (at stationary phase of growth). B) Enzymes involved in oxidative phosphorylation (complex I and IV). C) Pyruvate dehydrogenase activity with and without inhibitor (Gels are representative of 3 experiments; Ctl=control, Mn-treated).

Enzymes involved in KG homeostasis

As KG was a major metabolite generated in the presence of Mn, various enzymes involved in the homeostasis of this ketoacid were monitored. There was a significant increase in activities of such enzymes as ICDH-NAD as well as ICDH-NADP (Figure. 4.3A, B). In fact, three isoenzymes of ICDH-NAD were visualized by the in-gel activity assay. These were confirmed by incubating the appropriate sections of the gel separately in the substrates and monitoring the products. ICDH-NADP activity band was excised and treated with the isocitrate and NADP in order to monitor the production of KG by HPLC (Figure. 4.3C). Spectrophotometric assays revealed at least a 2-fold increase in ICDH-NADP activity (Table 4.1). These enzymes were also monitored at different growth intervals and maximal activity was observed at the stationary phase of growth for both ICDH-NADP/NAD (Figure. 4.3D). (Note that the activity at the earlier periods was evident only if the gel was incubated in the substrate

47

for longer time). In order to verify if indeed this increase in enzymatic activity was due to the presence of Mn, control cells were incubated in the Mn-media and Mn-grown cells were exposed to the control culture conditions. A reversal of ICDH activities was observed (Figure. 4.3E). Hence, the dependence of the increased activity of this enzyme on Mn was evident. α-Ketoglutarate dehydrogenase (KGDH), a TCA cycle enzyme involved in the decarboxylation of KG was shown to have diminished activity in the cells harvested from the Mn-media compared to the control cells (Figure. 4.3F). Aconitase (ACN), an enzyme referred to as the gate-keeper of the TCA cycle was increased 2-fold in activity in the Mn-supplemented media (Table 4.1).

Table 4.1 Enzymatic activities in CFE from control and Mn- *P. fluorescens* at the same growth phase as monitored by spectrophotometry.

Enzymes	Control	Mn
NAD+-dependent isocitrate Dehydrogenase [a]	0.64±0.07	1.07±0.11*
NADP+-dependent isocitrate Dehydrogenase [a]	0.4±0.014	0.84±0.009
Pyruvate carboxylase [b]	0.57±0.09	1.2±0.24*
Aconitase [c]	11±0.1	22±0.5*

[a] μmol NAD(P)H produced min^{-1} mg protein^{-1} as monitored at 340 nm(n = 3 ± standard deviation).
[b] μmol NADH consumed min^{-1} mg protein^{-1} as monitored at 340 nm(n = 3 ± standard deviation).
[C] Specific activity of aconitase (μmol aconitate min^{-1} mg protein^{-1} as monitored at 240 nm) (n = 3 ± standard deviation).

*Denotes a statistically significant differences compared with the control (P ≤ 0.05).
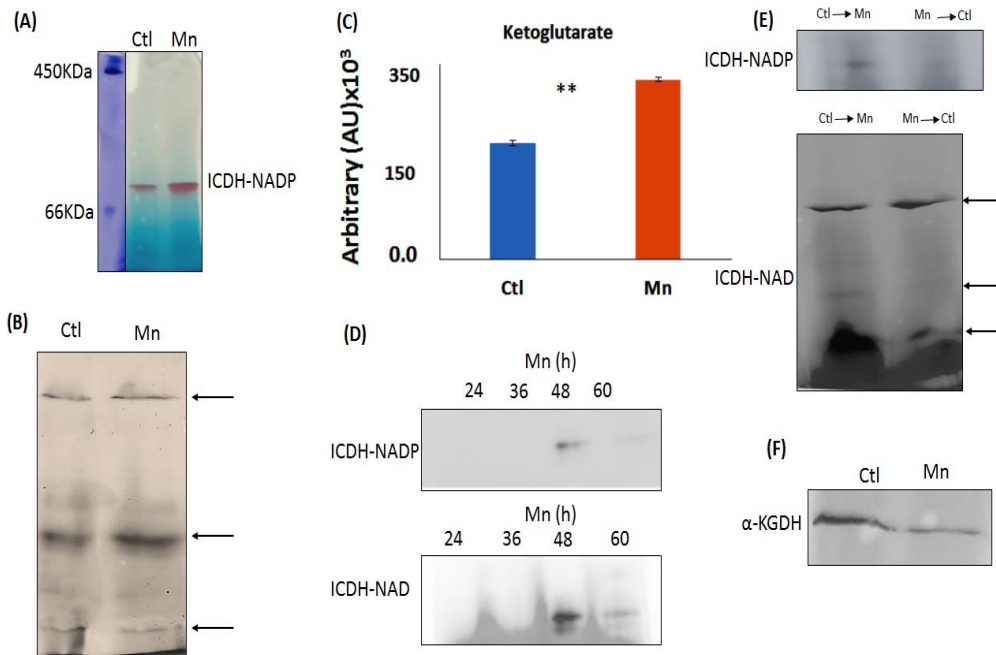
Figure 4.3: KG homeostasis in *P. fluorecens* grown in 10% glycerol.

A) In-gel enzymatic activity of isocitrate dehydrogenase (ICDH-NADP), Ferritin (450 KD) and BSA (60 KDa). B) In-gel enzymatic activity of isocitrate dehydrogenase (ICDH-NAD). C) HPLC analysis of excised band (A) incubated in 2 mM isocitrate, 0.5 mM NADP for 30 min. D) Time profile (h) of ICDH-NAD/NADP activities. E) In-gel activity of ICDH-NAD/NADP when control cells were incubated in Mn-cultures and Mn-treated cells were exposed to control media. F) In-gel KGDH activity. (Gels are representative of 3 independent experiments. Ctl = Control; Mn-treated).

The role of PC in oxaloacetate and PEP formation

For this organism to proliferate in glycerol, the 3-carbon nutrient has to be transformed into oxaloacetate, a moiety essential for the TCA cycle and gluconeogenesis. Pyruvate carboxylase (PC) a Mn-dependent enzyme that orchestrates the carboxylation of pyruvate into oxaloacetate with ATP as the cofactor would be a good candidate. This enzyme was characterized with elevated activity and two activity bands indicative of two isozymes that were associated with the cells grown in the Mn-enriched media (Figure. 4.4A). Incubation of excised

bands with pyruvate, HCO_3^-, and ATP yielded an oxaloacetate peak as revealed by HPLC. This metabolite was further confirmed enzymatically with the aid of malate dehydrogenase and NADH (data not shown). PC had a maximal activity at 48 h, a growth phase corresponding to the optimal production of KG (Figure. 4.4A).

As phosphoenol pyruvate (PEP) is an important precursor to the synthesis of pyruvate, the activity of PEPC, an enzyme responsible for the transformation of oxaloacetate to PEP was analyzed. The activity band was more intense in the cells obtained from the Mn-supplemented media. Furthermore, the presence of an isozyme was also detected (Figure. 4.4B). The PEP was readily converted to pyruvate by PPDK and PK as these enzymes were associated with markedly increased activity bands in the soluble CFE from the Mn-exposed cells compared to the control (Figure. 4.4B). To establish if PC, PEPC and PPDK may be working in tandem, the fate of labelled pyruvate (13C-3) and ATP was monitored. Following the formation of 13C labelled oxaloacetate by the PC activity band, this substrate was incubated with PEPC and PPDK band in the presence of AMP and PPi. The production of pyruvate and ATP were followed. Indeed this metabolic module fixed CO_2, produced oxaloacetate and regenerated pyruvate and ATP (Figure. 4.4C). The enhanced synthesis of oxaloacetate in the Mn-cultures propelled by PC may not only be an important contributor to ATP production via the formation of PEP but may help transform glutamate into KG.
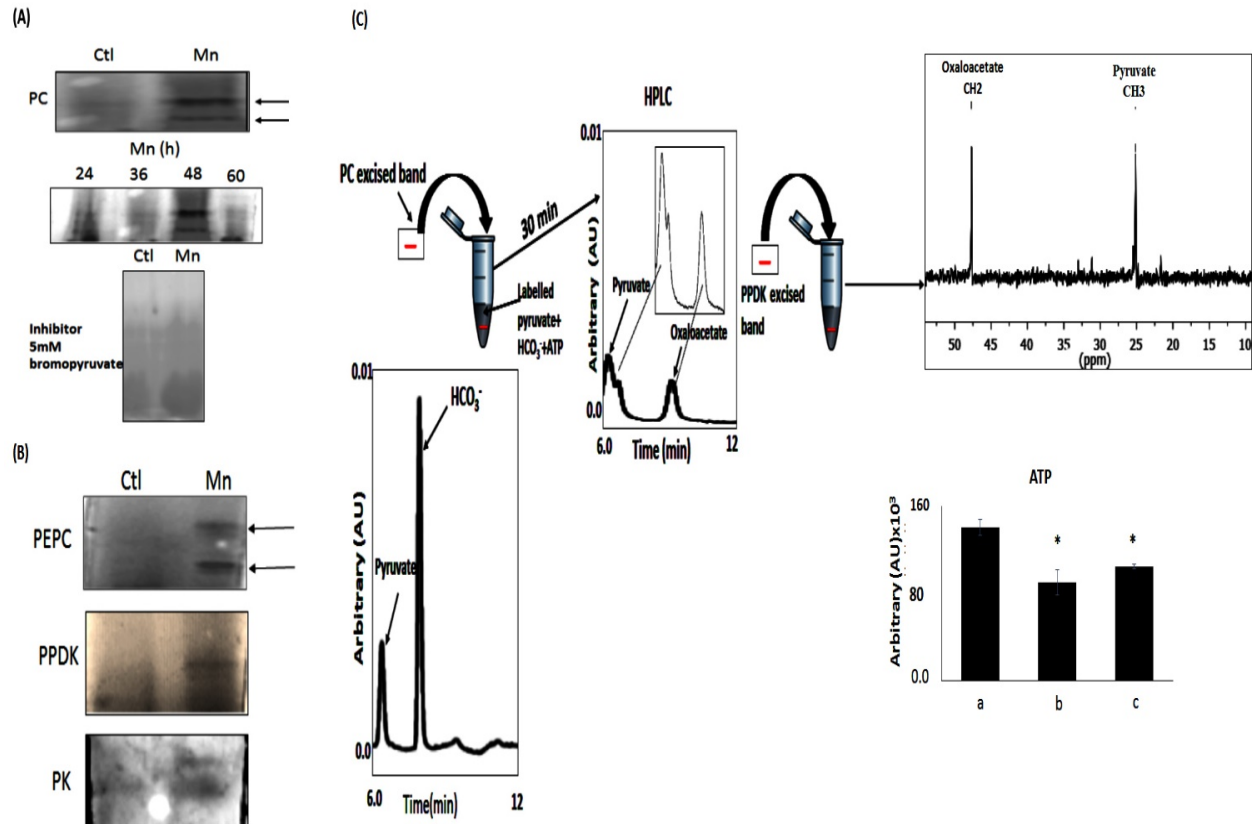
Figure 4.4: Pyruvate metabolism and ATP production

A) In-gel activity of pyruvate carboxylase (PC), activity at various time intervals and activity in the presence of inhibitor (5 mM bromopyruvate). B) Phosphoenolpyruvate carboxylase (PEPC), pyruvate orthophosphate dikinase (PPDK) and pyruvate kinase (PK) activity BN-PAGE. C) HPLC and NMR analyses of excised PC activity band (membrane CFE) and PEPC/PPDK activity band (soluble CFE) (note: oxaloacetate produced in the first reaction was incubated with PEPC/PPDK band in the presence of AMP and PPi. (Note: NMR peak corresponding to CH2 in oxaloacetate; ATP was monitored at time =0 a) ; then following the incubation with the PC band; b) and after reaction with PPDK/PEPC band in the presence of AMP; c); Note: ATP data were analysed by one-way ANOVA for the significance. Gels are representative of 3 independent experiments. Ctl = Control; Mn-treated.
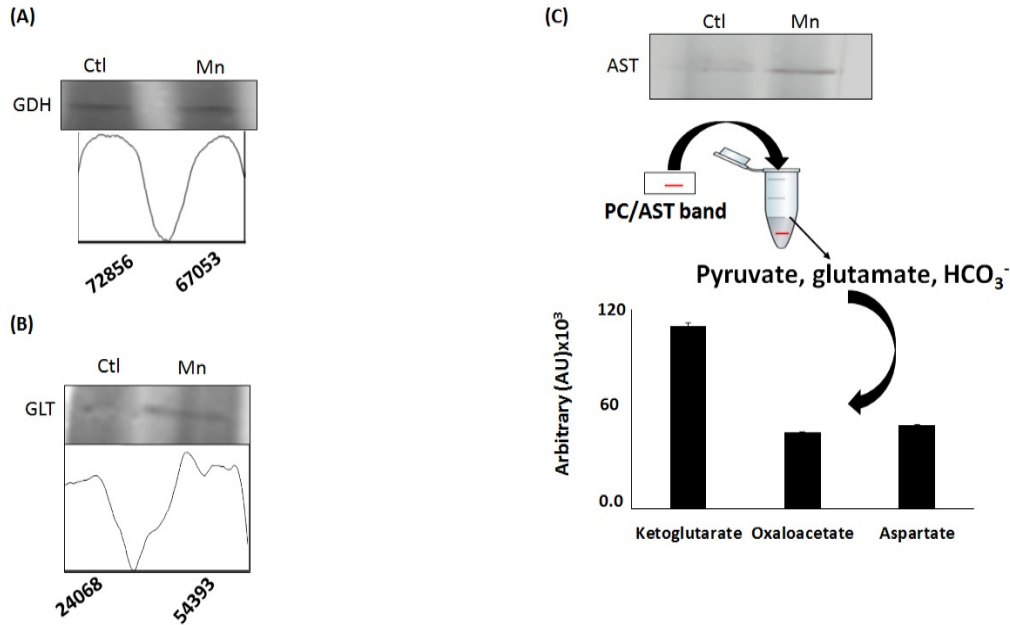
Figure 4.5: Glutamate-metabolizing and KG –producing enzyme activities by BN-PAGE and HPLC

A) Glutamate dehydrogenase (GDH) and densitometric reading of activity band. B) Glycine transaminase (GLT) and densitometric reading of activity band. C) Aspartate aminotransminase (AST) and HPLC analyses of excised band incubated with 2 mM glutamate, pyruvate and HCO_3^-. Note: the formation of KG; Gels are representative of 3 independent experiments; PC and AST bands co-migrated. Ctl = Control; Mn-treated. Densitometry was performed using Image J for windows.

Since transaminases and GDH play a role in the homeostasis of KG, these enzymes were monitored. AST and GLT were found to be elevated while GDH did not change significantly in the cells isolated from the Mn-cultures (Figure. 4.5A, B, C). As the lower PC band and AST co-migrated during the BN-PAGE, this band was excised. As it was harbouring these enzymes, its ability to form KG from pyruvate, glutamate, ATP and HCO_3^- was evaluated. Peaks indicative of KG, oxaloacetate and aspartate were obtained (Figure. 4.5C).

Mn-treated cells and biotransformation of industrial glycerol into KG

As the SF and CFE extract from the Mn cells were characterized by copious amounts of KG, it was essential to assess the ability of the intact cells to produce this value-added metabolite from glycerol. The whole cells were incubated in phosphate media devoid of a nitrogen source and at various time intervals, cells were centrifuged and KG was monitored using DNPH. After 24 h of incubation, the intact Mn-treated microbes synthesized approximately 1.2 mM KG from the industrial glycerol compared to 0.12 mM from the glycerol purchased from Sigma (commercial) (Figure. 4.6A). After 24 h of incubation, the Mn whole cells consumed 90% of the industrial starting material obtained from ROTHSAY, Canada compared to 60 % of the commercial one (data not shown).
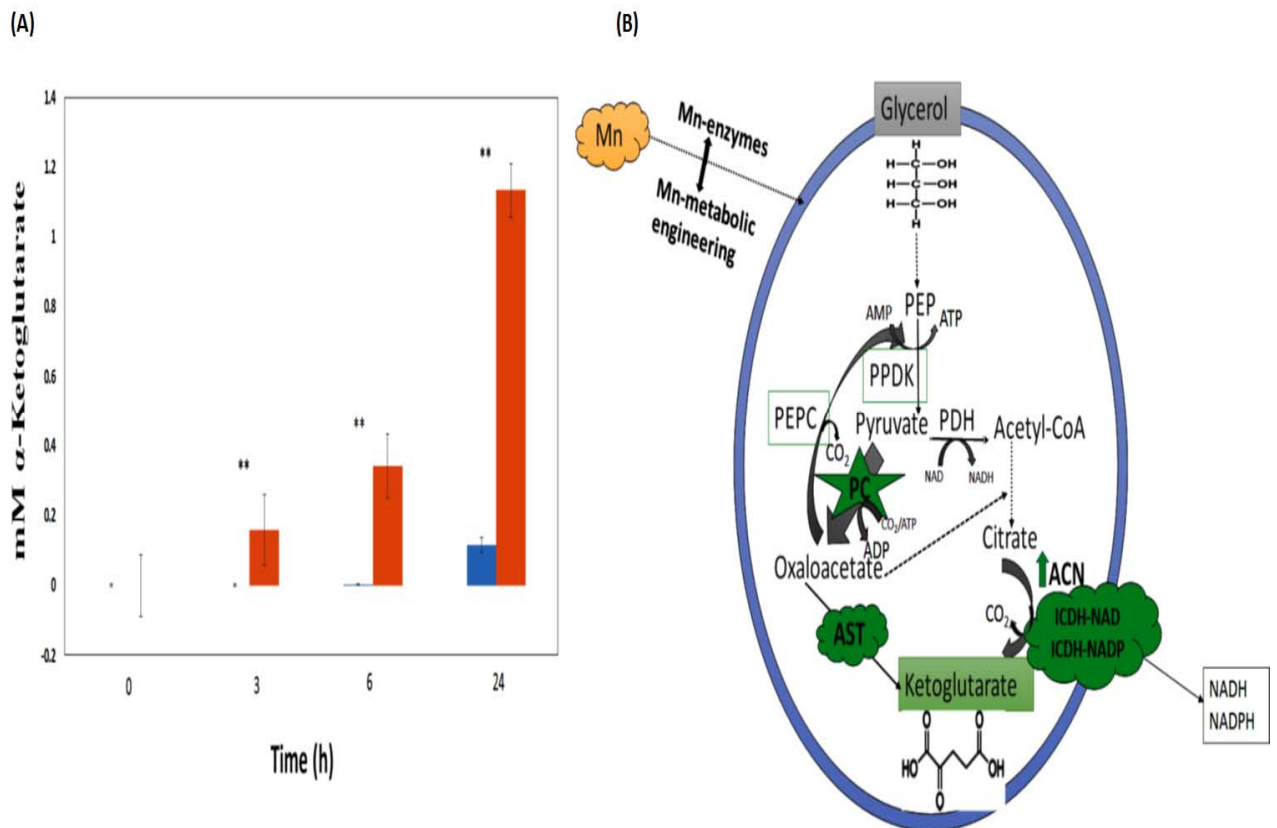
Figure 4.6: KG production by intact cells and Mn- dependent metabolic engineering involved in KG synthesis

A) KG formed when whole cells were incubated with commercial and industrial glycerol (Note: (60% and 90% of glycerol were consumed in the commercial (Sigma) and industrial (ROTHSAY, Canada) respectively, SD±2.0%, n=3). B) Scheme depicting a PC-propelled metabolic reconfiguration mediating the production of KG in *P. fluorescens* exposed to Mn. (Green indicates an increase).

Discussion

The foregoing data point to the ability of *P. fluorescens* to produce KG from glycerol in the presence of Mn. The metabolic re-engineering elicited by the interaction of the microbe with Mn exposes an intriguing strategy of how microbial systems can be coached to perform a desired commercial task. This divalent metal is involved in a variety of enzymatic reactions contributing to the metabolism of carbohydrates, in the fixation of CO_2, in anti-oxidative defence and in the carboxylation processes (79, 89-91). Pyruvate carboxylase is a Mn-dependent enzyme and is responsible for the addition of CO_2 to pyruvate with the concomitant formation of oxaloacetate. This reaction utilizes ATP as the co-factor (92, 93). The overexpression of the PC gene in a yeast has been shown to elicit the maximal secretion of this ketoacid when glycerol was the source of carbon (94). In this present study the expression of the two PC isozymes appeared to play a critical role in the enhanced production of KG observed when Mn was included in the cultures. The activity of PC was optimal at 48h of growth, a time that corresponded with the ability of the microbe to produce the maximal amounts of KG from glycerol. Since Mn was readily available, it is quite likely that the presence of the divalent metal in the medium may have promoted the expression of these isozymes. Metal-dependent proteins are intricately regulated and the availability of the metal tends to be a critical ingredient in this process (95). As 50 μM Mn enabled the microbe to produce the most KG, it is within the realm of possibility that this concentration of the divalent metal may be evoking the optimal enzymatic activity. Indeed Mn is

known to be toxic when present in elevated amounts. Depending on its concentration this divalent metal can be either essential or a toxin (96). The decrease in activity at higher Mn concentration may be attributed to its dose-dependent toxicity.

Oxaloacetate a key intermediate in a variety of metabolic networks may undergo numerous transformations in order to fuel the synthesis of KG. Aspartate transaminase (AST) is known to readily effect the conversion of glutamate and oxaloacetate into KG and aspartate (51). The activity of this enzyme was elevated in the cells harvested from the Mn-supplemented cultures. These two enzymes (PC/AST) co-migrated in the gel and the excised activity band yielded KG upon incubation with pyruvate, HCO_3^- and glutamate. This molecular arrangement would permit the funnelling of oxaloacetate to the production of KG. Indeed, the transient assemblage of enzymes dedicated to the synthesis of a desired product is a common biochemical phenomenon that facilitates the production of a select metabolite. Recently it was shown that the close proximity of citrate lyase, PEPC and PPDK allowed the survival of *P. fluorescens* challenged by nitrosative stress. This partnership among the enzymes enabled the production of ATP in an O_2-independent manner as oxidative phosphorylation was ineffective (54). In this instance the shuttling of PC-generated oxaloacetate towards the proximal AST would ensure the efficacy in the production of KG. The enhanced activity of glycine transaminase (GLT) observed in the Mn cultures, would also add to KG budget. Oxaloacetate is also a critical precursor of citrate synthesis, a reaction that is aided by a constant supply of acetyl CoA. Pyruvate dehydrogenase (PDH) activity was prominent in the Mn-treated cells as was the activity of aconitase (ACN). However, the enzymes mediating the decarboxylation of isocitrate into KG, a metabolite with numerous biological functions (97) were sharply enhanced in the Mn-enriched cultures. Indeed, both ICDHs, the NAD and NADP dependent were markedly elevated. The

ICDH-NAD dependent was evident as three isozymes. The overexpression of this enzyme in microbial systems has been utilized to promote the synthesis of KG from glycerol (54). The diminished activity of KGDH may be also contributing to the accumulation of KG, an enzyme with diminished activity in the cells harvested from the Mn-cultures. The enhanced activity of ICDH coupled with the concomitant diminution in the activity of KGDH may be an important stratagem this microbe may be resorting to in order to accumulate KG.

The enhanced activity of PC may not only be a source of the crucial oxaloacetate but may be also aiding in fulfilling the need for ATP. In this study, complex IV that mediates the final electron transfer step during ATP production by oxidative phosphorylation did not appear to be significantly affected. However, the demand for ATP by PC may have compelled the microbe to complement its energy-generating machinery by activating the substrate-level phosphorylation pathway. As oxaloacetate was abundantly being supplied by the overexpression of the Mn-dependent PC, the microorganism was readily tapping this ketoacid into the formation of the high-energy, PEP. This conversion catalyzed by PEPC is quite energy efficient as it necessitates inorganic phosphate (Pi) as the co-factor. The subsequent decarboxylation of oxaloacetate yields PEP that can be readily fixed into ATP in the presence of either ADP or AMP; pyruvate is produced as a consequence of this reaction. PPDK that uses AMP as the nucleotide was elevated in the cells isolated from the Mn cultures. This enzyme is known to provide organisms an adaptive advantage to survive conditions where oxidative phosphorylation is compromised due to oxidative stress, lack of oxygen, deficiency in iron or assault by macrophages (54, 56, 98). In this instance, other than augmenting the energy budget of the microbe, this metabolic network may also be contributing to pyruvate homeostasis, a pivotal feature in the Mn-induced KG

accumulation in *P. fluorescens*. This ketoacid fuels the fixation of CO_2 into oxaloacetate by PC, an enzyme whose expression and activity are responsive to Mn (61, 92, 99).

The seminal experiments with the membrane localized PC and the soluble cellular component with PEPC and PPDK where oxaloacetate, and ATP were produced provided compelling evidence that these enzymes may be working in tandem. Furthermore the regeneration of the initial 13C-3 labelled pyruvate vividly illustrates that this organism may be utilizing this metabolic network not only to produce oxaloacetate but also to synthesize ATP. It is also within the realm of possibility to argue for the notion that Mn has compelled *P. fluorescens* to fix CO_2 in the presence of glycerol to fulfill its energy and metabolic needs. By invoking this process, the organism has abundant access to oxaloacetate and ATP. The former can be readily transaminated in order to produce KG and converted to citrate, a critical precursor to KG via isocitrate. Since one of the objectives of this investigation was to generate value-added products from glycerol, a waste from the biodiesel industry, the ability of intact cells to transform this trihydroxy alcohol into KG was evaluated. The maximal KG was obtained after 24 h of incubation and industrial glycerol yielded more ketoacid compared to the commercial variety. Although further investigation needs to be undertaken in order to unravel the commercial application of these findings, it is not unlikely that the composition of these starting materials may be the contributing factor. Manganese supplementation provides a relatively facile operation aimed at triggering a plethora of metabolic networks dedicated to the production of KG.

In conclusion, this work reveals the significance of abiotic change in modulating biochemical behaviour. The presence of Mn has a profound influence on glycerol metabolism leading to the accumulation of KG. The overexpression in the activities of such Mn-requiring

enzymes as PC, PPDK and PEPC provides an effective route to oxaloacetate and ATP. The former was an important source of KG, a value-added product that was made easily accessible due the enhanced activities of transaminases and ICDH (Figure. 4.6B). The metabolic shift prompted by Mn presents a relatively facile stratagem to program microbes to execute assignments of economic importance. These metabolic networks evoked by Mn provide a relatively inexpensive means of synthesizing KG from glycerol. This is the first demonstration of a metabolic reprogramming involving the synthesis of oxaloacetate, acetyl CoA and ATP, three ingredients propelling the enhanced production of KG from industrial glycerol. Optimization of these biochemical processes has the potential of yielding biofactories that may assist the biodiesel industry to be more profitable and environmentally neutral.

Acknowledgment

Conflict of Interest

All authors declare that they have no conflict of interest.

5. Chapter 5: The role γ-aminobutyric acid (GABA) and Succinate Semialdehyde in α Ketoglutarate (KG) production

α Ketoglutarate (KG) is a crucial keto-acid due to its participation in a plethora of biological activities. It is involved in protein synthesis, immune response, anti-oxidative defence, collagen formation and energy production. While clinically, KG is utilized in wound healing, to treat chronic kidney deficiency and to decrease uraemia, this metabolite can also be processed into heterocyclic compounds, dietary supplements and succinate. Hence, it is critical to uncover effective and environmentally neutral processes to commercially synthesize KG. Glycerol, a waste by-product from the biodiesel industry has been utilized to enhance the production of KG in *Pseudomonas fluorescens* in the presence of manganese.

In this Chapter an intriguing metabolic pathway orchestrated by GABA and succinate semialdehyde that fuels the formation of KG from glycerol has been unraveled. The homeostasis of succinate a key precursor in the biosynthesis of succinate semialdehyde is described. The production of this dicarboxylic acid is mediated by increased activity of isocitrate lyase (ICL) and fumarate reductase (FRD). Succinate is converted to succinate semialdehyde by succinate semialdehyde dehydrogenase (SSADH). The succinate semialdehyde budget is also supplemented by GABA via GABA transaminases (GABAT). The carboxylation of succinate semialdehyde by α ketoglutarate decarboxylase (KDC) results in the copious secretion of KG, the final product

This seminal observation whereby GABA fuels the synthesis of KG extends the repertoire of metabolic networks contributing to the formation of this ketoacid from glycerol and provides a microbially-assisted technology to improve the efficacy of the biodiesel industry.

γ-Aminobutyric acid (GABA) aminotransaminase and succinate semialdehyde dehydrogenase mediate the synthesis of α-ketoglutarate in *Pseudomonas fluorescens*.

(Original research)

Azhar A. Alhasawi, Sean C. Thomas, Sujeethar Tharmalingam, Felix Legendre and Vasu

D. Appanna*

(In preparation)

Abstract:

Glycerol is an important by-product of the biodiesel industry and its transformation into value-added products is being actively pursued in order to improve the efficacy of this renewable energy sector. Here we report that the enhanced production of α-ketoglutarate (KG) effected by *Pseudomonas fluorescens* in a mineral medium supplemented with manganese (Mn) is propelled by the increased activities of GABA transaminase, succinate semialdehyde dehydrogenase (SSADH) and isocitrate lyase (ICL). The latter generates glyoxylate and succinate to key metabolites involved in this process. Fumarate reductase (FRD) also aids in augmenting the pool of succinate, a precursor of succinate semialdehyde (SSA). The latter is then carboxylated to KG with the assistance of α ketoglutarate decarboxylase (KDC). These enzymes work in tandem to ensure a copious secretion of the keto-acid. When incubated with glycerol in the presence of bicarbonate, cell-free extracts readily produce KG with a metabolite finger print attributed to glutamate, GABA, succinate and succinate semialdehyde. Further targeted metabolomic and functional proteomic studies with HPLC, NMR and gel electrophoresis techniques provided molecular insights into this KG-generating machinery. This the first report of a metabolic network where dopamine transaminase and SSADH orchestrate the enhanced production of KG from glycerol. It affords a biochemical process that can be harnessed to improve the efficiency of the biodiesel industry.

Key Words: GABA, Succinate semialdehyde, α-ketoglutarate, biofuel, enzymes, metabolic engineering

Introduction

The ability of microbial systems to transform chemical wastes and renewable biomass into value-added products has been widely exploited industrially. Citrate and glutamate are two common metabolites that are synthesized with the aid of microbes. The manipulation of metabolic networks is key if these industrial processes are to be efficient. Genetic modification and abiotic modulation are central to the strategy aimed at reconfiguring metabolic modules designed to efficaciously obtain a desired product. α Ketoglutarate (KG) is a keto-acid of immense commercial interest due to its wide-ranging applications. Apart from being a pivotal chemical ingredient that participates in a variety of biological processes including protein synthesis, immune response, and anti-oxidative defence, it is also utilized clinically in wound healing, to treat chronic kidney deficiency and to decrease uraemia (100-102). This keto-acid is found in food flavouring, in cosmetics and as a nutritional supplement.

The chemical synthesis of this keto-acid requires the participation of toxic ingredients and leads to the formation of undesirable products. For instance, it can be obtained from succinic acid and oxalic acid diethyl esters using cyanohydrines or by hydrolysis of acyl cyanide (103). These multi-step synthetic methods have a lot of drawbacks due to the use of hazardous chemicals such as cyanides and the generation of toxic wastes. Biotechnology offers a cleaner and more selective route to synthesize KG. Recently, the ability of the nutritionally-versatile *Pseudomonas fluorescens* to produce copious amount of KG from glycerol in the presence of the micronutrient, Mn was reported (104). This affords a facile means to reprogram metabolic pathways compared to the procedures involving genetic transformation. The key participants in conversion of glycerol to KG are isocitrate dehydrogenase (ICDH-NAD(P)) and pyruvate

carboxylase (PC). The overexpression of these two genes in numerous organisms have been routinely utilized to mediate the conversion of glycerol to KG. PC mediates the carboxylation of pyruvate into oxaloacetate, a precursor of citrate. ICDH then generates KG through the reductive decarboxylation of isocitrate. In an effort to assess if any other metabolic networks are contributing to the enhanced production of KG in the Mn-supplemented cultures, a targeted metabolomic and functional proteomic study was undertaken to identify the metabolites and enzymes that orchestrate the formation of this keto-acid. Mn is known to be required for numerous enzymes to function effectively and can easily substitute for magnesium in biomolecules that depend on this divalent metal for optimal activity (79).

In this report we demonstrate the ability of *P. fluorescens* to invoke an alternative network to produce KG from glycerol. Isocitrate lyase (ICL), succinate semialdehyde dehydrogenase (SSADH), fumarate reductase (FRD) and α-ketoglutarate decarboxylase (KDC) appear to be the critical contributors to this KG-generating pathway. The pool of succinate that is supplemented by FRD and ICL is readily processed into succinate semialdehyde. KDC subsequently interacts with HCO_3^- and SSA to produce KG. The significance of intact cells to secrete KG and the overexpression of genes responsible for this Mn-evoked metabolic engineering are discussed.

Materials and Methods:

Microbial growth conditions and cellular fractionation

Pseudomonas fluorescens (ATCC 13525), obtained from the American Type Culture Collection, was grown and maintained in a mineral medium comprising Na_2HPO_4 (6 g), KH_2PO_4

(3 g), NH$_4$Cl (0.8 g), MgSO$_4$.7H$_2$O (0.2 g) per liter of deionized water. Trace elements (1 mL) were added as well in concentrations as described previously (55). The pH was adjusted using 2 N NaOH to 6.8. Glycerol (10% v/v: 1.37 M) from Sigma Aldrich (Oakville, Canada) was added to the medium as the sole source of carbon. This glycerol media was dispensed in 200 mL aliquots in 500 mL Erlenmeyer flasks and inoculated with 1 mL of stationary phase mL of (450 µg protein equivalent) of the control *Pseudomonas fluorescens* culture. The 50 µM Mn supplemented media was used for comparison with control. The cultures were then aerated on a gyratory water bath shaker (model G76, New Brunswick Scientific) at 26℃ and 140 rpm. The bacterial cells were isolated by centrifugation at stationary growth phases (40 h for control and 48 h for Mn-treated) and then re-suspended in a cell storage buffer (CSB) consisting of 50 mM Tris-HCl, 5 mM MgCl$_2$, 1 mM phenylmethylsulfonylfluoride PMSF (pH 7.3). The cells were lysed by sonication using a Brunswick Sonicator on power level 4 for 15 sec, 4 times and with 5 minutes intervals in between. In order to obtain the cell free extracts [(CFE) soluble and membranous fractions], the cells were centrifuged for 3 h at 180,000×*g* at 4℃. The unbroken cells were initially removed by centrifugation at 10,000×*g* for 20 min. The Bradford assay was performed in triplicate to determine the protein concentration of both fractions using bovine serum albumin (BSA) as the standard (58). Additionally, the cells were harvested at different time intervals by centrifugation at 10,000×g for 20 min. The bacterial pellets were treated with 1 mL of 1 N NaOH and the biomass was measured with the aid of the Bradford assay. All comparative studies were performed with cells at the same growth phases i.e. 40 h for the controls and 48 h for the Mn-treated cells (104). In order to confirm if the metabolic changes were indeed induced by the addition of Mn, control cells were added to Mn-treated media while cells isolated from the Mn cultures were incubated in control media and re-evaluated. To afford

an accurate comparison, these cells were gathered at the same growth phase and following their incubation at 26 °C for 6 h in a gyratory water bath, the cells were harvested as previously mentioned (32).

Blue Native Polyacrylamide Gel Electrophoresis (BN-PAGE) and two-dimensional (2D) SDS-PAGE

BN- PAGE was utilized to assess the activities of various enzymes involved in the production of KG. To verify optimal protein separation, 4–16% linear gradient gels were cast with the Bio-Rad MiniProteanTM2 (Hercules, CA) systems using 1 mm spacers. Sixty micrograms of soluble cell-free extract protein were loaded into the wells and the gels were electrophoresed under native conditions (50 mM e-aminocaproic acid, 15 Bis-Tris, pH 7.0, 4°C) at a final concentration of 4 mg of protein per ml. The membrane proteins were set in a similar preparation except 1% (v/v) b-dodecyl-D-maltoside was added to the preparation to assist in the solubilisation of the membrane-bound proteins. Blue cathode buffer [50 mM Tricine,15 mM, Bis-Tris, 0.02% (w/v) Coomassie G-250 (pH 7)] was replaced with a colourless cathode buffer [50 mM Tricine, 15 mM Bis-Tris, (pH 7)] at 4°C when the running front was half-way through the resolving gel. The in-gel visualization of enzyme activity was carried out with the utilization of formazan precipitation. The gels were incubated in a reaction mixture containing equilibration buffer, 5 mM substrate, 0. 5 mM cofactor with 0.2 mg/ mL of phenazine methosulfate (PMS) or DCPIP and 0.4 mg/ mL of iodonitrotetrazolium (INT). succinate semialdehyde dehydrogenase (SSADH) activity was visualized using reaction buffer with 5 mM succinate, NAD(P)H and confirmed with referees reaction using 5 mM succinate semialdehyde, 0.5 NAD(P) (105). Fumarate reductase (FRD) activity was also monitored in the gel using reaction buffer

containing (5 mM fumarate, 0.5 mM NADH) (57). Isocitrate lyase (ICL) activity was detected as described (54). The activity of α-ketoglutarate decarboxylase (KDC) was visualized by utilizing enzyme-coupled assays as described (60). This was confirmed with lead nitrate as well as the shift reagent (106). GABA aminotransminases (GABAT) activities were visualized by using (5 mM GABA, 5 mM KG, pyruvate or oxaloacetate) (107-109). Reactions were stopped using destaining solution (40% methanol, 10% glacial acetic acid) once the activity bands reached their desired intensity. To ensure equal loading, control CFE and stressed CFE were electrophoresed and stained with Coomassie blue. As a control, the activity of glutamate dehydrogenase (GDH), an enzyme known not to appear to change significantly, was also probed as described (104). The activity of isocitrate lyase (ICL), fumarate reductase (FRD), succinate semialdehyde dehydrogenase (SSADH) as well as ketoglutarate decarboxylase (KDC) were further confirmed by incubating the activity bands with the appropriate substrates and monitoring the products by HPLC. Inhibitors like 5 mM sodium arsenite were used for SSADH and 4 mM malonate used to inhibit (ICL) activity (52, 110, 111). Also, the control reaction was verified by substituting succinate or NADH in (SSADH) activity. Reactions were stopped using a destaining solution (40% methanol, 10% glacial acetic acid) when the activity bands had gotten the required intensity. Reactions performed without the addition of a substrate or cofactor or inhibitor in the reaction mixture ensured specificity. Densitometry was done using Image J for Windows.

The activity of select enzymes were verified by spectrophotometric studies. Malate dehydrogenase (MDH) (2 mM malate and 0.5 NAD), α-ketoglutarate dehydrogenase (αKGDH) (2 mM KG, 0.5 NAD), and succinate semialdehyde dehydrogenase (SSADH) (2 mM succinate, 0.5 mM NADH) were monitored at 340 nm. (5,5-dithio-bis-(2-nitrobenzoic acid) was utilized to analyze succinyl-CoA synthetase (Williams et al., 1998). The reaction mixture contained 2 mM

succinate, 1 mM ATP, 0.1 mM CoA in 25 mM Tris-HCl, 5 mM $MgCl_2$ buffer (pH 7.3). The decrease in absorbance due to consumption of CoA by DTNB ion was monitored at 10 sec intervals for 10 min at 412 nm ($\varepsilon = 13.6$ $mM^{-1} \cdot cm^{-1}$) (41, 112).

In-cell Western assays were modified from the Odyssey® Infrared Imaging System protocol document (Li-cor doc# 988-08599). Briefly, *P. fluorescens* were grown in control and Mn treated cells. Subsequently, the proteins were measured to ensure that they had equal protein loaded. The cells were seeded in 96-well plates and then the cells were then fixed with 37% formaldehyde for 20 min at room temperature. Upon removing the fixing solution, the cells were washed thrice with phosphate buffered saline (PBS) [136.8 mM NaCl, 2.5 mM KCl, 1.83 mM Na_2HPO_4, and 0.43 mM KH_2PO_4 at pH 7.4]. The PBS was then removed and the cells were soaked with PBS containing 0.1% tween-20. Odyssey® blocking buffer was used as the blocking agent for 30 min. Primary antibody incubations occurred over a 1 h period with gentle shaking. Mouse monoclonal anti-SSADH (Gibson) was diluted to a concentration of 1:200 in blocking buffer. Secondary antibodies consisted of donkey anti-mouse IR 680 (Li-cor; red) was diluted to 1:1000. The cells were probed with secondary antibodies only to account for any unspecific binding and to further confirm the loading of equal amount of cells (54).

Metabolite analysis

Metabolite levels were examined by high performance liquid chromatography (HPLC) in which soluble cell free extract (CFE) was taken promptly in order to reduce any degradation products and then boiled for 10 min to precipitate proteins prior to analysis. Quenching with 60% methanol afforded similar results (56). Samples of soluble CFE were injected into an Alliance HPLC equipped with a C18 reverse-phase column (Synergi Hydro-RP; 4 μm; 250 × 4.6 mm,

Phenomenex) operating at a flow rate of 0.7 mL/min at ambient temperature. A Waters dual absorbance detector was used as described in (113). Activity bands gained by electrophoresis were excised from the gel and placed in a reaction mixture containing 2 mM substrates. After 30 min of incubation, 100 μL of the sample was removed and diluted with Milli-Q water for HPLC analysis. Mobile phase containing 20 mM KH_2PO_4 (pH 2.9) was used at a flow rate of 0.7 mL/min at ambient temperature to separate the substrates and products, which were measured at 210 nm to detect carbonyl groups. To confirm the metabolite identity biological samples were spiked with known standards, and peaks were quantified using the Empower software (Waters Corporation). Also, to confirm that glycerol was being converted to KG, 4 mg of intact cells harvested from the Mn-supplemented cultures were incubated with 10% glycerol, 10 mM NH_4Cl and 10 mM HCO_3^-. The cells were stopped after 2 h and 24 h by heating. Then, the metabolites were analysed by HPLC. To identify the metabolic pathway involved in KG synthesis the membrane CFE was reacted with glyoxylate, GABA, and HCO_3^- in the presence sodium azide. Similar experiments were performed with fumarate, HCO_3^-, and NADH as substrates.

NMR studies

To establish if indeed these enzymes were a source of succinate semi aldehyde and α-ketoglutarate, the activity bands attributable to these enzymes were incubated sequentially to the substrates and the products were assessed. 13C-NMR analyses were achieved using a Varian Gemini 2000 spectrometer operating at 50.31 MHz for 13C. Samples were analyzed with a 5 mm dual probe (35u pulse, 1-s relaxation delay, 8 kilobytes of data, and 3000 scans). Chemical shifts were established by comparing to standard compounds under equivalent conditions (52). The formation of succinate semi aldehyde was first examined by incubating the excised band of

SSDAH from the membrane CFE of Mn cultures for 1 h in phosphate reaction buffer containing (2 mM succinate labelled 13C-1, 4 and NADH). The reaction was stopped by eliminating the excised gel and heating at 60 ^{0}C. Once, the reaction was done, the products were examined by NMR. Once, the reaction was done, the products were examined by NMR. CFE was incubated with 2 mM GABA, 2 mM glyoxylate and labelled $H^{13}CO_3^-$. The presence of carboxylation of SSA into KG were monitored.

Statistical analysis

Data were expressed as means ± standard deviations (SD). Statistical correlations of the data were tested for significance using the Student t test (*p ≤ 0.05, ** p ≤ 0.01) and all experiments were performed in triplicate in biological duplicate.

Results

When *Pseudomonas fluorescens* is cultured in glycerol medium with Mn (50 μM), the microbe secretes copious amount of α-KG compared to the control cells at stationary phase of growth (104). The soluble CFE isolated at the same growth phase had more metabolites in the Mn-supplemented bacteria attributable to glyoxylate, succinate semialdehyde, GABA, 4-hydroxybutyrate and succinate. Oxaloacetate levels were relatively similar (Figure 5.1). The succinate was increased approximately two fold while GABA was nearly nine fold higher compared to the control CFE. As succinate levels were markedly higher, this prompted us to evaluate how the homeostasis of this dicarboxylic acid was maintained and whether it was utilized in the biogenesis of KG, a metabolite in the spent fluid.
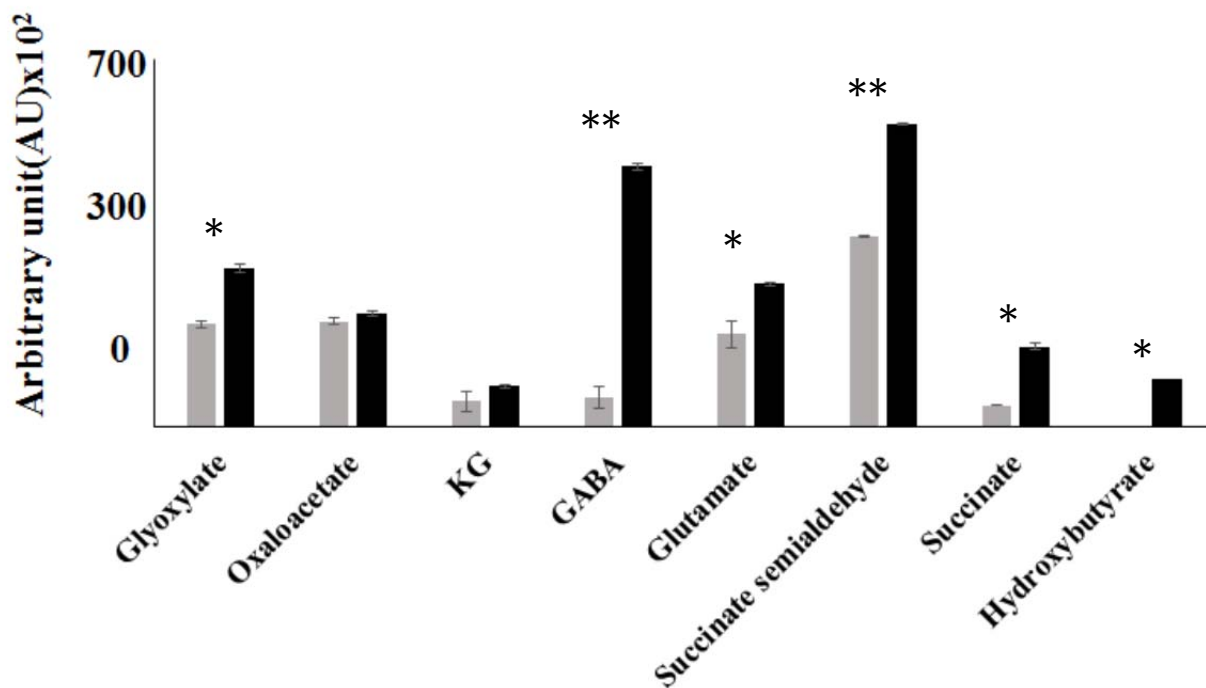
Figure 5.1: HPLC of metabolic profiles from control and Mn-treated cells (at stationary phase of growth). Data is representative of 3 experiments; Ctl=control, Mn-treated). *Denotes a statistically significant differences compared with the control (P ≤ 0.05) and**Denotes the differences (P ≤ 0.01).

The presence a glyoxylate peak in the CFE pointed to isocitrate lyase (ICL) as a possible enzyme involved in this process. Indeed in the Mn-treated cells, the activity band indicative of this enzyme was intense. No ICL activity band in the control cells was discerned after an incubation period of 30 min (Figure. 5.2A). The enzyme was inhibited by malonate. When the ICL activity band was excised and treated with the isocitrate, peaks attributed to glyoxylate and succinate were observed by HPLC (Figure. 5.2B). In order to prove if indeed this increase in enzymatic activity was due to the presence of Mn in the medium, control cells were incubated in the Mn-media and Mn-grown cells were exposed to the control culture conditions. A reversal of ICL activity was detected (Figure. 5.2C).
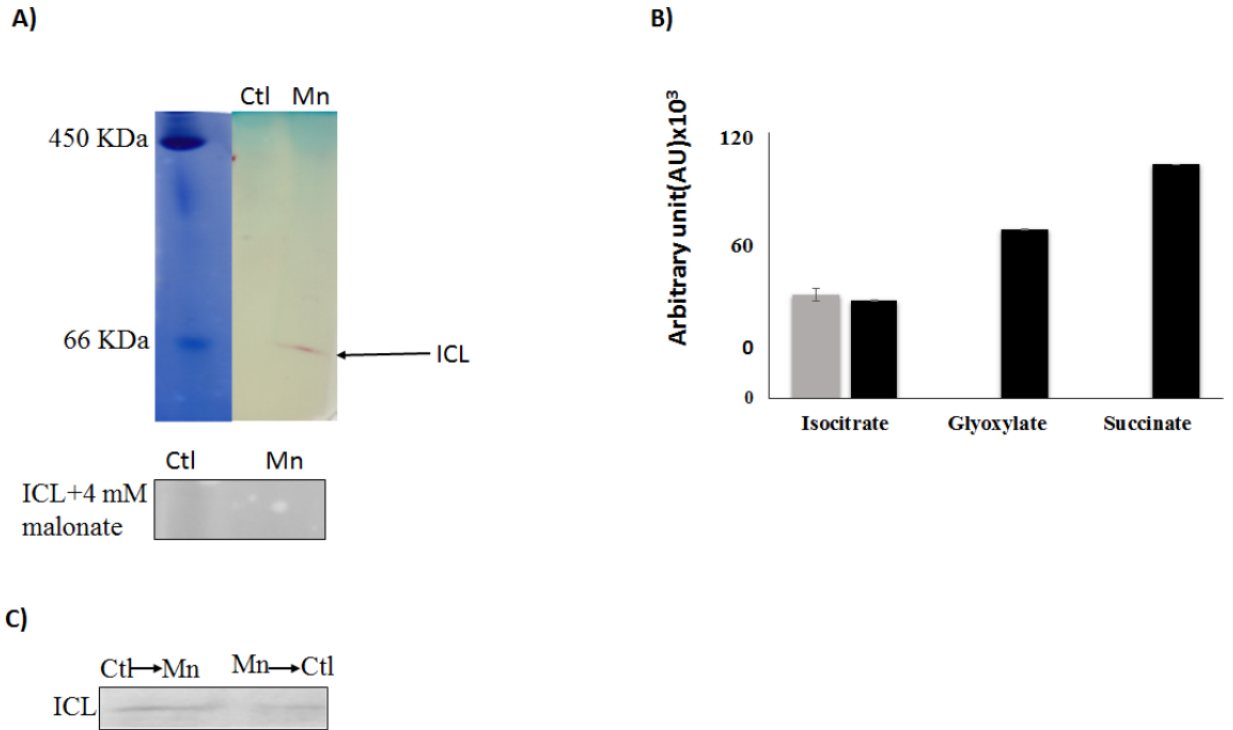
Figure 5.2: Succinate generating isocitrate lyase.

A) In-gel enzymatic activity of isocitrate lyase (ICL), Ferritin (450 KD) and BSA (66 KDa) and with inhibitor (4 mM malonate). B) HPLC analysis of Mn excised band (A) incubated in 2 mM isocitrate, 0.5 mM NAD for 30 min. Grey color: 0 min; Black color: 30 min. C) In-gel activity of ICL when control cells were incubated in Mn-cultures and Mn-treated cells were exposed to control media (Gels are representative of 3 independent experiments. Ctl = Control; Mn-treated; ICL activity band was observed in the control after extended incubation periods).

Fumarate reductase (FRD) is another enzyme that can contribute to the succinate budget. While the fumarase (FUM) was down in Mn-treated cells, the activity of FRD that mediates the conversion of fumarate into succinate with concomitant oxidation of NADH was elevated in the Mn-supplemented cultures (Figure. 5.3A, B). The maximal activity was observed at stationary phase of growth (Figure. 5.3C). The activity band attributable to FRD generated a succinate peak when incubated with fumarate and NADH (Figure. 5.3A). The synthesis of this dicarboxylic acid via KGDH did not appear to play a major role in the increased succinate observed in the cell free extracts of the Mn-supplemented cells as this enzyme was markedly

diminished (Table 5.1). Also, succinyl CoA synthetase was markedly reduced in the Mn-treated

cells (Table 5.1).
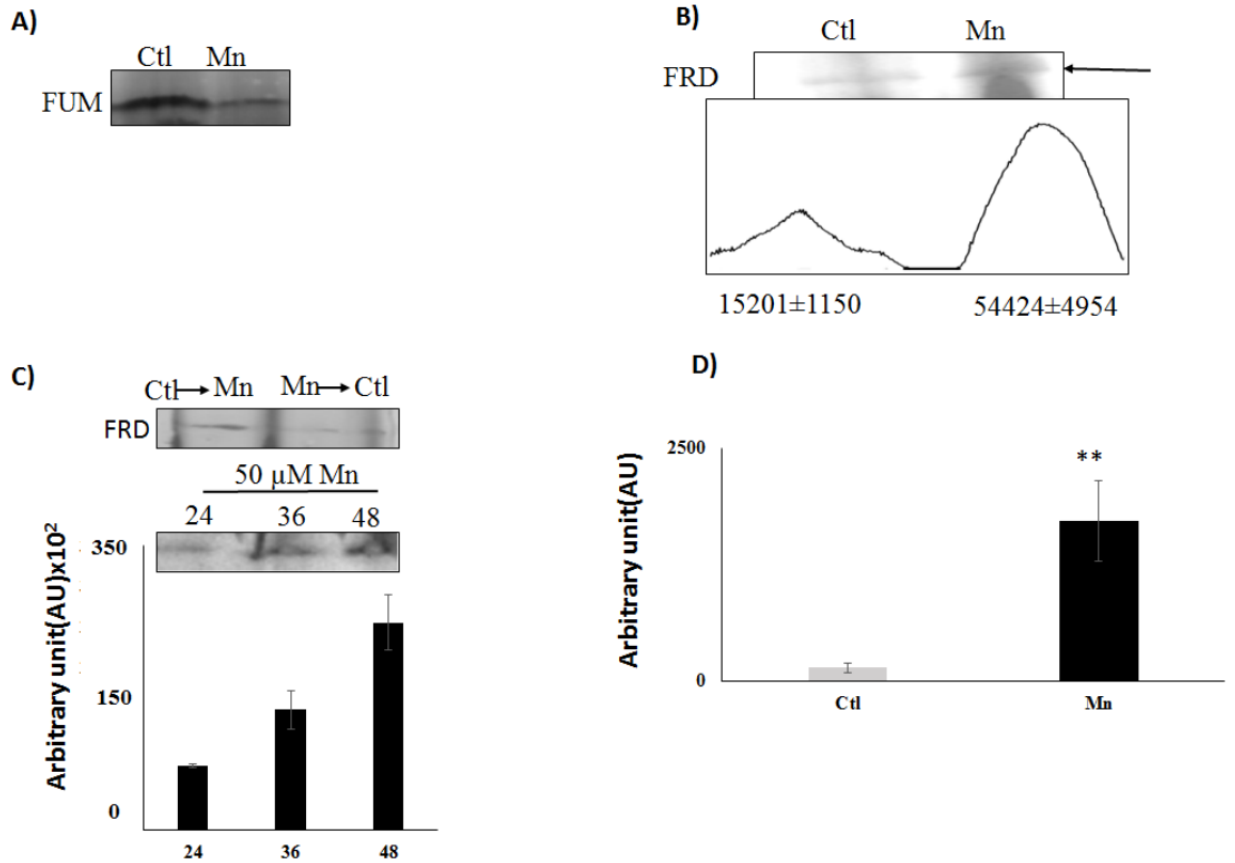
Figure 5.3: Fumarate metabolizing enzymes.

A) In-gel activity of fumarase (FUM). B) Fumarase reductase (FRD) activity BN-PAGE and densitometric reading of activity band. C) In-gel activity of FRD when control cells were incubated in Mn-cultures and Mn-treated cells were exposed to control media and activity at various time intervals with densitometric values. D) Succinate analysis by HPLC of control and Mn excised band (B) from incubated in 2 mM fumarate, 0.5 mM NADH for 1 h. Gels are representative of 3 independent experiments. Ctl = Control; Mn=Mn-treated.

Table 5.1 Enzymatic activities in the CFE from control and Mn-treated *P. fluorescens* at the same growth phase as monitored by spectrophotometry.

Enzymes	Control	Mn
Malate dehydrogenase (MDH) [a]	0.32±0.07	0.22 ±0.09
α-Ketoglutarate dehydrogenase (αKGDH)[a]	0.51±0.14	0.44±0.03
Succinate semialdehyde dehydrogenase[b]	0.45±0.19	1.58±0.33*
Succinyl-CoA synthetase[c]	0.12± 0.04	0.025±0.01*

[a] μmol NAD(P)H produced min^{-1} mg $protein^{-1}$ as monitored at 340 nm(n = 3 ± standard deviation).

[b] μmol NADH consumed min^{-1} mg $protein^{-1}$ as monitored at 340 nm(n = 3 ± standard deviation).

[c] Activity of succinyl-CoA by the consumption of CoA A412(ε= 13.6 $mM^{-1} \cdot cm^{-1}$) (n = 3 ± standard deviation).

*Denotes a statistically significant differences compared with the control ($P \leq 0.05$).

Succinate metabolism and KG synthesis

Succinate can be consumed via succinate semialdehyde dehydrogenase (SSADH) and succinate dehydrogenase (SDH). The former converts succinate into succinate semialdehyde in the presence of NADH or NADPH. This enzyme was found to be elevated in the cells grown in the presence of Mn (Figure 5.4A). Excised activity bands readily generated succinate when incubated with succinate semialdehyde and NAD or NADP (Figure 5.4B). Sodium arsenite inhibited the activity of SSADH (110). The influence of Mn on this enzyme was demonstrated by subjecting the Mn-treated cells to a control medium and the control cells to a Mn-supplemented medium. In this instance a reversal of SSADH activity was observed (Figure. 5.4C). It had a maximal activity at 48 h of growth, an incubation period coinciding with the optimal secretion of KG (104) (Figure. 5.4C). In cell Western blot assays indicated an overexpression of this protein in cells harvested from the Mn-supplemented cultures compared to

the controls (Figure. 5.4D). The ability of the SSADH to produce succinate semialdehyde was confirmed by ^{13}CNMR spectroscopy when the activity band incubated with labelled succinate ^{13}C-1, 4. The peaks indicative of aldehyde and carboxylic groups were detected (Figure. 5.4F).
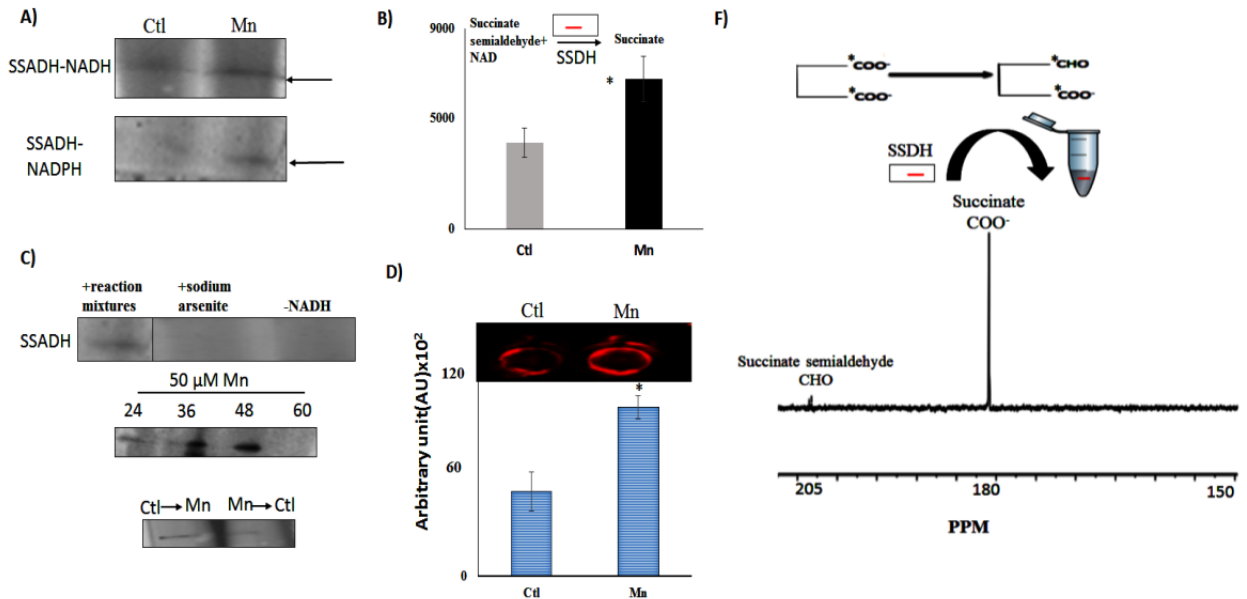
Figure 5.4: Analyses of Succinate aldehyde dehydrogenase (SSADH).

 A) In-gel enzymatic activity of succinate semialdehyde dehydrogenase (SSADH) dependent NADH and NADPH. B) HPLC analysis of succinate production of SSADH activity band incubated in 2 mM succinate semialdehyde and 0.5 mM NAD after 1 h. C) Activity of the SSADH, with inhibitor (5 mM sodium arsenite) and without cofactor NADH as negative control ; at various time intervals; D) In cell western blots with SSADH antibody (Note: the control and Mn-treated CFE were exposed to secondary antibody only in order to account for any unspecific binding and to further confirm equal loading; no change in the intensity was observed (data not shown). F) ^{13}C NMR chromatogram of SSADH excised band incubated in 1, 4 labelled succinate with NADH after 1 h (Note the aldehyde peak at 205 ppm). Gels are representative of 3 independent experiments; Ctl = Control; Mn-treated. Densitometry was performed using Image J for windows.

The presence of GABA in the CFE prompted the assessment of enzymes contributing to the SSA homeostasis. GABA aminotransaminase (GABAT) can mediate the conversion of this ketoacids into the corresponding amino-acids and SSA. Activity bands corresponding to the

transaminases converting GABA into SSA in presence of glyoxylate, pyruvate and KG were identified (Figure 5.5A). The formation of KG from glutamate and SSA that is effected by GABA-glutamate transaminase was also evident (Figure. 5.5B). HPLC experiments with the excised bands helped established the substrate-specificity of these enzymes (Figure 5.5B). Succinate semialdehyde can be converted into KG by the α-ketoglutarate decarboxylase (KDC), a biochemical transformation that necessitates the requirement of HCO_3^- (Figure. 5.5C). The activity band corresponding to this enzyme was detected in the membrane CFE by both formazan and lead carbonate precipitation. The latter detects the decarboxylation reaction while the former helps visualize the formation of SSA with INT. Also, the KDC excised band was confirmed by incubating the enzyme with KG and succinate semialdehyde production was analysed (Figure 5.5D). This enzyme was also verified by 1D BN-PAGE followed by 2D SDS. The molecular mass of 56 KDa corresponded to that reported in the literature (Figure. 5.5F) (114).
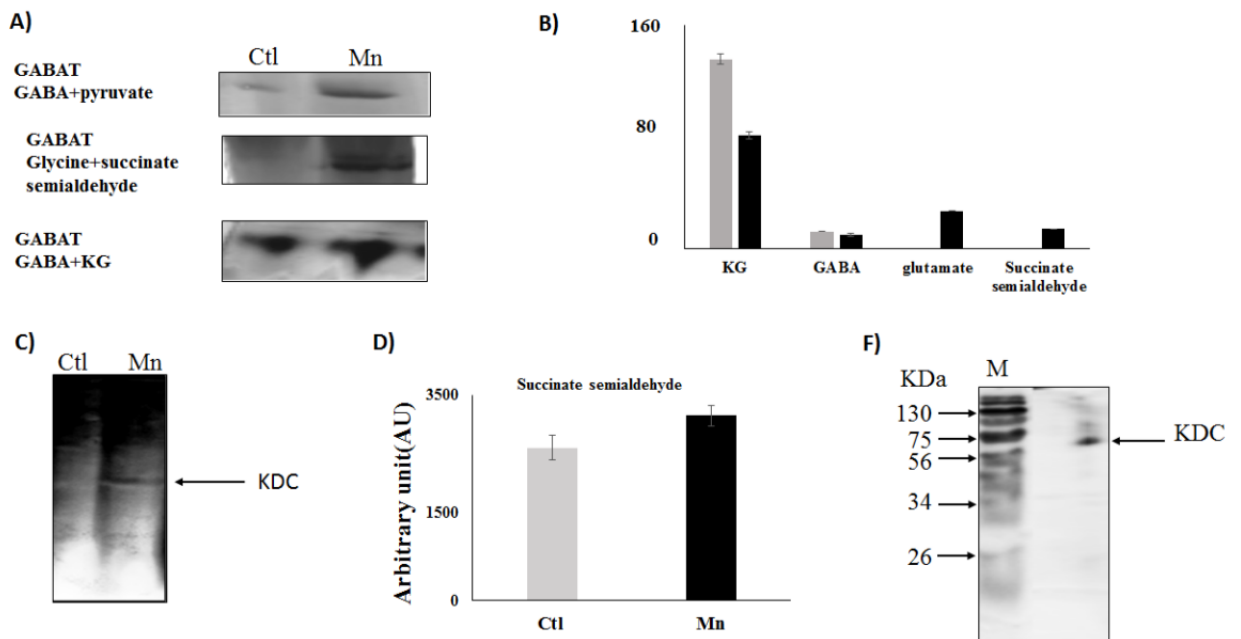
Figure 5.5: GABAT and succinate semialdehyde synthesis.

A) In-gel activity of GABAT; metabolite analysis following the incubation of GABA and pyruvate with excised band; B) In-gel activity of GABAT; product formation following the incubation of the excised band with GABA and KG. C) α- ketoglutarate decarboxylase (KDC) activity by lead nitrate precipitation. D) HPLC analyses of succinate semialdehyde production from KDC excised band incubated in 5 mM of KG after 1 h. F) 2D SDS gel of native KDC with blue Coomassie staining after 1D BN PAGE; (M: Molecular Mass KDa).

Identification of metabolic pathways: ^{13}C NMR and HPLC analyses of CFE and intact cells.

As numerous enzymes that participated in the synthesis of various metabolites leading to the production of KG were identified by BN-PAGE, it became critical to evaluate if the intact cells and/or CFE would generate metabolic fingerprint of this biochemical pathway. The incubation of the intact cells with glycerol, HCO_3^- and NH_4Cl yielded pyruvate, oxaloacetate, succinate, GABA, SSA, and KG peaks (Figure 5.6A). The membrane CFE revealed the presence of KG, oxaloacetate, SSA, and succinate in presence of fumarate, NADH and HCO_3 (Figure 6B). Also, when membrane CFE was subjected to GABA, glycine and HCO_3^-, SSA, glyoxylate and KG were produced after 1 h of incubation (Figure. 5.6C). When subjected to labelled $H^{13}CO_3$, glyoxylate and GABA, a characteristic peak at 164 ppm corresponding to 1-carboxylic group of KG was evident (Figure. 5.6D). The keto-acid was further confirmed by HPLC and DNPH assay. To limit the consumption of substrates via oxidation phosphorylation, these experiments were performed in the presence of sodium azide (5 mM).
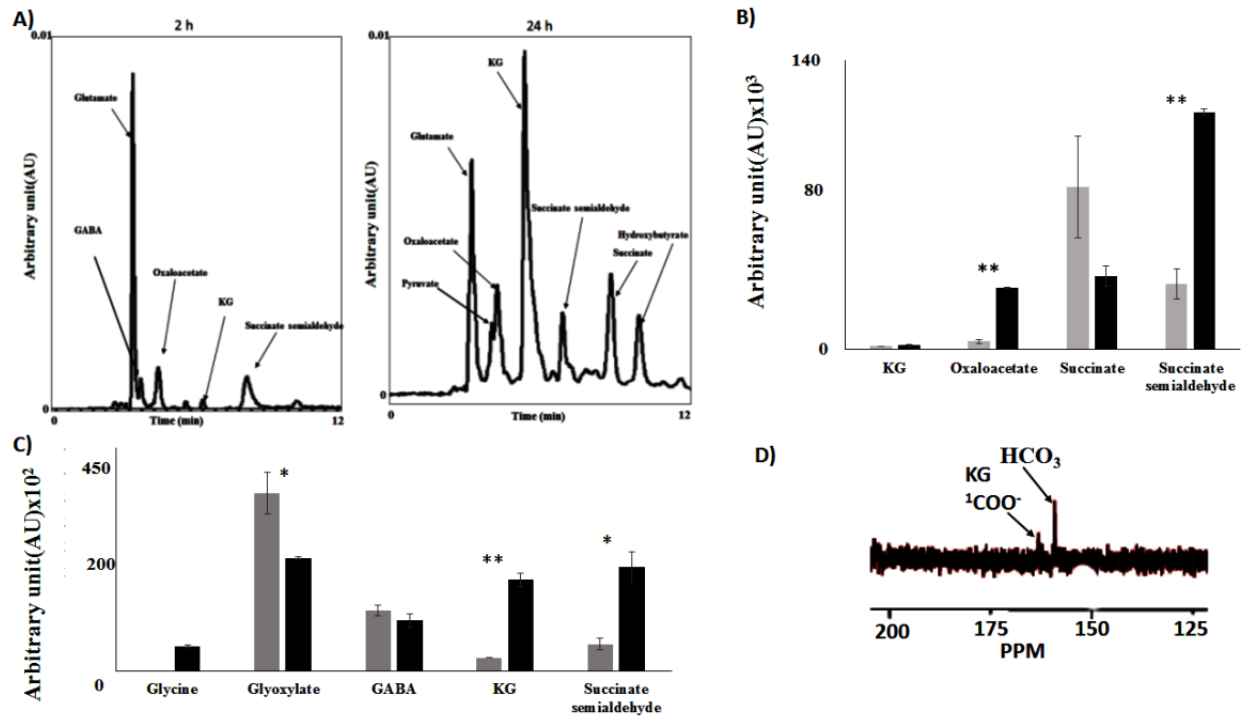
Figure 5.6: Experiments with intact cells and CFE.

A) HPLC analysis of metabolites when intact cells were incubated with glycerol and NH_4Cl. B) Membrane CFE upon incubation with fumarate HCO_3^-. C) GABA and glyoxylate. D) GABA, glyoxylate and labelled $H^{13}CO_3$.

Discussion

The data in this study point to a pivotal role of succinate and SSA in the enhanced production of KG triggered by the micro-nutrient Mn when *P. fluorescens* is grown in a mineral medium with glycerol as the sole carbon source. The biosynthesis of KG from glycerol via the reductive decarboxylation of isocitrate, a reaction mediated by the enzyme ICDH (NAD/NADP) has been reported in numerous microbial systems (94). In this instance, pyruvate carboxylase (PC) provides oxaloacetate, the precursor that fuels this metabolic process. Insertion of multiple copies of genes harbouring these two enzymes in the yeast, *Yarrowia lipolytica* resulted in 19%

78

increase in the synthesis of KG. In *P. fluorescens,* the presence of Mn triggered a 5-fold augmentation in KG formation again propelled by PC and ICDH (104). The activity of aconitase (ACN) that underwent a 2-fold increase would help replenish isocitrate, a key ingredient in this metabolic network (115).

Although ICDH and PC are critical in the conversion of glycerol into KG, the current investigation reveals that succinate, GABA and succinate semialdehyde are also key intermediates orchestrating the production of the keto-acid. The overexpression of ICL and FRD contributes to the increased formation of succinate observed in the Mn-supplemented cultures. The former produces succinate following the cleavage of isocitrate while the latter adds to the budget of the dicarboxylic acid through its interaction with fumarate and NADH (57, 60). The glyoxylate liberated when ICL reacts with isocitrate can be a source of malate that can be transformed into fumarate. FRD- fuelled production of succinate is a common strategy invoked by numerous organisms dedicated to the secretion of this moiety (60). It is important to note that ICL activity was barely evident in the control cultures and did not appear to be linked to malate synthetase (MS) as part of the glyoxylate shunt. When confronted by aluminum (Al) toxicity, *P. fluorescens* has been reported to overexpress ICL aimed at increasing the synthesis of oxalate, a metabolite known to sequester Al (32, 85, 116). Hence, it is within the realm of possibility that this microbe utilizes ICL and FRD in tandem to enhance the formation of succinate, a metabolite that is then channelled toward the synthesis of KG.

The presence of peaks in the HPLC chromatograph characteristic of SSA and GABA would argue for the involvement of these moieties in the metabolic network mediating the enhanced production of KG. SSADH and GABA transaminases are known to participate in the formation of SSA. These enzymatic activities were markedly elevated in the Mn-cultures. The

79

transamination of glyoxylate, pyruvate and oxaloacetate in the presence of GABA liberates SSA and the corresponding amino acids. SSADH reduces succinate with the aid of either NADH or NADPH. These two enzymes participate in GABA metabolism in most organisms (107, 117). The amino-carboxylic acid that is a well-documented signalling molecule is also secreted during abiotic stress in plants and bacteria. It is involved in wound healing in plants while in microbes GABA contributes to acid tolerance (118-121). The SSA generated by the concerted action of SSADH and GABA-transaminases can readily fuel the synthesis of KG, a process mediated by either KDC or GABA-glutamate transaminase. These enzymes were indeed elevated in the cultures with added Mn. The carboxylation of SSA by KDC coupled with its transamination propelled by glutamate would provide an effective pathway to KG with the concomitant formation of GABA. The later can become an ideal target of other GABA-transaminases in order to replenish the pool of SSA. KDC occurs in numerous microbes where various modified TCA cycle are operative (114, 122). KDC has a similar E1 component like KGDH but does not require any cofactors like Co-enzyme A and NAD. It can decarboxylate KG to SSA and add HCO_3^- to SSA to generate KG (114). GABA-glutamate transaminase is a critical enzyme involved in modulating the homeostasis of GABA. Following its signalling role, GABA is eliminated with assistance of this enzyme (120, 125, 126). In this instance, it may contribute to enhanced KG formation. The data with the intact cells incubated with either glycerol in the presence of HCO_3^- and NH_4^+ would argue for such a possibility. Owing to the ability of Mn to participate directly in numerous enzymatic reactions and /or to substitute metals like Mg in a variety of proteins, it is not unlikely that the abundance of this micro-nutrient may be triggering this metabolic reprogramming dedicated to KG synthesis. ICL has been reported to be influenced by this divalent metal (126). Furthermore, it may also be involved in promoting the expression of

proteins that require Mn to function (126). It has been well-established that lack of a metal represses the transcription of the corresponding metallo-proteins (127). They may help in the stabilization, modification, activation and elimination of transcription factors (128, 129). These moieties can also modulate enzymatic activities (130, 131). Oxidative and nitrosative stress are known to trigger the production of keto-acids in numerous organisms. Hence, metabolite synthesis triggered by metal nutrients and abiotic stress is not an uncommon occurrence (132-135).

In conclusion, the evidence presented in this study reveals a remarkable metabolic engineering evoked by Mn in order to transform glycerol into KG. Succinate, SSA, fumarate and GABA are the main participants driving this biochemical phenomenon with the assistance of the enzymes ICL, FRD, SSADH, GABA-aminotransaminases and KDC. To our knowledge, this is the first report on a metabolic network dedicated to the production of KG via SSA. Although the exact role of Mn and the accompanying metabolites in this metabolic reconfiguration has to await further elucidation, it is within the realm of possibility that these modulators either individually or in concert guide the metabolism of glycerol to a pathway leading to copious KG production, an observation that may have important implications for the biofuel industry.
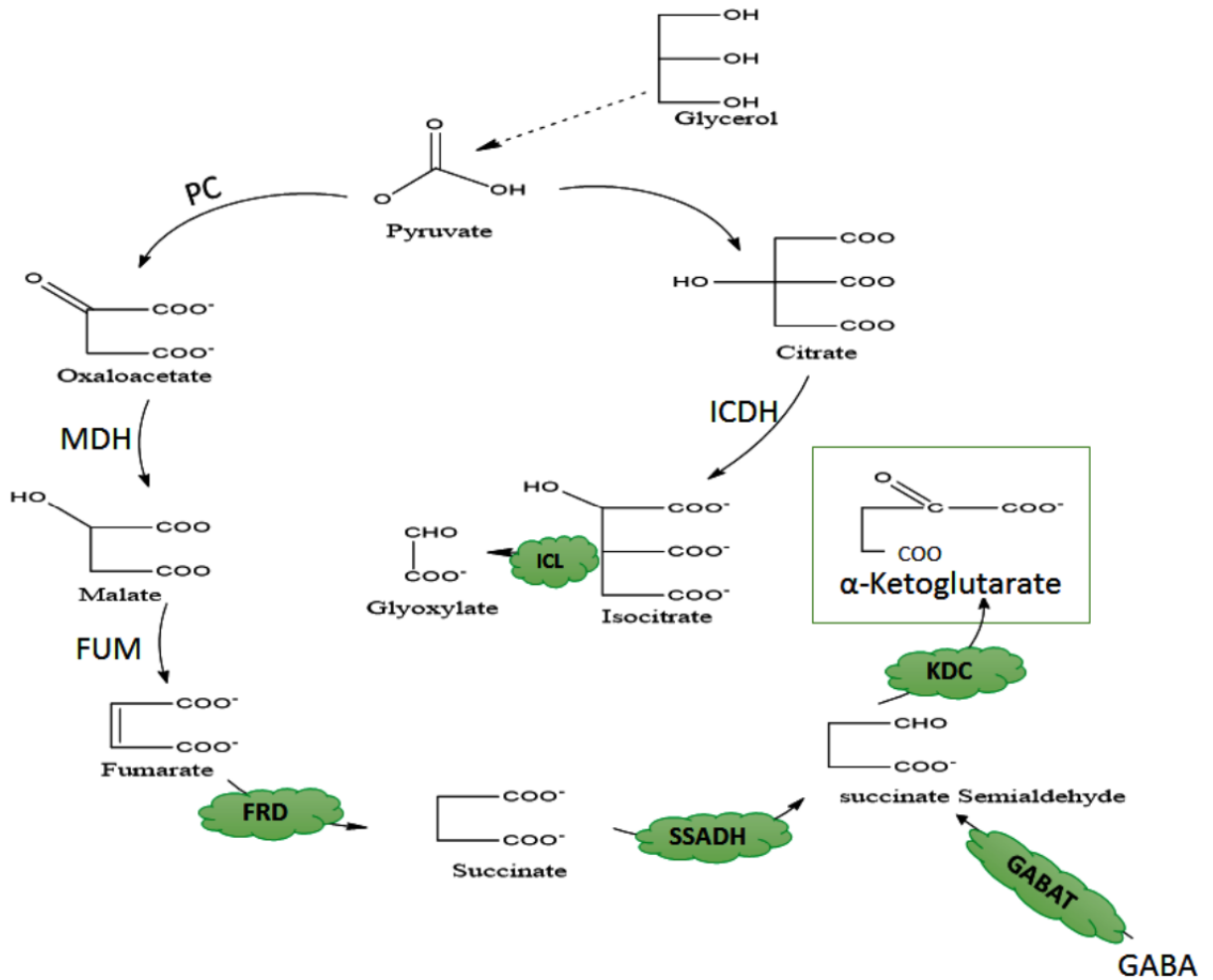
Figure 5.7: Metabolic Scheme contributing to KG production.

MDH: malate dehydrogenase; FUM: fumarase; ICDH: isocitarate dehydrogenase; ICL: isocitrate lyase; FRD: fumarate reductase; SSADH: succinate semialdehyde dehydrogenase; KDC: ketoglutarate dehydrogenase and GABAT: GABA aminotransaminase.

Acknowledgement:

6. Conclusions and future directions

The search for renewable energy has prompted scientists to incorporate physical, chemical and biochemical approaches to find the proper solution. The upcoming energy economy will likely be established on a wide-ranging of substitute energy platforms including wind, water, sun, nuclear fission and fusion, as well as biomass. Thus, the reliance on petroleum can be alleviated due to the possibility of converting renewable and readily available biomass to value-added commodities. Changing society's dependence from non-renewable fossil fuel to renewable biomass-based energy is commonly seen as key to the expansion of a maintainable industrial progress, energy independence, and to the active controlling of greenhouse gas emissions (31). Biomass is utilized as feedstock to produce biofuels such as bioethanol and biodiesel.

Biodiesel can be a critical substitute fuel, however its processing generates crude glycerol as a waste by-product. The bioconversion of glycerol waste to valuable products is a viable approach that can make the biodiesel industry more economically and environmentally competitive. With the advent of directed advancement and biological strategies, bioconversion methods appear to be a feasible source of economic expansion. This approach also helps maintain the delicate environmental balance (23). The biodiesel industry, which is supplying a significant amount of global energy can be more effective if glycerol, a by-product can be converting to value added products. Recently, direct use of glycerol from biodiesel industry in agriculture and as livestock feed has attracted much attention. However, crude glycerol in huge quantities can pose a hazard to the environment. Therefore, there is a necessity to transform this crude glycerol into economic products using biotechnological routes. Glycerol-derived from the

biodiesel industry can be used as a raw material for biopolymers, polyunsaturated fatty acids, ethanol, hydrogen and n-butanol production (23).

Much consideration has been given to microorganisms, which have the potential to substitute our dependence on fossil fuels. Such research will broaden our knowledge of microbial technology and will provide an economical and environmentally-friendly alternate for the production of chemicals. Although genetic enrichments have been employed in an effort to diminish inhibitory by-products or increase the consumption of glycerol (136), genetically modified organisms have inherent threats and necessitate strict control mechanisms (137). Environmental modulation can improve the trait by natural means as well as has more economical advantages. This can be fulfilled by using microbes subjected to a variety of stressors aimed at increasing the production of desired products. Metabolic engineering is one of the foremost strategies dedicated to channeling the power of a specific pathway to produce industrial goods.

The H_2O_2 stress that contributes to increase pyruvate synthesis in *P. fluorescens* may offer a facile approach to adapt microbial systems for this job. It seems that the metabolic reconfiguration provoked by the oxidant powers the bacterium to fulfil its ATP needs via substrate-level phosphorylation with the associated secretion of pyruvate. This alternate ATP-producing scheme contributes to the synthesis of various amounts of PEP and pyruvate. The production of these metabolites is achieved via the enhanced activities of numerous enzymes including pyruvate carboxylase (PC) and phosphoenolpyruvate carboxylase (PEPC). The high-energy PEP is consequently transformed into ATP with the aid of pyruvate phosphate dikinase (PPDK), phosphoenolpyruvate synthase (PEPS) and pyruvate kinase (PK) with the concomitant formation of pyruvate. This by-product of the metabolic shift is indeed a value-added product

84

with several uses. The involvement of the phosphotransfer enzymes like adenylate kinase (AK) and acetate kinase (ACK) ensures the efficacy of this O_2-independent energy-producing system. Hence, the H_2O_2-prompted metabolic changes in this microbe can provide a green means of producing biochemicals with wide-ranging applications.

Micro-nutrient supplementation such manganese (Mn) can also alter metabolic machinery leading to the accumulation to desired products. This divalent metal is essential for the optimal activity of a variety of enzymes including pyruvate carboxylase (PC), pyruvate kinase (PK), and phosphoenol pyruvate carboxylase (PEPC) that are critical for the metabolism of glycerol. The ability of *Pseudomonas fluorescens* to produce copious amounts of ketoglutarate is achieved by supplementing the glycerol media with Mn. The increased activities of isocitrate dehydrogenase (ICDH)-(NAD)P dependent and aminotransaminases facilitated the exocellular secretion of ketoglutarate. The overexpression of pyruvate carboxylase (PC) that is evident in the Mn-treated cells provides oxaloacetate, an essential precursor that fuels the production of KG.

Another metabolic network propelled by enzymes like isocitrate lyase (ICL), fumarate reductase (FUMR) and GABA transaminases (GABAT) also contributes to the copious synthesis of α-ketoglutarate. In this instance, succinate is funneled toward the keto-acid with the aid of succinate semialdehyde dehydrogenase (SSADH) and α-ketoglutarate decarboxylase (KGD). The former converts succinate into succinate semialdehyde. The latter is also generated via the transamination of GABA. This intermediate is subsequently transformed into KG by the addition of CO_2 with the assistance of KDC. Hence, these two abiotic modulators H_2O_2 and Mn evoke disparate metabolic shifts resulting into two distinct glycerol-derived metabolites that are of economic benefit.

Figure 6.1: Abiotic modulators and the metabolic networks leading to glycerol-derived ketoacids

These findings can be applied to operate in a bioreactor of 100 L with the aid of immobilized cells. Various physico-chemical parameters can be monitored to ensure the efficacy of this process in converting industrial glycerol into pyruvate and KG. Additionally, the participation of other mineral nutrients like Ca, Co, Cr and Fe can be utilized to ascertain if other valuable metabolites can be generated. Alternate pathways essential for the synthesis of commercially important chemicals can be assessed. It has been show that some microbes can produce lactic acid in the presence of Cu, Zn, and Fe (138). Additionally, nutrient starvation is another promising route for production of viable products naturally. Studies have shown chemoheterotrophic marine bacteria produced methane under phosphate starvation (139). Furthermore, the influence of different concentrations of glycerol on the growth, metabolism and adaptation capability of *P. fluorescens* can be evaluated. It has been reported that *C. butyricum*

DSP1 can grow in 70 g/L crude glycerol without significant decrease in biomass (136). Metabolic flux can also be assessed with the aid of software tools like MatLab to optimize the generation of desired products. Microbe-driven technologies have lot to offer to the energy sector.
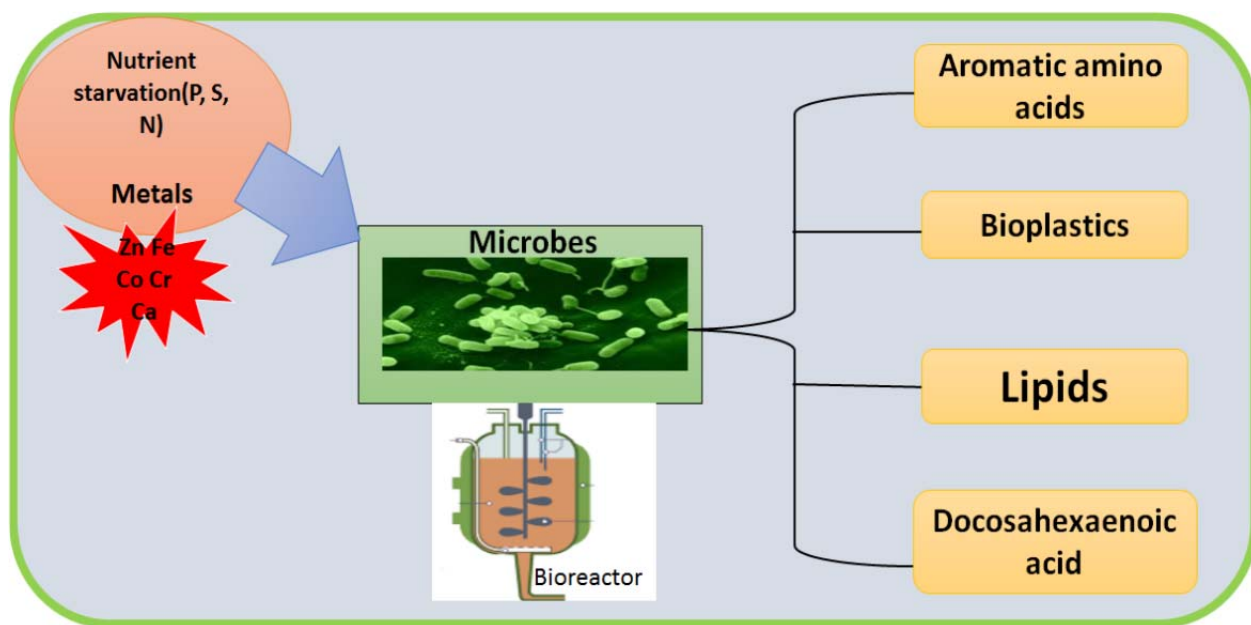
Figure 6.2: Future studies on the production and optimization of valuable products from glycerol in *P. fluorescens*.

7. References:

1. History: Energy Information Administration (EIA), International Energy Annual 2004 (May-July 2006), web site www.eia.doe.gov/iea. Projections: EIA, System for the Analysis of Global Energy Markets (2007).

2. Dellomonaco, C., Fava, F., Gonzalez, R. (2010). The path to next generation biofuels: successes and challenges in the era of synthetic biology. Microb Cell Fact 9, 1-15.

3. McKendry, P. (2002). Energy production from biomass (part 1): overview of biomass. Bioresour Technol 83, 37-46.

4. Erickson, B., Winters, P. (2012). Perspective on opportunities in industrial biotechnology in renewable chemicals. Biotechnol J 7, 176-185.

5. Bomb, C., McCormick, K., Deurwaarder, E., Kåberger, T. (2007). Biofuels for transport in Europe: Lessons from Germany and the UK. Energy Policy 35, 2256-2267.

6. Larsen, U., Johansen, T., Schramm, J. (2009). Ethanol as a fuel for road transportation. Main Report. IEA-AMF report 100, 1-87.

7. Balat, M., Balat, H., Öz, C. (2008). Progress in bioethanol processing. Progr Energy Combust Sci 34, 551-573.

8. Van Zyl, W. H., Chimphango, F.A., Den Haan, R., Görgens, J. F., Chirwa, P. W. C. (2011). Next-generation cellulosic ethanol technologies and their contribution to a sustainable Africa. Interface Focus 1, 196-211.

9. Li, C., Lesnik, K. L., Liu, H. (2013). Microbial conversion of waste glycerol from biodiesel production into value-added products. Energies 6, 4739-4768.

10. Yang, F., Hanna, M. A., Sun, R. (2012). Value-added uses for crude glycerol--a byproduct of biodiesel production. Biotechnol Biofuels 5, 13.

11. Gerpen, J. V. (2005). Biodiesel processing and production. Fuel Process Technol 86, 1097-1107.

12. Anand, P., Saxena, R. K. (2012). A comparative study of solvent-assisted pretreatment of biodiesel derived crude glycerol on growth and 1, 3-propanediol production from *Citrobacter freundii*. N Biotechnol 29, 199-205.

13. Nanda, M. R., Yuan, Z., Qin, W., Poirier, M. A., Chunbao, X. (2014). Purification of crude glycerol using acidification: effects of acid types and product characterization. Austin J Chem Eng 1, 1-7.

14. Sivasankaran, C., Ramanujam, P. K., Balasubramanian, B., Mani, J. (2016). Recent progress on transforming crude glycerol into high value chemicals: a critical review. Biofuels, 1-6.

15. Leoneti, A. B., Aragao-Leoneti, V., De Oliveira, S. V. W. B. (2012). Glycerol as a by-product of biodiesel production in Brazil: Alternatives for the use of unrefined glycerol. Renew Energy 45, 138-145.

16. Chen, Z., Liu, D. (2016). Toward glycerol biorefinery: metabolic engineering for the production of biofuels and chemicals from glycerol. Biotechnol Biofuels 9, 205.

17. Okoye, P. U., Hameed, B. H. (2016). Review on recent progress in catalytic carboxylation and acetylation of glycerol as a byproduct of biodiesel production. Renew Sustain Energy Rev 53, 558-574.

18. Bagheri, S., Julkapli, N. M., Yehye, W. A. (2015). Catalytic conversion of biodiesel derived raw glycerol to value added products. Renew Sustain Energy Rev 41, 113-127.

19. Wilkens E., Ringel A. K., Hortig D., Willke T., Vorlop K. D. (2012). High-level production of 1,3-propanediol from crude glycerol by *Clostridium butyricum* AKR102a. Appl Microbiol Biotechnol 93, 1057-1063.

20. Clomburg, J. M., Gonzalez, R. (2011). Metabolic engineering of *Escherichia coli* for the production of 1, 2-propanediol from glycerol. Biotechnol Bioeng 108, 867-879.

21. Oh, B. R., Heo, S. Y., Lee, S. M., Hong, W. K., Park, J. M., Jung, Y. R., Kim, C. H. (2014). Erratum to: Production of isobutanol from crude glycerol by a genetically-engineered *Klebsiella pneumoniae* strain. Biotechnol Lett 36, 397-402.

22. Rywińska, A., Rymowicz, W., Żarowska, B., Skrzypiński, A. (2010). Comparison of citric acid production from glycerol and glucose by different strains of *Yarrowia lipolytica*. World J Microbiol Biotechnol 26, 1217-1224.

23. Garlapati, V. K., Shankar, U., Budhiraja, A. (2016). Bioconversion technologies of crude glycerol to value added industrial products. Biotechnol Rep 9, 9-14.

24. Szymanowska-Powałowska, D., Kubiak, P. (2015). Effect of 1, 3-propanediol, organic acids, and ethanol on growth and metabolism of *Clostridium butyricum* DSP1. Appl Microbiol Biotechnol 99, 3179-3189.

25. Teeka, J., Imai, T., Reungsang, A., Cheng, X., Yuliani, E., Thiantanankul, J., Yamamoto, K. (2012). Characterization of polyhydroxyalkanoates (PHAs)

biosynthesis by isolated *Novosphingobium* sp. THA_AIK7 using crude glycerol. J Ind Microbiol Biotechnol 39, 749-758.

26. Naranjo, J. M., Posada, J. A., Higuita, J. C., Cardona, C. A. (2013). Valorization of glycerol through the production of biopolymers: The PHB case using *Bacillus megaterium*. Bioresour Technol 133, 38-44.

27. Fu, W., Mathews, A. P. (1999). Lactic acid production from lactose by *Lactobacillus plantarum*: kinetic model and effects of pH, substrate, and oxygen. Biochem Eng J 3, 163-170.

28. Coelho, L. F., De Lima, C. J. B., Rodovalho, C. M., Bernardo, M. P., Contiero, J. (2011). Lactic acid production by new *Lactobacillus plantarum* LMISM6 grown in molasses: optimization of medium composition. Braz J Chem Eng 28, 27-36.

29. Del Pozo, J. C., Allona, I., Rubio, V., Leyva, A., De La Peña, A., Aragoncillo, C., Paz-Ares, J. (1999). A type 5 acid phosphatase gene from *Arabidopsis thaliana* is induced by phosphate starvation and by some other types of phosphate mobilising/oxidative stress conditions. Plant J 19, 579-589.

30. Aislabie, J., Saul, D. J., Foght, J. M. (2006). Bioremediation of hydrocarbon-contaminated polar soils. Extremophiles 10, 171-179.

31. FitzPatrick, M., Champagne, P., Cunningham, M. F., Whitney, R. A. (2010). A biorefinery processing perspective: treatment of lignocellulosic materials for the production of value-added products. Bioresour Technol 101, 8915-8922.

32. Alhasawi, A., Appanna, N. D, Auger, A., Appanna, V. (2015). Metabolic networks involved in the decontamination of a multiple metal environment by *Pseudomonas fluorescens*. J Biotechnol 200, 38-43.

33. Simões, M., Simões, L. C., Vieira, M. J. (2008). Physiology and behavior of *Pseudomonas fluorescens* single and dual strain biofilms under diverse hydrodynamics stresses. Int J Food Microbiol 128, 309-316.

34. Jaleel, C. A., Manivannan, P., Sankar, B., Kishorekumar, A., Gopi, R., Somasundaram, R., Panneerselvam, R. (2007). *Pseudomonas fluorescens* enhances biomass yield and ajmalicine production in *Catharanthus roseus* under water deficit stress. Colloids Surf B Biointerfaces 60, 7-11.

35. Amelio, I., Cutruzzolá, F., Antonov, A., Agostini, M., Melino, G. (2014). Serine and glycine metabolism in cancer. Trends Biochem Sci 39, 191-198.

36. Alhasawi, A., Castonguay, Z., Appanna, N.D., Auger, C., Appanna, V.D. (2015). Glycine metabolism and anti-oxidative defence mechanisms in *Pseudomonas fluorescens*. Microbiological Res 171, 26-31.

37. Mailloux, R., Lemire, J., Appanna, V.D. (2011). Metabolic networks to combat oxidative stress in *Pseuodomonas fluorescens*. Antonie van Leeuwenhoek J Microbiol 99, 433-442.

38. Chénier, D., Bériault, R., Mailloux, R., Baquie, M., Abramia, G., Lemire, J., Appanna, V. D. (2008). Metabolic adaptation in *Pseudomonas fluorescens* evoked by aluminum and gallium toxicity: involvement of fumarase C and NADH oxidase. Appl Environ Microbiol 74, 3977- 84.

39. Höper, D., Bernhardt, J., Hecker, M. (2006). Salt stress adaptation of *Bacillus subtilis*: a physiological proteomics approach. Proteomics 6, 1550-1562.

40. Bériault, R., Hamel, R., Chénier, D., Mailloux, R., Joly, J., Appanna, V. D. (2007). The overexpression of NADPH-producing enzymes counters the oxidative stress evoked by gallium, an iron mimetic. Biometals 20, 165-176.

41. Bignucolo, A., Appanna, V.P., Thomas, S. C., Auger, C., Han, S., Omri, A., Appanna, V. D. (2013). Hydrogen peroxide stress provokes a metabolic reprogramming in *Pseudomonas fluorescens*: enhanced production of pyruvate. J Biotechnol 167, 309-15.

42. Appanna, V. D. Preston, C. M. (1987). Manganese elicits the synthesis of a novel exopolysaccharide in an arctic Rhizobium. FEBS let 215, 79-82.

43. Zeller, T., Klug, G. (2004). Detoxification of hydrogen peroxide and expression of catalase genes in Rhodobacter. Microbiology 150, 3451-62.

44. Bruno-Bárcena, J. M., Azcárate-Peril, M. A., Hassan, H. M. (2010). Role of antioxidant enzymes in bacterial resistance to organic acids. Appl Environ Microbiol 76, 2747-53.

45. Sato, I., Shimizu, M., Hoshino, T., Takaya, N. (2009). The glutathione system of *Aspergillus nidulans* involves a fungus-specific glutathione S-transferase. J Biol Chem 284, 8042-53.

46. Singh, R., Mailloux, R. J., Puiseux-Dao, S., Appanna, V. D. (2007). Oxidative stress evokes a metabolic adaptation that favors increased NADPH synthesis and decreased NADH production in *Pseudomonas fluorescens*. J Bacteriol 189, 6665-6675.

47. Singh, R., Lemire, J., Mailloux, R.J., Appanna, V.D. (2008). A novel strategy involved anti-oxidative defense: the conversion of NADH into NADPH by a metabolic network. PLoS One 3, e2682.

48. Sandoval, J. M., Arenas, F.A., Vásquez, C. C. (2011). Glucose-6-phosphate dehydrogenase protects *Escherichia coli* from tellurite-mediated oxidative stress. PLoS One 6, e25573.

49. Middaugh, J., Hamel, R., Jean-Baptiste, G., Beriault, R., Chenier, D., Appanna, V.D. (2005). Aluminum triggers decreased aconitase activity via Fe-S cluster disruption and the overexpression of isocitrate dehydrogenase and isocitrate lyase: a metabolic network mediating cellular survival. J Biol Chem 280, 3159-3165.

50. Kim, D., Yu, B. J., Kim, J. A., Lee, Y., Choi, S., Kang, S. (2003). The acetyl proteome of Gram-positive model bacterium *Bacillus subtilis*. Proteomics 13, 1726-1736.

51. Han, S., Auger, C., Castonguay, Z., Appanna, V. P., Thomas, S. C., Appanna, V. D. (2013). The unravelling of metabolic dysfunctions linked to metal-associated diseases by blue native polyacrylamide gel electrophoresis. Anal Bioanal Chem 405, 1821-1831.

52. Singh, R., Lemire, J., Mailloux, R. J., Chénier, D., Hamel, R., Appanna, V.D. (2009). An ATP and oxalate generating variant tricarboxylic acid cycle counters aluminum toxicity in *Pseudomonas fluorescens*. PLoS One 4, e7344.

53. Auger, C., Appanna, V., Castonguay, Z., Han, S., Appanna, V. D. (2012). A facile electrophoretic technique to monitor phosphoenolpyruvate-dependent kinases. Electrophoresis 33, 1095-1101.

54. Auger, C., Lemire, J., Cecchini, D., Bignucolo, A., Appanna, V. D. (2011). The metabolic reprogramming evoked by nitrosative stress triggers the anaerobic utilization of citrate in *Pseudomonas fluorescens*. PloS One 6, e28469.

55. Anderson, S., Appanna, V. D., Huang, J., Viswanatha, T. (1992). A novel role for calcite in calcium homeostasis. FEBS let 308, 94-96.

56. Alhasawi, A., Leblanc, M., Appanna, N. D., Auger, C., Appanna, V.D. (2015). Aspartate metabolism and pyruvate homeostasis triggered by oxidative stress in *Pseudomonas fluorescens*: a functional metabolomics study. Metabolomics 11, 1792-1801.

57. Thomas, S. C., Alhasawi, A., Auger, C., Omri,A., Appanna, V. D. (2015). The role of formate in combatting oxidative stress. Antonie van Leeuwenhoek 2015, 1-9.

58. Bradford, M. M. (1976). A Rapid and sensitive method for the quantitation of microgram quantities of protein utilizing the principle of protein-dye binding. Anal Biochem 72, 248-254.

59. Schägger, H., von Jagow, G. (1991). Blue native electrophoresis for isolation of membrane protein complexes in enzymatically active form. Anal Biochem 199, 223-231.

60. Auger, C., Appanna, V. D. (2014). A novel ATP-generating machinery to counter nitrosative stress is mediated by substrate-level phosphorylation. Biochimica Biophysica Acta (BBA) 1850, 43-50.

61. Kuhn, J., Müller, H., Salzig, D., Czermak, P. (2015). A rapid method for an offline glycerol determination during microbial fermentation. Electr J Biotechnol 18, 252-255.

62. Da Silva, G.P., Mack, M., Contiero, J. (2009). Glycerol: a promising and abundant carbon source for industrial microbiology. Biotechnol Adv 27, 30-39.

63. Suhaimi, S.N., Phang, L. Y., Maeda, Abd-Aziz, S., Wakisaka, M., Shirai, Y., Hassan, M. A. (2012). Bioconversion of glycerol for bioethanol production using isolated *Escherichia coli* SS1. Braz J Microbiol 43, 506-516.

64. Szpetnar, M., Luchowska-Kocot, D., Boguszewska-Czubara, A., Kurzepa, J. (2016). The influence of manganese and glutamine intake on antioxidants and neurotransmitter amino acids levels in rats' brain. Neurochem Res 41, 2129-2139.

65. Aschner, J. L., Aschner, M. (2005). Nutritional aspects of manganese homeostasis. Mol Aspects Med 26, 353-362.

66. Kumar, M., Gayen, K. (2011). Developments in biobutanol production: new insights. Appl Ener 88, 1999-2012.

67. Hoekman, S. K. (2009). Biofuels in the US-challenges and opportunities. Renew Ener 34, 14-22.

68. Behera, S., Singh, R., Arora, R., Sharma, N. K., Shukla, M., Kumar, S. (2014). Scope of algae as third generation biofuels. Front Bioeng Biotechnol 2, 90.

69. Saxena, R. C., Adhikari, D. K., Goyal, H. B. (2009). Biomass-based energy fuel through biochemical routes: a review. Renew Sust Energ Rev 13, 167-178.

70. Ullah, K., Ahmad, M., Sharma, V. K., Lu, P., Harvey, A., Zafar, M., Anyanwu, C. N. (2014). Algal biomass as a global source of transport fuels: Overview and development perspectives. Prog Nat Sci Mater Int 24, 329-339.

71. Elkins, J.G., Raman, B., Keller, M. (2010). Engineered microbial systems for enhanced conversion of lignocellulosic biomass. Curr Opin Biotechnol 21, 657-662.

72. Papagianni, M. (2012). Recent advances in engineering the central carbon metabolism of industrially important bacteria. Microb Cell Fact 11, 1-13.

73. Liao, J. C., Mi, L., Pontrelli, S., Luo, S. (2016). Fuelling the future: microbial engineering for the production of sustainable biofuels. Nat Rev Microbiol 14, 288-304.

74. Suero, S. R., Ledesma, B., Álvarez-Murillo, A., Al-Kassir, A., Yusaf, T. (2015). Glycerin, a Biodiesel by-product with potentiality to produce hydrogen by steam gasification. Energies 8, 12765-12775.

75. Luna, C., Verdugo, C., Sancho, E. D., Luna, D., Calero, J., Posadillo, A., Romero, A. A. (2014). Production of a biodiesel-like biofuel without glycerol generation, by using Novozym 435, an immobilized *Candida antarctica* lipase. Bioresour Bioprocess 1, 1-11.

76. Johnson, D. T, Taconi, K. A. (2007). The glycerin glut: Options for the value-added conversion of crude glycerol resulting from biodiesel production. Environ Prog 26, 338-348.

77. Fan, X., Chen, R., Chen, L., Liu, L. (2016). Enhancement of alpha-ketoglutaric acid production from l-glutamic acid by high-cell-density cultivation. J Mol Catal B: Enzym 126, 10-17.

78. Appanna, V. D. (1988). Alteration of exopolysaccharide composition in *Rhizobium meliloti* JJ-1 exposed to manganese. FEMS Microbiol Lett 50, 141-144.

79. Kehres, D. G., Maguire, M. E. (2003). Emerging themes in manganese transport, biochemistry and pathogenesis in bacteria. FEMS Microbiol Rev 27, 263-290.

80. Jakubovics, N.S., Jenkinson, H.F. (2001). Out of the iron age: new insights into the critical role of manganese homeostasis in bacteria. Microbiology 147, 1709-1718.

81. Culotta, V. C., Daly, M. J. (2013). Manganese complexes: diverse metabolic routes to oxidative stress resistance in prokaryotes and yeast. Antioxid Redox Signal 19, 933-944.

82. Appanna, V. D. (1988). Stimulation of exopolysaccharide production in *Rhizobium meliloti* JJ-1 by manganese. Biotechnol lett 10, 205-206.

83. Otto, C., Yovkova, V., Barth, G. (2011). Overproduction and secretion of α-ketoglutaric acid by microorganisms. Appl Microbiol Biotechnol 92, 689-695.

84. Hamel, R., Appanna, V. D. (2003). Aluminum detoxification in *Pseudomonas fluorescens* is mediated by oxalate and phosphatidylethanolamine. Biochim Biophys Acta (BBA) 1619, 70-76.

85. Hamel, R., Appanna, V. D., Viswanatha, T., Puiseux-Dao, S. (2004). Overexpression of isocitrate lyase is an important strategy in the survival of

Pseudomonas fluorescens exposed to aluminum. Biochem Biophys Res Commun 317, 1189-1194.

86. Appanna, V. D., Gazs, L. G., Pierre, M. S. (1996). Multiple-metal tolerance in *Pseudomonas fluorescens* and its biotechnological significance. J Biotechnol 52: 75-80.

87. Frank, J., Pompella, A., Biesalski, H. K. (2000). Histochemical visualization of oxidant stress. Free Radical Biol Med 29, 1096-1105.

88. Lietzan, A. D., Maurice, M. S. (2013). Insights into the carboxyltransferase reaction of pyruvate carboxylase from the structures of bound product and intermediate analogs. Biochem Biophys Res Commun 441, 377-382.

89. Whittaker, J. W. (2002). Prokaryotic manganese superoxide dismutases. Methods Enzymol 349, 80-90.

90. Igarashi, T., Kono, Y., Tanaka, K. (1996). Molecular cloning of manganese catalase from *Lactobacillus plantarum*. J Biol Chem 271, 29521-29524.

91. Tseng, H. J., Srikhanta, Y., McEwan, A. G., Jennings, M. P. (2000). Accumulation of manganese in Neisseria gonorrhoeae correlates with resistance to oxidative killing by superoxide anion and is independent of superoxide dismutase activity. Mol Microbiol 40, 1175-118.

92. Zeczycki, T. N., Menefee, A. L., Jitrapakdee, S., Wallace, J. C., Attwood, P. V., St. Maurice, M., Cleland, W. W. (2011). Activation and inhibition of pyruvate carboxylase from *Rhizobium etli*. Biochem 50, 9694-9707.

93. Adina-Zada, A., Jitrapakdee, S., Wallace, J. C., Attwood, P. V. (2014). Coordinating role of His216 in MgATP binding and cleavage in pyruvate carboxylase. Biochem 53, 1051-1058.

94. Yovkova, V., Otto, C., Aurich, A., Mauersberger, S., Barth, G. (2014). Engineering the α-ketoglutarate overproduction from raw glycerol by overexpression of the genes encoding NADP-dependent isocitrate dehydrogenase and pyruvate carboxylase in *Yarrowia lipolytica*. Appl Microbiol Biotechnol 98, 2003-2013.

95. Lietzan, A. D., Maurice, M. S. (2013). A substrate-induced biotin binding pocket in the carboxyltransferase domain of pyruvate carboxylase. J Biolog Chem 288, 19915-19925.

96. Li, Q., Chen, L. S., Jiang, H. X., Tang, N., Yang, L. T., Lin, Z. H., Yang, G. H. (2010). Effects of manganese-excess on CO_2 assimilation, ribulose-1, 5-bisphosphate carboxylase/oxygenase, carbohydrates and photosynthetic electron transport of leaves, and antioxidant systems of leaves and roots in *Citrus grandis* seedlings. BMC Plant Boil 10, 42-10.

97. Mailloux, R. J., Puiseux-Dao, S., Appanna, V. D. (2009). α-ketoglutarate abrogates the nuclear localization of HIF-1α in aluminum-exposed hepatocytes. Biochimie 91, 408-415.

98. Husain, A., Sato, D., Jeelani, G., Soga, T., Nozaki, T. (2012). Dramatic increase in glycerol biosynthesis upon oxidative stress in the anaerobic protozoan parasite *Entamoeba histolytica*. PLoS Negl Trop Dis 6, e1831.

99. Kimura, M., Ujihara, M., Yokoi, K. (1996). Tissue manganese levels and liver pyruvate carboxylase activity in magnesium-deficient rats. Biol Trace Elem Res 52, 171-179.

100. Bayliak, M. M., Shmihel, H. V., Lylyk, M. P., Vytvytska, O. M., Storey, J. M., Storey, K. B., Lushchak, V. I. (2015). Alpha-ketoglutarate attenuates toxic effects of sodium nitroprusside and hydrogen peroxide in Drosophila melanogaster. Environ Toxicol Pharmacol 40, 650-659.

101. Wu, N., Yang, M., Gaur, U., Xu, H., Yao, Y., Li, D. (2016). Alpha Ketoglutarate: physiological functions and applications. Biomol Ther (Seoul) 24, 1-8.

102. Tapiero, H., Mathe, G., Couvreur, P., Tew, K. D. (2002). Glutamine and glutamate. Biomed Pharmacother 56, 446-457.

103. Stottmeister, U., Aurich, A., Wilde, H., Andersch, J., Schmidt, S., Sicker, D. (2005). White biotechnology for green chemistry: fermentative 2-oxocarboxylic acids as novel building blocks for subsequent chemical syntheses. J Ind Microbiol Biotechnol 32, 651-664.

104. Alhasawi, A. A., Appanna, V. D. (2016). Manganese orchestrates a metabolic shift leading to the increased bioconversion of glycerol into α-ketoglutarate. AIMS Bioengineering 4, 12-27.

105. Kumar, S., Kumar, S., Punekar, N. S. (2015). Characterization of succinic semialdehyde dehydrogenase from *Aspergillus niger*. Indian J Exp Biol 53, 67-74.

106. Yin, L., Mano, J. I., Wang, S., Tsuji, W., Tanaka, K. (2010). The involvement of lipid peroxide-derived aldehydes in aluminum toxicity of tobacco roots. Plant physiol 152, 1406-1417.

107. Shelp, B. J., Bown, A. W., McLean, M. D. (1999). Metabolism and functions of gamma-aminobutyric acid. Trends Plant Sci. 4, 446-452.

108. Han, S., Auger, C., Appanna, V. P., Lemire, J., Castonguay, Z., Akbarov, E., Appanna, V. D. (2012). A blue native polyacrylamide gel electrophoretic technology to probe the functional proteomics mediating nitrogen homeostasis in *Pseudomonas fluorescens*. J Microbiol Methods 90, 206-210.

109. Choi, S. Y., Kim I., Jang S.H, Lee S.J., Song M.S., Lee Y.S., Cho S.W. (1993). Purification and properties of GABA transaminase from bovine brain. Mol Cells 3, 397-401.

110. Jakoby, W. B., Scott, E. M. (1959). Aldehyde oxidation III. Succinic semialdehyde dehydrogenase. J Biol Chem 234, 937-940.

111. Pathare, V., Srivastava, S., Suprasanna, P. (2013). Evaluation of effects of arsenic on carbon, nitrogen, and sulfur metabolism in two contrasting varieties of *Brassica juncea*. Acta physiol plant 35, 3377-3389.

112. Williams, A. J., Coakley, J. and Christodoulou, J. (1998). Automated analysis of mitochondrial enzymes in cultured skin fibroblasts. Anal Biochem 259, 176-180.

113. Alhasawi, A., Auger, C., Appanna, V. P., Chahma, M., Appanna, V. D. (2014). Zinc toxicity and ATP production in *Pseudomonas fluorescens*. J Appl Microbiol 117, 65-73.

114. Zhang, S., Bryant, D. A. (2011). The tricarboxylic acid cycle in cyano-bacteria. Science 334, 1551-155.

115. Holz, M., Förster, A., Mauersberger, S. Barth, G. (2009). Aconitase overexpression changes the product ratio of citric acid production by *Yarrowia lipolytica*. Appl Microbiol Biotechnol 81, 1087-1096.

116. Auger, C., Han, S., Appanna, V. P., Thomas, S. C., Ulibarri, G., Appanna, V. D. (2013). Metabolic reengineering invoked by microbial systems to decontaminate aluminum: Implications for bioremediation technologies. Biotechnol Adv 31, 26-273.

117. Dhakal, R., Bajpai, V. K., Baek, K. H. (2012). Production of GABA (γ-aminobutyric acid) by microorganisms: a review. J Pediatr Epilepsy 43, 1230-1241.

118. Scholz, S. S., Malabarba, J., Reichelt, M., Heyer, M., Ludewig, F., Mithöfer, A. (2017). Evidence for GABA-Induced Systemic GABA Accumulation in *Arabidopsis* upon Wounding. Front Plant Sci 8.

119. Bown, A. W., Shelp, B. J. (2016). Plant GABA: not just a metabolite. Trends Plant Sci 21, 811-813.

120. Feehily, C., Karatzas, K. A. G. (2013). Role of glutamate metabolism in bacterial responses towards acid and other stresses. J Appl Microbiol 114, 11-24.

121. Su, M. S., Schlicht, S., Gänzle, M. G. (2011). Contribution of glutamate decarboxylase in *Lactobacillus reuteri* to acid resistance and persistence in sourdough fermentation. Microb Cell Fact 10, S8.

122. Sykes, S., Szempruch, A., Hajduk, S. (2015). The krebs cycle enzyme α-ketoglutarate decarboxylase is an essential glycosomal protein in bloodstream African trypanosomes. Eukaryotic cell 14, 206-215.

123. Green, L. S., Li, Y., Emerich, D. W., Bergersen, F. J., Day, D. A. (2000). Catabolism of α-ketoglutarate by a sucA mutant of *Bradyrhizobium japonicum*: evidence for an alternative tricarboxylic acid cycle. J bacteriol 182, 2838-2844.

124. Mazzoli, R., Pessione, E. (2016). The neuro-endocrinological role of microbial glutamate and GABA signaling. Front Microbiol 7, 1934.

125. Dunn, M. F., Ramirez-Trujillo, J. A., Hernández-Lucas, I. (2009). Major roles of isocitrate lyase and malate synthase in bacterial and fungal pathogenesis. Microbiology 155, 3166-3175.

126. Waldron, K. J., Rutherford, J. C., Ford, D., Robinson, N. J. (2009). Metalloproteins and metal sensing. Nature 460, 823-830.

127. Hohle, T. H., O'brian, M. R. (2014). Magnesium-dependent processes are targets of bacterial manganese toxicity. Mol Microbiol, 93, 736-747.

128. Rosch, J.W, Gao, G., Ridout, G., Wang, Y.D., Tuomanen, EI. (2009). Role of the manganese efflux system mntE for signalling and pathogenesis in *Streptococcus pneumoniae*. Mol Microbiol 72, 12-25.

129. Appanna, V.D., Preston, C. (1987). Manganese elicits the synthesis of a novel exopolysacchride in an arctic *Rhizobium*. FEBS Lett 215, 79-82.

130. Gubert, P., Puntel, B., Lehmen, T., Bornhorst, J., Avila, D.S., Aschner, M., Soares, F.A.A. (2016). Reversible reprotoxic effects of manganese through daf-16 transcription factor activation and vitellogenin downregulation in *Caenorhabditis elegans*. Life Sci 151, 218-223.

131. Karki, P., Smith, K., Johnson, J., Jr, Aschner, M., Lee, E. (2014). Role of transcription factor yin yang 1 in manganese-induced reduction of astrocytic

glutamate transporters: Putative mechanism for manganese-induced neurotoxicity. Neurochem Int S0197-0186, 00185-5.

132. Tharmalingam, S., Alhasawi, A., Appanna, V.P., Lemire, J., Appanna, V.D. (2017). Reactive nitrogen species (RNS) resistant microbes: adaptation and medical implications. Biol Chem. doi.org/10.1515/hsz-2017-0152.

133. Lemire, J., Alhasawi, A., Appanna, V. P, Tharmalingam, S., Appanna, V.D. (2017). Metabolic defense against oxidative stress: The road less travelled-so far. J Appl Microbiol. doi: 10.1111/jam.13509.

134. Mailloux, R., Lemire, J., Appanna, V.D. (2008). A novel metabolic network leads to enhanced citrate biogenesis in *Pseudomonas* exposed to aluminum toxicity. Extremophiles 12, 451- 59.

135. Lemire, J., Milandu, J. Y., Auger, C., Bignucolo, A., Appanna, V.P., Appanna, V.D. (2010). Histidine is a source of the anti-oxidant a-ketoglutarate in *Pseudomonas fluorescens* challenged by oxidative stress. FEMS Microbiol 309, 170-177.

136. Li, C., Lesnik, K. L., Liu, H. (2013). Microbial conversion of waste glycerol from biodiesel production into value-added products. Energies 6, 4739-4768.

137. Schmidt, G., Kleppin, L., Schr der, W., Breckling, B., Reuter, H., Eschenbach, C., Windhorst, W., ltl, K., Wurbs, A., Barkmann, J., Marggraf, R., Thiel, M. (2009). Systemic risks of genetically modified organisms in crop production: interdisciplinary perspective. Gaia 18, 119-126.

138. He, Y., Chen, Z., Liu, X., Wang, C., & Lu, W. (2014). Influence of trace elements mixture on bacterial diversity and fermentation characteristics of liquid diet fermented with probiotics under air-tight condition. PloS One 9, e114218.

139. Carini, P., White, A.E., Campbell, E.O., Giovannoni, S.J. (2014). Methane production by phosphate-starved SAR11 chemoheterotrophic marine bacteria. Nat Commun 5, 4346.

Appendix: Other contribution in the conversion of renewable biomass into value-added products

Like glycerol, chitin is another important renewable chemical that can be transformed into value-added products. However, to achieve this objective, efficient technologies involved in the hydrolysis of chitin has to be unraveled. As part of my work, *Pseudomonas fluorescens* was explored as a potential source of chitinase, an enzyme known to degrade chitin into N-acetylglucosamine (NAG). In this study, we uncovered a unique exocellular chitinase with intriguing physico-chemical attributes.

Enhanced extracellular chitinase production in *Pseudomonas fluorescens*: biotechnological implications

(Original research)

Azhar A. Alhasawi and Vasu D. Appanna*

(Published in Aims Bioengineering)

Alhasawi A, Appanna VD (2017) Enhanced extracellular chitinase production in *Pseudomonas fluorescens*: biotechnological implications. Aims bioengineering. 2017, 4: 366-376.

Abstract

Chitin is an important renewable biomass of immense commercial interest. The processing of this biopolymer into value-added products in an environmentally-friendly manner necessitates its conversion into N-acetyl glucosamine (NAG), a reaction mediated by the enzyme chitinase. Here we report on the ability of the soil microbe *Pseudomonas fluorescens* to secrete copious amounts of chitinase in the spent fluid when cultured in mineral medium with chitin as the sole source of carbon and nitrogen. Although chitinase was detected in various cellular fractions, the enzyme was predominantly localized in the extracellular component that was also rich in NAG and glucosamine. Maximal amounts of chitinase with a specific activity of 80 µmol NAG produced mg^{-1} protein min^{-1} was obtained at pH 8 after 6 days of growth in medium with

0.5 g of chitin. In-gel activity assays and Western blot studies revealed three isoenzymes. The enzyme had an optimal activity at pH 10 and a temperature range of 22–38 . It was stable for up to 3 months. Although it showed optimal specificity toward chitin, the enzyme did readily degrade shrimp shells. When these shells (0.1 g) were treated with the extracellular chitinase preparation, NAG [3 mmoles (0.003 g-mol)] was generated in 6 h. The extracellular nature of the enzyme coupled with its physico-chemical properties make this chitinase an excellent candidate for biotechnological applications.

1.   Introduction

Chitin, the second most widely occurring bio-polymer in nature after cellulose, is composed of β (1→4) linked N-acetylglucosamine (GlcNAc). Unlike cellulose, chitin has an acetamide group and can be a source of carbon and nitrogen. Chitin is a major structural component in the cell walls of fungi and the shells of crustaceans such as lobsters, crabs and shrimp. Worldwide, chitin is an important renewable solid waste generated from the processing of shellfish, krill and shrimps [1] that can be utilized in the production of value-added products. Owing to their biocompatibility, biodegradability, bioactivity, non-toxicity and adsorption properties, chitin and its derivatives [2, 3] are used in wastewater treatment, drug delivery, wound healing, and dietary fibre [4].

Hence, the transformation of chitin into commercial products is an ongoing research endeavour. Although chemical solubilisation of the polymer is routinely utilized industrially, it is time consuming, requires harsh conditions such as strong acids and high temperatures and produces waste products [1]. Enzymatic degradation has become a technology of choice in the bioconversion of chitin as it is economical, environmentally-friendly and generates relatively no by-products. Microorganisms are widely utilized for the degradation of polymers and this process has received significant attention in recent years [5, 6].

Chitinase (EC 3.2.1.14), that catalyzes the hydrolysis of the β-1-4-glycosidic linkage, is widely distributed in nature and can be found not only in fungi and crustaceans, but is also present in bacteria, viruses, higher plants and humans [7]. Chitinase is known to fulfill numerous physiological roles including the maintenance of cellular morphology, providing nutrients, and promoting infection. It can be obtained from numerous sources and has found applications in medical, agricultural and food industries [8-10]. However, its ability to degrade chitin effectively is gaining prominence in biotechnological processes. This enzyme that belongs to the glycoside hydrolase family has the ability to release N-acetyl glucosamine like lysozyme (EC 3.2.1.17) [8].

As part of our study to explore the nutritional versatility of the soil microbe *Pseudomonas fluorescens*, we have examined its ability to use chitin as the sole source carbon and produce chitinase under various growth conditions [11, 12]. This soil microbe is widely used in biotechnological applications and is known not only to produce commercially important metabolites but is also resistant to numerous metal pollutants, an attribute central in the management of metal wastes [12-15]. Furthermore, its application in the agriculture industry as biofertilizers is well-established [16]. In this report the optimal synthesis of chitinase and its extracellular localization

110

are reported. The significance of these findings in the bioconversion of chitin and shrimp shells into value-added products is discussed.

2. Materials and Methods

2.1. Growth conditions and biomass

The bacterial strain *Pseudomonas fluorescens* (ATCC 13525), was maintained and grown in 250 mL phosphate mineral medium containing $NaHPO_4$ (1.5 g), KH_2PO_4 (0.75 g), and $MgSO_4 \cdot 7H_2O$ (0.05 g) [17]. Chitin was utilised as the source of carbon and nitrogen in these cultures. In select experiments, NH_4Cl (0.2 g) was used as a nitrogen source and/or the medium was supplemented with 50 μM $FeCl_3$. To optimize the yield of microbial biomass and exocellular chitinase production, the amount of chitin was varied from 0.1 g to 2 g. Trace elements were added as described previously [15]. The effect of pH on microbial growth was investigated by varying the pH of culture media from 4–10. The medium was dispensed in an aliquot of 250 mL into 500 mL Erlenmeyer flasks with foam plugs. Inoculations were made with 1 mL stationary phase cells grown in a chitin culture and aerated on a gyratory water bath shaker (Model 76; New Brunswick Scientific) at 26   and 140 rpm. Cell growth was monitored by measuring bacterial proteins with the aid of the Bradford assay [18]. Ten mL of culture medium was isolated at different growth intervals and following the centrifugation of the bacterial pellet, it was treated with 1 mL of 0.5 M NaOH. The soluble protein content was subsequently measured [19].

2.2. Cellular fractionation and metabolite analyses

Bacteria were harvested at the stationary phase of growth by centrifugation at 10,000 × g and

4   for 15 min. The spent fluid was collected and the pellets were washed with 0.85% (w/v) NaCl and the pellet was re-suspended in cell storage buffer (CSB; 50 mM Tris-HCl pH 7.6, 5 mM MgCl$_2$, 1 mM dithiothreitol and 1 mM phenylmethylsulphonyl fluoride (PMSF)). To obtain the cell free extract (CFE), the bacteria were lysed via sonication and centrifuged at 180,000 × g for 3 h at 4   , yielding soluble and membrane fractions [15]. The latter was re-suspended in 500 μL of CSB. The protein content in the soluble and membrane fractions was determined using the Bradford assay [18].

Metabolite levels were examined using high performance liquid chromatography (HPLC). The spent fluid and soluble CFE were injected into an Alliance HPLC equipped with a C18 reverse-phase column (Synergi Hydro-RP; 4 μm; 250 × 4.6 mm, Phenomenex) operating at a flow   rate   of 0.2 mL min–1 at ambient temperature. A mobile phase consisting of 20 mM KH$_2$PO4 (pH 2.9) was used to separate organic acids, which were detected using a Waters dual absorbance detector at 210 nm. Metabolites were identified using known standards, and peaks were quantified with the aid of the Empower software (Waters Corporation). The spent fluid was analysed for metabolites as were chitin, shrimp, glycol chitin and chitosan following incubation with the spent fluid [20].

2.3.   Chitinase assay

The spent fluid, soluble CFE and membrane CFE were added with 1 mg chitin. The mixture was incubated at room temperature for 1 h. One hundred μL of 0.8 mM sodium

tetraborate ($Na_2B_4O_7$) was added and then boiled for 3 min. Chitinase activity was measured by the amount of NAG produced by adding 3 mL p-dimethylaminobenzaldehyde (DMAB). DMAB was prepared as described [21] and the absorbance at 585 nm was recorded. Chitinase (1 U) is defined as the amount of enzyme which releases 1 µmol of NAG min^{-1} [22]. D-glucose was assayed using dinitrosalicylic acid (DNS) and was monitored at 540 nm as described [23].

2.4. Polyacrylamide gel electrophoresis and western blot analyses

After the culture was harvested at the stationary phase, the cells were isolated by centrifugation at 10,000 × g for 15 min at 4 . The cell-free supernatant was collected and precipitated by ammonium sulphate (70%) saturation and allowed to stand overnight at 4 . The precipitates were centrifuged, dialysed, and re-suspended with cell storage buffer (50 mM Tris-HCl, 1 mM phenylmethylsulfonylfluoride, and 1 mM dithiothreitol pH: 7.6). The molecular mass and activity of chitinase was assessed by SDS-PAGE. The latter was performed as described previously [24-27] with 0.01% glycol chitin added but devoid of 2-mercaptoethanol. Following electrophoresis, the gel was re-natured by incubation in phosphate buffer (pH 8) with 1% triton X-100 overnight. Upon completion, the glycol chitin containing gel was then stained with 0.01% (w/v) calcofluor white M2R (Sigma) in Tris-HCl buffer (50 mM, pH 7.4 for 30 min). Then, the brightener solution was removed and the gel was washed with distilled water for 1 h at room temperature. The enzyme activity zone was detected by placing the gels on UV-transilluminator and photographed [28, 29].

Western blot assays were modified from the Odyssey H Infrared Imaging System protocol document (Li-cor doc# 988-08599). Briefly, the proteins from the SDS gel were electroblotted onto a nitrocellulose membrane using protein transfer buffer (PTS) consisting of (25 mM Tris,

192 mM glycine) at 20 V for 16 h. The fixing solution was then removed and the cells were

rinsed   with

TBS (4 g Tris-HCl, 10 g NaCl, pH. 7.6 at 4   ) containing 0.1% tween-20. The membrane was

subsequently incubated in a skim milk blocking buffer for 1 h. Primary antibody (barley

chitinase anti-rabbit antibody, a gift from Dr. S. Muthukrishnan, Kansas State University, USA)

interactions occurred over a 1 h period with gentle shaking. Primary antibodies were added for 1

h in TBS containing 0.1% Tween-20 and the membrane was washed with TTBS (0.1% Tween-

20 with TBS) three times for 10 to 15 minutes each time to remove the unbound antibodies. The

membrane was then treated with secondary antibodies diluted to a concentration of 1:1000.

Secondary antibodies consisted of goat anti-rabbit (Sigma).

2.5.   Physico-chemical and biotechnological studies

In order to define the optimum pH and temperature for chitinase activity, 500 μL of the

spent fluid was assayed in various pH ranges from 4–12 and at temperatures ranging from 18–48

   for 1 h. The formation of chitinase was monitored at 585 nm. To determine the stability, the

enzyme was monitored at various time intervals over a period of three months. To evaluate the

substrate specificity of the enzyme preparation, 500 μL of the spent fluid was incubated for 1 h

with 1 mg of substrates such as chitin, shrimp shells, glycol chitin, chitosan, cellulose and starch

[30]. NAG was measured by the DMAB assay at 585 nm while the glucose production was

monitored by DNS assay at 540 nm. To evaluate the biotechnological potential of this enzymatic

preparation, de-proteinated shrimp shells as described [31] (0.1 g) were subjected to 10 mL of

spent fluid (0.3 mg protein equivalent) for up to 12 h and NAG production was evaluated.

2.6.   Statistical analysis

All experiments were performed in triplicate and in biological duplicate. Data were expressed as mean ± standard deviation (SD).

3.   Results and Discussion

In an effort to evaluate the optimal expression of chitinase activity in *P. fluorescens* ATCC 13525, the microbe was cultured in various nutritional conditions. Chitin was readily utilized both as a source of carbon and nitrogen. At pH 8.3 in the presence of 0.5 g of chitin, the optimal biomass of 0.549 mg protein equivalent per mL of culture was obtained. The inclusion of increased amounts of chitin and NH_4Cl did not ameliorate growth rate or cellular yield. Microbial multiplication was negatively influenced at lower pH. At pH 4 there was a 3-fold reduction in biomass while at pH 10 the cellular yield was 30% compared to that recorded during the optimal growth conditions. Addition of $FeCl_3$ was also inhibitory. As the 0.5 g chitin medium at pH 8.3 devoid of ammonium salt afforded the optimal condition, this medium was subsequently utilized to further characterize the degradation of this polymer by *Pseudomonas fluorescens* (Tables 1). Bacterial growth was evident after 2 days and stationary phase of growth was attained within 5–6 days. There was a concomitant increase in protein in the spent fluid (Figure 1A). In effort to elucidate how chitin was degraded the soluble CFE isolated at stationary phase of growth was monitored by HPLC. Peaks that were attributed to NAG and glucosamine were prominent (Figure. 1B). Hence, it became evident that chitinase, an enzyme involved in the depolymerisation of chitin into NAG was involved in this process. Various cellular fractions

were subsequently probed for chitinase activity. As the spent fluid had the most chitinase activity, the nature of the enzyme was probed in this fraction at various growth periods. At day 6, both the activity and the protein levels were the highest. When chitin was added to the spent fluid, NAG was readily released as confirmed by colorimetric assay and HPLC (Figure. 2A).

Table 1. Optimization of microbial yield at different concentration of chitin. B) Influence of pH and nutrient on biomass production with 0.5 g chitin. $100\% = 0.549$ mg^{-1} mL^{-1}, n = 3, SD ± 1%.

A)

Chitin concentrations	Biomass
2 g	57%
1 g	95%
0.5 g	100%
0.1 g	64%

$100\% = 0.54$ mg protein mL^{-1}, n = 3 ± 1%

B)

pH	Cellular yield

116

4	33%
8	100%
10	30%

Nutrients	Cellular yield
NH_4Cl	97%
$FeCl_3$	55%
Phosphate (64 mM)	100%
Phosphate (25 µM)	65%

$100\% = 0.549$ mg^{-1} mL^{-1}, n=3.
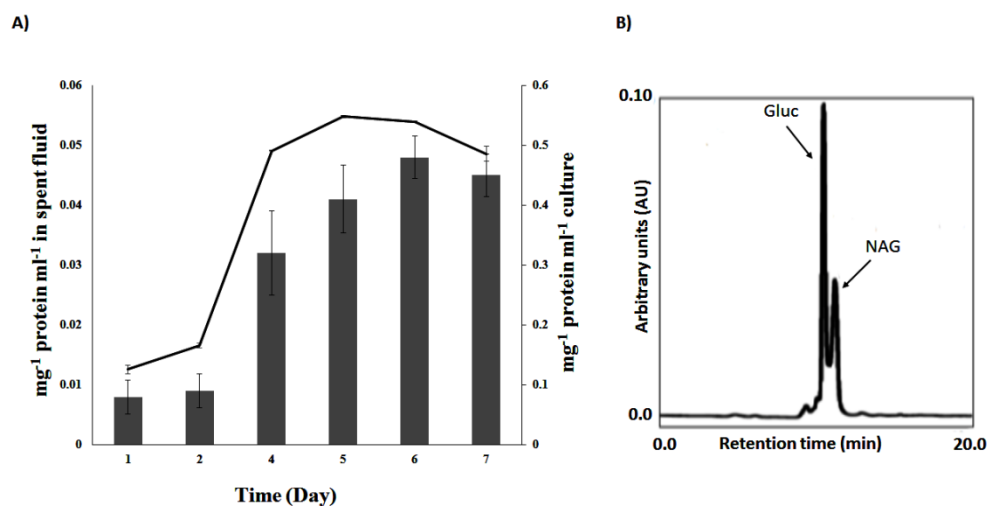
Figure 1. *P. fluorescens* cultured in the optimal chitin medium: A) Cellular yield (line graph) and extracellular protein concentration of spent fluid (bar chart). B) Metabolite profile at the stationary phase in the spent fluid, as measured by high performance liquid chromatography (HPLC). Gluc = Glucosamine, NAG = N-acetylglucosamine.

The spent fluid at the stationary phase of growth was isolated and treated with ammonium sulphate (($NH_4)_2SO_4$) in order to precipitate the proteins. (Note: No cell lysis was discerned). The pellet was reconstituted and examined for chitinase by gel electrophoresis and Western

blotting. Immunoblot studies revealed bands indicative of chitinase (Figure. 2B). In an effort to confirm the nature of the isoforms of the enzyme, the proteins were electrophoresed in a SDS gel [25]. Following the re-naturing of the enzymes, three activity bands were obtained, thus pointing to the three isoforms that were being secreted in the exocellular environment (Figure 2C). The spent fluid harboured the most enzymatic activity while the membranous fraction had a specific activity that was the lowest with a value of 27 μmol of NAG mg^{-1} protein min^{-1} (Figure 2D). Although the chitinases in the spent fluid did degrade shrimp shell, chitosan and glycol chitin, chitin appeared to be the preferred substrate. NAG was the product generated when the shrimp shells were incubated with the spent fluid (Figure. 3A). No discernable amount of D-glucose was released upon the incubation of either cellulose or starch with the exocellular chitinase (data not shown). The enzyme appeared to have an optimal activity in the pH range of 9–10 (Figure. 3B). There was a drastic reduction in activity at acidic pH. The chitinase was stable when kept at 4 for 3 months. No significant change of activity was evident when enzymatic preparations were monitored over this period (data not shown). The activity ranged between 70–100% at temperature varying from 18–48 (Figure 3C).


118
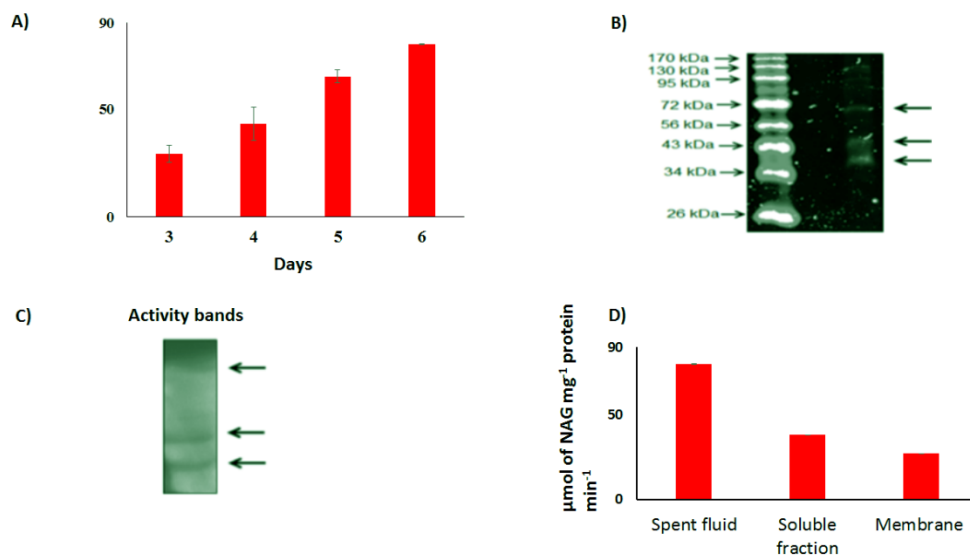
Figure 2. Studies on extracellular chitinase: A) Time profile of chitinase activity in the spent fluid, as measured by the DMAB assay. B) Chitinase expression in spent fluid, as probed by Western blot following SDS-PAGE. C) Chitinase activity bands measured via calcofluor white following re-naturing. D) Specific activity of chitinase in various cellular fractions obtained from the optimal medium.
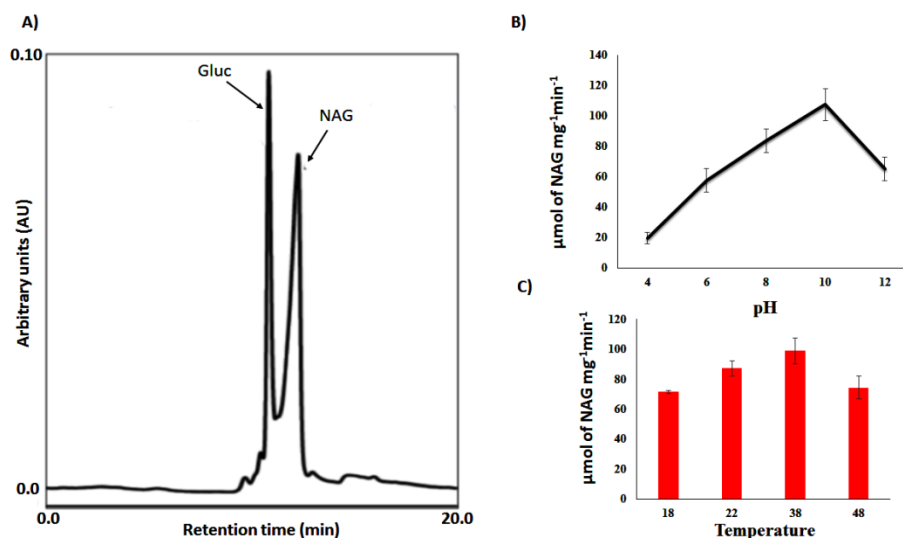
Figure 3. Physico-chemical properties of chitinase: A) HPLC analysis showing NAG production when spent fluid is incubated with 0.1 g of shrimp cells. B) Chitinase activity as measured by the DMAB assay over a range of pH. C) Chitinase activity as measured by the DMAB assay over a range of temperatures. Gluc = Glucosamine, NAG = N-acetylglucosamine.

When de-proteinated shrimp shells were incubated with the spent fluid, NAG was obtained. After a 6 h enzymatic treatment using the *P. fluorescens* spent fluid, 3 mmole (0.003 g-mol) of NAG was released from 0.1 g of shrimp waste (Figure 4A). While chitin elicited the most chitinase activity, other substrates like chitosan and chitin-glycol were also rapidly broken down into NAG when incubated with the spent fluid (Figure 4B). The foregoing data point to the ability of *P. fluorescens* to secrete chitinase when chitin is the sole source of carbon and nitrogen. An alkaline pH appears to evoke the maximal bacterial growth and release of extracellular chitinase in mineral medium with no added ammonium salt or cofactors. The enzyme was stable for a period of 3 months and showed maximal activity at pH

10. Recently, an alkaline chitinase with an optimal activity at pH 9.0 and having a molecular mass in the range of 50–125 kDa was reported in *Bacillus* [30, 32]. In this instance, the enzyme was intracellular. Even though in our studies the enzyme was localized in various cellular components, the chitinase in the spent fluid was the most abundant and active. The presence of extracellular chitinases has been reported in *P. fluorescens* isolated from different plant sources with activities mostly in the range of acidic pH [33]. The physico-chemical properties of the chitinase revealed in this study coupled with its exocellular location makes this enzyme an excellent candidate in the industrial digestion of chitin wastes (Figure 4C). The presence of the enzyme in the spent fluid and its activity in the alkaline pH range make this chitinase more amenable to industrial application compared to those localized intracellularly. Indeed, the efficacy of the spent fluid in generating NAG and glucosamine from shrimp shells may provide interesting biotechnological applications [10].
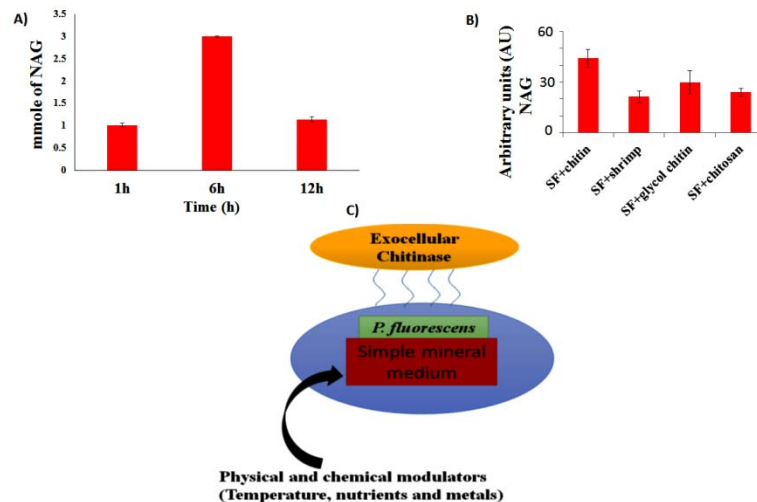
Figure 4. Exocellular chitinase and biotechnological implications: A) Enzymatic degradation was measured by incubating 10 mL of spent fluid with 0.1 g

of shrimp shells for 1, 6 and 12 h. NAG production was measured by the DMAB assay. B) HPLC analysis of NAG production when disparate substrates (1 mg of chitin, glycol chitin, chitosan or shrimp shells) were incubated with 500 µL of spent fluid. C) Increased exocellular chitinase production in *Pseudomonas fluorescens*.

4. Conclusion

Chitin is an important renewable biomass of immense economic benefit and chitinase provides a controlled route to effectively transform this polymer into value-added products. The discovery of the enhanced production of this enzyme with exceptional attributes by *P. fluorescens* ATCC 13525 presents a unique opportunity to tailor this microbe and its components for commercial application in the renewable biomass industry. This extracellular chitinase can be readily harnessed as nanofactories designed to convert this renewable biopolymer into chemicals aimed at the agricultural, energy, food and medical sectors.

Conflicts of interest

The authors declare that they have no conflict of interest.

References

1. Khoushab F, Yamabhai M (2010) Chitin research revisited. *Mar Drugs* 8: 1988-2012.

2. Cheba BA (2011) Chitin and chitosan: marine biopolymers with unique properties and versatile applications. *Global J Biotech Bio-Chem* 6: 149-153.

3. Thiagarajan V, Revathi R, Aparanjini K, et al. (2011) Extra cellular chitinase production by *Streptomyces* sp.PTK19 in submerged fermentation and its lytic activity on *Fusarium oxysporum* PTK2 cell wall. *Int J Curr Sci* 1: 30-44.

4. Dahiya N, Tewari R, Hoondal GS (2006) Biotechnological aspects of chitinolytic enzymes: a review. *Appl Microbiol Biotechnol* 71: 773-782.

5. Haggag WM, Abdallh E (2012) Purification and characterization of chitinase produced by *Endophytic ptomyceshygroscopicus* against some phytopathogens. *J Microbiol Res* 2: 145-151.

6. Reissig JL, Strominger JL, Leloir LF (1955) A modified colorimetric method for the estimation of N-acetylamino sugars. *J Biol Chem* 21: 959-966.

7. Kamil Z, Saleh M, Moustafa S (2007) Isolation and identification of rhizosphere soil chitinolytic bacteria and their potential in antifungal biocontrol 1. *Global J Mol Sci* 2: 57-66.

8. Bhattacharya D, Nagpure A, Gupta RK, (2007) Bacterial chitinases: properties and potential. *Crit Rev Biotechnol* 27: 21-28.

9. Hamid R, Khan MA, Ahmad M, et al. (2013) Chitinases: an update. *J Pharm Bioallied Sci* 5: 21-29.

10. Narayanan K, Chopade N, Raj PV, et al. (2013) Fungal chitinase production and its application in biowaste management. *J Sci Indust Res* 72: 393-399.

11. Appanna VD, Pierre MS (1996) Aluminum elicits exocellular phosphatidylethanolamine production in *Pseudomonas fluorescens*. *Appl Environ Microbiol* 62: 2778-2782.

12. Auger C, Han S, Appanna VP, et al. (2013) Metabolic reengineering invoked by microbial systems to decontaminate aluminum: implications for bioremediation technologies. *Biotechnol Adv* 31: 266-273.

13. Appanna VD, Gazsó LG, Pierre MS (1996) Multiple-metal tolerance in *Pseudomonas fluorescens* and its biotechnological significance. *J Biotechnol* 52: 75-80.

14. Bignucolo A, Appanna VP, Thomas SC, et al. (2013) Hydrogen peroxide stress provokes a metabolic reprogramming in *Pseudomonas fluorescens*: enhanced production of pyruvate. *J Biotechnol* 167: 309-315.

15. Middaugh J, Hamel R, Jean-Baptiste G, et al. (2005) Aluminum triggers decreased aconitase activity via Fe-S cluster disruption and the overexpression of isocitrate dehydrogenase and isocitrate lyase: a metabolic network mediating cellular survival. *J Biol Chem* 280: 3159-3165.

16. Yanes ML, Bajsa N. Fluorescent *Pseudomonas*: a natural resource from soil to enhance crop growth and health. In microbial models: from environmental to industrial sustainability 2016 (pp. 323-349). Springer Singapore.

17. Chenier D, Beriault R, Mailloux R, et al. (2008) Involvement of fumarase C and NADH oxidase in metabolic adaptation of *Pseudomonas fluorescens* cells evoked by aluminum and gallium toxicity. *Appl Environ Microbiol* 74: 3977-3984.

18. Bradford MM (1976) A rapid and sensitive method for the quantitation of microgram quantities of protein utilizing the principle of protein-dye binding. *Anal Biochem* 72: 248-254.

19. Mailloux R, Lemire J, Kalyuzhnyi S, et al. (2008) A novel metabolic network leads to enhanced citrate biogenesis in *Pseudomonas fluorescens* exposed to aluminum toxicity. *Extremophiles* 12: 451-459.

20. Alhasawi A, Auger C, Appanna VP, et al. (2014) Zinc toxicity and ATP production in *Pseudomonas fluorescens*. *J appl microbial* 117: 65-73.

21. Sharp RG (2013) A review of the applications of chitin and its derivatives in agriculture to modify plant-microbial interactions and improve crop yields. *Agronomy* 3: 757-793.

22. Neiendam Nielsen M, Sørensen J (1999) Chitinolytic activity of *Pseudomonas fluorescens* isolates from barley and sugar beet rhizosphere. *FEMS Microbiol Ecol* 30: 217-227.

23. Negrulescu A, Patrulea V, Mincea MM, et al. (2012) Adapting the reducing sugars method with dinitrosalicylic acid to microtiter plates and microwave heating. *J Braz Chem Soc* 23: 2176-2182.

24. Auger C, Lemire J, Cecchini D, et al. (2011) The metabolic reprogramming evoked by nitrosative stress triggers the anaerobic utilization of citrate in *Pseudomonas fluorescens*. *PloS One* 6: e28469.

25. Laemmli UK (1970) Cleavage of structural proteins during the assembly of the head of bacteriophage T4. *Nature* 277: 680-685.

26. Liu CL, Shen CR, Hsu FF, et al. (2009) Isolation and identification of two novel SDS-resistant secreted chitinases from *Aeromonas schubertii*. *Biotechnol Prog* 25: 124-131.

27. Loni PP, Patil JU, Phugare SS, et al. (2014) Purification and characterization of alkaline chitinase from *Paenibacillus pasadenensis* NCIM 5434. *J Basic Microbiol* 54: 1080-1089.

28. Velusamy P, Ko HS, Kim KY (2011) Determination of antifungal activity of *Pseudomonas* sp. A3 against *Fusarium oxysporum* by high performance liquid chromatography (HPLC). *Agric Food Annal Bacteriol* 1: 15-23.

29. Zou X, Nonogaki H, Welbaum GE (2002) A gel diffusion assay for visualization and quantification of chitinase activity. *Mol Biotechnol* 22: 19-23.

30. Karunya SK (2011) Optimization and purification of chitinase produced by *Bacillus subtilis* and its antifungal activity against plant pathogens. *Intl J Pharma Biol Arch* 2: 1680-1685.

31. Viarsagh MS, Janmaleki M, Falahatpisheh HR, et al. (2010) Chitosan preparation from Persian Gulf shrimp shells and investigating the effect of time on the degree of deacetylation. *J Paramed Sci* 1: 2-6.

32. Kuzu SB, Güvenmez HK, Denizci AA (2012) Production of a thermostable and alkaline chitinase by *Bacillus thuringiensis* subsp. kurstaki strain HBK-51. *Biotechnol Res Int* 2012: 1-6.

33. Park SH, Lee JH, Lee HK (2000) Purification and characterization of chitinase from a marine bacterium, *Vibrio* sp. 98CJ11027. *J Microbiol* 38: 224-229.